EOM 3901

Master thesis in Energy and Environment in the North

The Fugløy cold-water coral reefs on the south-western Barents Sea shelf: their morphology, distribution and environmental setting

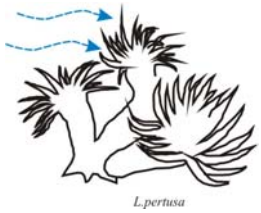

Heike Moumets

December, 2008

FACULTY OF SCIENCE

Department of Geology

University of Tromsø

EOM 3901

Master thesis in Energy and Environment in the North

The Fugløy cold-water coral reefs on the south-western Barents Sea shelf: their morphology, distribution and environmental setting

Heike Moumets

December, 2008

FACULTY OF SCIENCE

Department of Geology

University of Tromsø

ACKNOWLEDGEMENTS

I am very grateful to my supervisors Assoc.Prof. Stefan Bűnz and Prof.Dr. Jűrgen Mienert, whom have shared their vast knowledge about marine surveying, geology and hydrodynamics in the study area, effort to broaden my horizons and providing useful literature for this study. I must especial thank are to Stefan Bűnz for information and assistance, and for maintaining my enthusiasm marine research.

Thanks are to the captain and crew of R/V Jan Mayen for help to acquire the data. I gratefully acknowledge the friendship and support by the faculty, staff and students of the department during my two years at the University of Tromsø. Special thanks go to Anita Pettersen and Geir Antonsen. They always have been helpful and friendly to sort out all kinds of administrative questions. My special thanks are also provided to Matthias Forwick and Nicole Baeten for reading my thesis and giving helpful comments. I am also grateful for comments received from Riko Noormets, which helped to improve this thesis. I thank Julia Casado for spending long hours in the seismic lab with me and struggling with GMT.

Lastly, but not least, I wish to thank my dear brothers and sisters and of course my father for all the love and support that made my education possible and allowed me to pursue my childhood dreams.

Heike Moumets

Tromsø

December 15th 2008

Kallid õed-vennad (Viktor, Merle, Mardo, Maido, Hedit ja Erika) ja muidugi isa ja kasuema Agnes- suur aitäh teie toetuse ja abi ees. Ilma teie abi ja hoolivuseta õigel ajal õiges kohas ei oleks ma jõudnud nii kaugele! Vanaema, Valve, oled mul hinges ja sűdames…Alati…..

Tervitusetega Heike,
15.detsember 2008

THE FUGLØY COLD-WATER CORAL REEFS ON THE SOUTH-WESTERN BARENTS SEA SHELF: THEIR MORPHOLOGY, DISTRIBUTION AND ENVIRONMENTAL SETTING

Heike Moumets | Department of Geology, Faculty of Science in University of Tromsø
Dramsveien 201 NO-9037 Tromsø

ABSTRACT

The Fugløy area is located on the continental shelf, off the coast of Troms County in northern Norway about 300 km north of the Arctic Circle. The multibeam echosounder bathymetry data, backscatter data, high-resolution seismic profiles and acoustic attribute maps were used to identify cold-water coral reefs. Together 12 cold-water coral reefs up to 126 m wide, 241 m long and with an average slope angle of 15° were mapped in the study area. Coral reefs cover an area about 508147 m² and exist only at water depths between 115 and 163 m. The coral reefs appear as sub-circular low backscatter patches on the backscatter image and as cone-shaped, acoustically semi-transparent features on the low frequency data.

Coral reefs have the highest density up to 1.39 reefs per km² at ridges of morainic origin and local elevations. Reefs have an elongated form with mostly single crest aligned parallel to the moraine ridges. Coral reefs occur only in areas where the seafloor represents by hard bottom sediments. It seems that the pre-existing morainic ridge morphology dictates the shape and orientation of *L.pertusa* reef. Moraine ridges are often cut by erosional channels; those have probably positive influence on the transport and concentration of food particles and provide additionally control factors on the distribution of *L.pertusa* reefs.

Numerous pockmarks (in total 49) were observed in the sedimentary basin in the north and northeast from the main coral reef concentration. The pockmarks are mostly circular in planar view and show no sediment infill, which indicates that pockmarks have been recently active or are still active. The data suggest that the development and lateral distribution of reefs in the Fugløy area is dictated by an interaction between biological growth processes and factors like seepage of fluid from the pockmarks, local topography, hard ground and the current regime. The vertical distribution is most likely controlled by physical oceanographic conditions like temperature, salinity and density.

The size of cold-water coral reefs (up to 27 m high) indicates that reefs have optimal conditions for growth in the Fugløy area.

This study shows that high-resolution multibeam data together with backscatter and seismic data are effective tools to cold-water coral reef distributions in relation to the geological and oceanographic environment.

TABLE OF CONTENTS

1. INTRODUCTION

The continental margin and coastline of northern Norway have received continuously increasing attention over the last decades, mostly because of developing economic activities in various fields such as oil and gas production, seabed engineering, shipping, fisheries, offshore windmill parks (Sawhill et al. 2006). Marine resources, both renewable (fish) and not-renewable (petroleum), have played a key role in social and economic development in Norway and in this northern area. In particular the northern Norwegian coastline is expected to have a significant development potential in the future. Due to the ongoing development, this region attracts many scientific and commercial research activities related to the fields such as geosciences, oceanography, physics, chemistry and biology. The marine ecosystems at the northern Norwegian continental margin and coastline have a high environmental value and are rich in natural resources (Olsen et al. 2007). Therefore, those areas are particularly valuable and vulnerable, and in many cases, it will be a great challenge to combine environmental interests with the need for economic development. It is important that new growing activities do not damage ecosystems and natural seafloor habitats.

One of the most interesting and spectacular ecosystems in this area are cold-water coral reefs. Cold-water coral, *Lophelia pertusa* (=*L.pertusa*; Linné 1758), is one of the reef forming stony corals. It has a cosmopolitan distribution, where a dense belt of *L.pertusa* occurrences stretches from the south-western Barents Sea along the eastern Atlantic continental margin down to West Africa (Mortensen 1995; Rogers 1999; Fosså et al. 2000; Freiwald et al. 2002). Unlike their tropical counterparts, cold-water corals are less known to the public. Remarkably, cold-water coral reefs can have levels of biological diversity comparable to the tropical reefs (Rogers 1999). Examples of *L.pertusa* reef biodiversity are illustrated in figure 1.1. *L.pertusa* corals are an important component of benthic biodiversity and structural habitat complexity in cold-water marine ecosystems (Côté and Reynolds 2006). Cold-water coral ecosystems are slow growing (from 1 to 25 mm per year), but due to their long life span they are able to form massive reef complexes (Mortensen and Rapp 1998; Mortensen 2001). One of the greatest known *L.pertusa* reef structures today is the Sula reef on the Norwegian shelf. This reef structure is more than 13 km long, up to 450–500 m wide and more

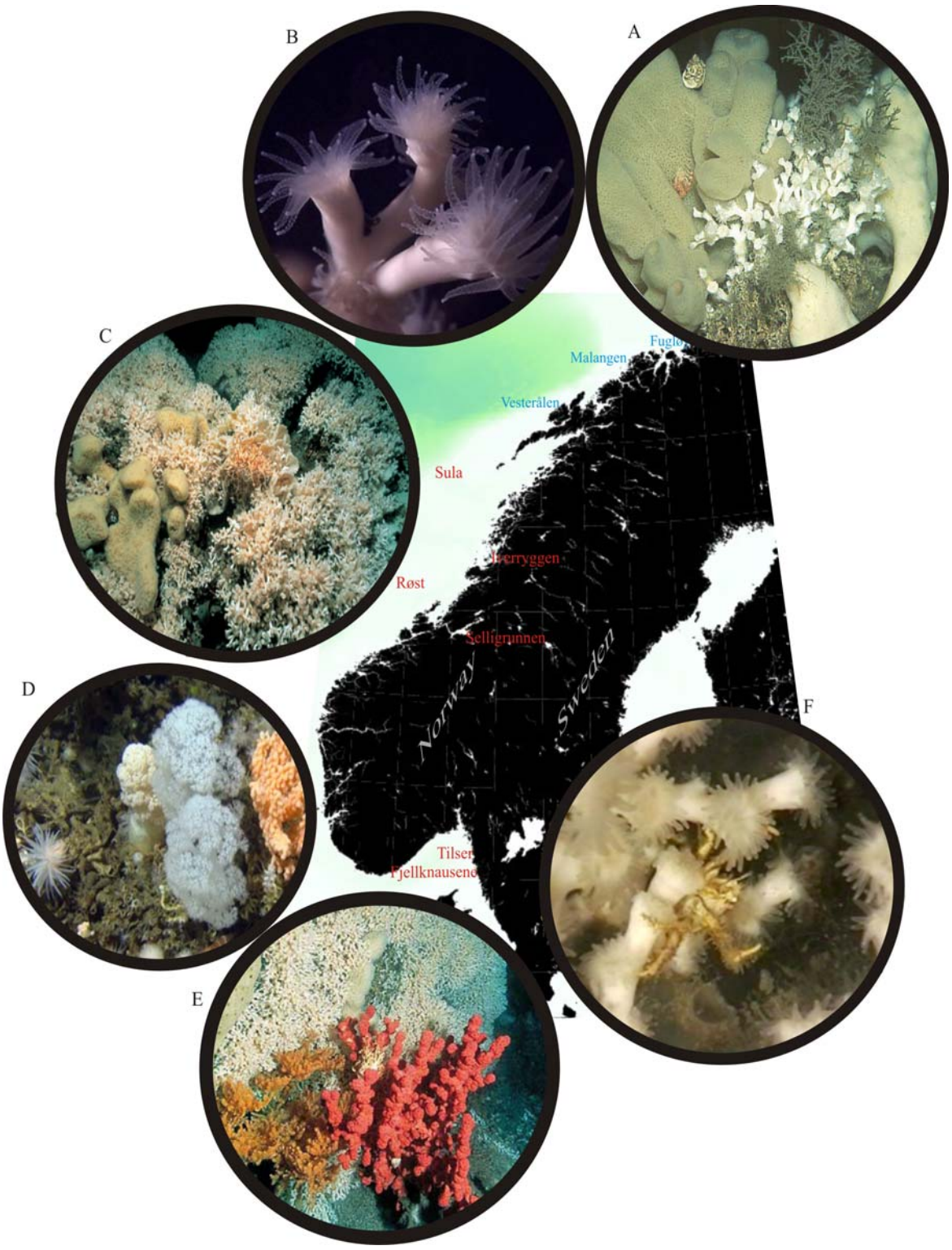

Figure 1.1. A *L.pertusa* and *Mycale lingua* from Skarnsundet, in Trondheimsfjorden (©F.E.Moen), **B** *L.pertusa* (©P.B.Mortensen), **C** an example of *L.pertusa* colony in Kosterfjord (©T.Lundälv), **D** soft coral (*Capnella glomerata*), sea corn (*Primnoa resedaeformis*) and a small pink *L.pertusa* on death *L.pertusa* rubble, **E** hvite *Lophelia*-reef and red horny coral (*Paragorgia arborea*) in Skarnsundet, Trondheimsfjorden (©E.Svensen), and **F** *L.pertusa* in Tisler (©T.Lundälv). With red colour are marked banned cold-water reefs. The Malangen and Vesterålen reefs were discovered by MAREANO spring-cruise in 2007. In Hola near Vesterålen was mapped over 330 coral reefs.

than 8500 years old (Mortensen et al. 2001). Spectacular reefs such as the Sula Ridge appear to be rare, but there are more than 700 verified smaller cold-water coral reef systems on the Norwegian continental margin (MAREANO). Due to the longevity, slow growth and low reproductive rate these ecosystems are vulnerable and sensitive to anthropogenic disturbance, especially activities such as fishing, and oil and gas production (Fosså et al. 2002; Roberts 2002; Gass and Roberts 2006). All fishing methods affect coral reefs, but the physically most damaging method is bottom trawling (National Research Council 2002). When fishing trawl is dragged along the sea floor, it breaks coral reefs, kills corals and destroys a habitat that takes centuries to recover, if it does at all (Rogers 1999). So far, the bottom trawling is banned on 6 cold-water coral reefs in Norway, but more areas are proposed for protection (Norwegian Directorate of Fisheries 2004; Langaas 2008)

The distribution of cold-water corals is relatively well studied in Norwegian coastal and offshore regions (Mortensen et al. 2001; Fosså et al. 2002; Hovland et al. 2002; Hovland et al. 2005; Lindberg et al. 2007; Lumsden et al. 2007), but the knowledge of coral reef occurrences is yet incomplete. New coral reefs are continually being described as the result of the advantage of new seafloor mapping technologies and considerable research and developing efforts in these areas. However, additional studies are needed to obtain more detailed records of cold-water reef locations and their sensitivity to anthropogenic and environmental change. These studies would allow us to better determine and manage potential anthropogenic and environmental impacts to those reefs, whether from commercial trawl fisheries or from the offshore oil and gas industry, or due to the ongoing global warming. As our understanding of *Lophelia pertusa* reefs is growing, it becomes easier to protect those communities and habitats, and save them for the future.

The Fugløy Reef was discovered accidentally by Statoil in 1982 during a pipe-line survey (Fosså et al. 2000; Hovland and Risk 2003). The Fugløy Reef area is one of the northernmost verified locations of cold-water reefs, and is located about 300 km north of the Arctic Circle. This reef complex has been studied in recent years (Lindberg et al. 2005a, 2005b & 2007). However, this is the first study to utilize high-resolution multibeam data set of the Fugløy Reef area to provide a more comprehensive analysis of coral-reef complexes in their environmental setting. The new multibeam data allows a more detailed mapping and integrated interpretation of individual coral reefs including existing backscatter and seismic data.

The objectives of this study are:

- provide representative maps of the sea floor in the Fugløy reef area;
- identify cold-water coral reefs and visualise and interpret their environmental settings;
- examine the size, distribution and origin of cold water coral reefs in the Fugløy area;
- contemplate the physical parameters that control coral reefs growth in this area;
- assess the sensitivity of the Fugløy reef system;

2. BACKGROUND

2.1. *LOPHELIA PERTUSA*

Lophelia pertusa (=L.pertusa) was first described by Linnaeus (1758) in the mid 18th century. The coral *L.pertusa* is the most well studied and common habitat-forming cold-water coral globally (Dons 1944; Hovland and Mortensen 1998; Fosså et al. 2000; 2002).

2.1.1. GEOGRAPHICAL DISTRIBUTION

L.pertusa has a global distribution, forming reefs along the continental margins, seamounts and banks throughout the world's oceans (Rogers 1999; Wheeler et al. 2007). These corals have been found most frequently in the North Atlantic, in particular south of Iceland (Copley et al. 1996), around the Faroe Islands (Fredriksen et al. 1992), on the banks west of Ireland and Scotland and on the Norwegian continental margin (Fig. 2.1a; Hovland et al. 1998; Fosså et al. 2000). Abundant *L.pertusa* are also recorded in the western Atlantic from Nova Scotia to Brazil, in the Gulf of Mexico, in the eastern Atlantic, the Mediterranean, the eastern Pacific, and the Indian Ocean (Reed et al. 2004; Roberts et al. 2006). The northernmost known occurrence of *L.pertusa* is in the south-western Barents Sea close to Hjelmsøybank at 71°21N and 24°00E (Fosså et al. 2000), while the southernmost location is known from the subantarctic Macquarie Ridge off New Zealand at 51°00S and 162°01E (Clarins 1982; Rogers 1999). Figure 2.1b shows that *L.pertusa* reefs are evenly distributed along the coast of Norway from the Tisler reef in Skagerrak close to the Swedish border in the south, to the Barents Sea c.71°N.

Most of the reefs are located near the continental shelf break between 200 m and 400 m water-depth, but there are a number of records from the entrances to fjords as well (Fosså et al. 2000). The precise number of reefs in Norwegian waters is not yet known. However, the Mareano (2008) database contains more than 700 geographically referenced *L.pertusa* locations. Furthermore, Fosså et al. (2000) estimated that total spatial coverage is about 2000 km² of Norwegian margin, mostly located on elevated moraines and boulder levees of ploughmarks (Freiwald et al. 1999).

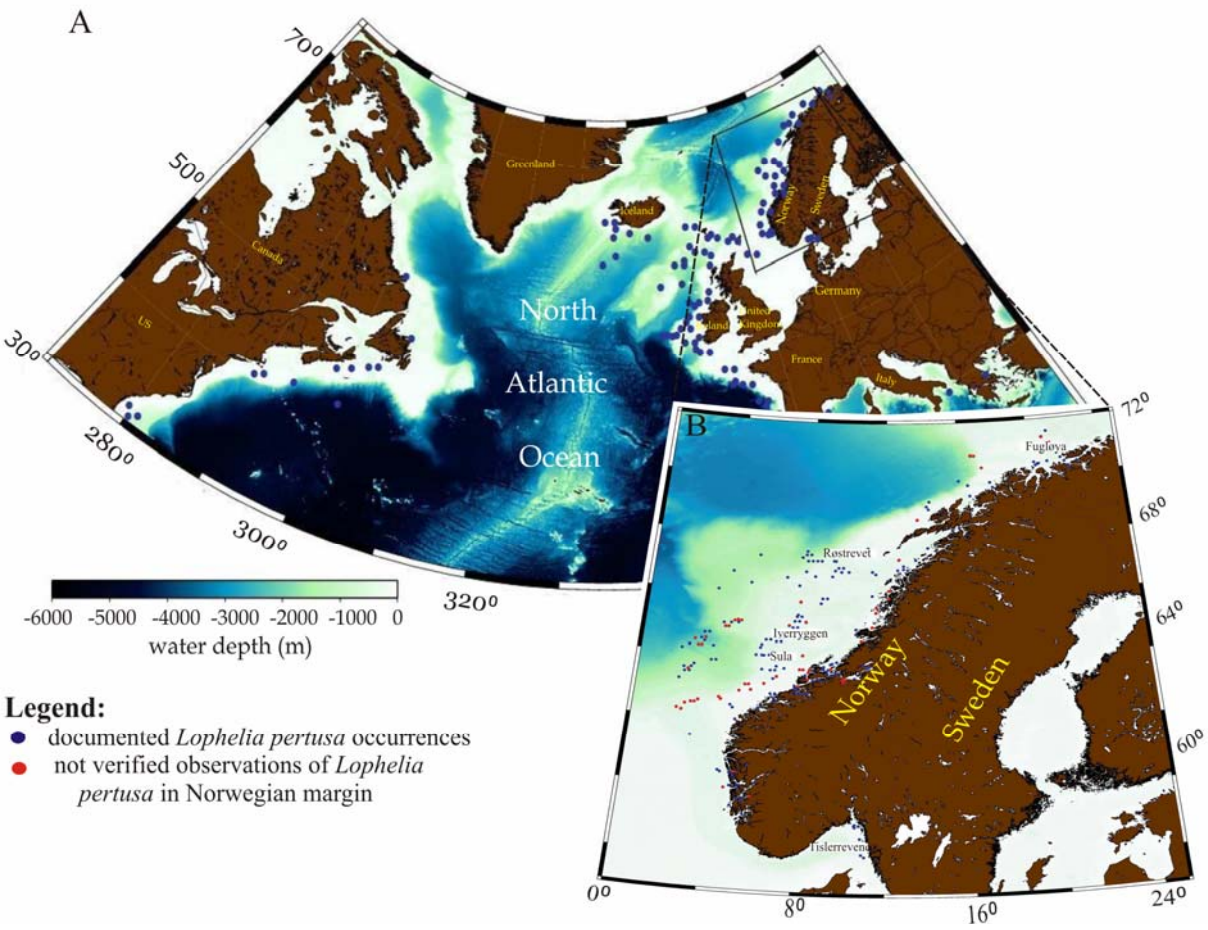

Figure 2.1. A *L.pertusa* occurrences on the northern hemisphere. *L.pertusa* has a global distribution. The blue points correspond to the occurrences of framework-forming cold-water corals reported in literature. **B** Map of the Norwegian continental margin showing the distribution of verified and not verified observations of *L.pertusa* reef. Modified from UNEP-CWCM report Cold-water Coral Reefs (2006) and Havforskningsinstituttet/MAREANO-maps, Coral reefs and oil.

2.1.2. ECOLOGY

Cold-water coral forms massive, bushy colonies, with anastomosing branches (Fig. 2.2). *L.pertusa* grows in colonies up to 2 m high. They can build calcium carbonate skeletons as they grow, forming giant and complex reef-like structures (Mortensen and Rapp 1998), commonly called coral banks, bioherms, lithoherms, patches or reefs (Freiwald et al. 1997; Paull et al. 2000). In this thesis such accumulation structures are called reefs. The sizes and morphologies of the reefs are very variable: circular, dome-shaped or elongate, in distinct irregular patches or arranged in lines of islands (Fosså et al. 2000; Wheeler et al. 2005). The growth rate of *L. pertusa* in the northeast Atlantic has been estimated to be from 5 to 26 mm per year. They are able to form massive reef complexes usually several kilometres long and more then 30 m high (Mortensen and Rapp 1998; Mortensen 2001).

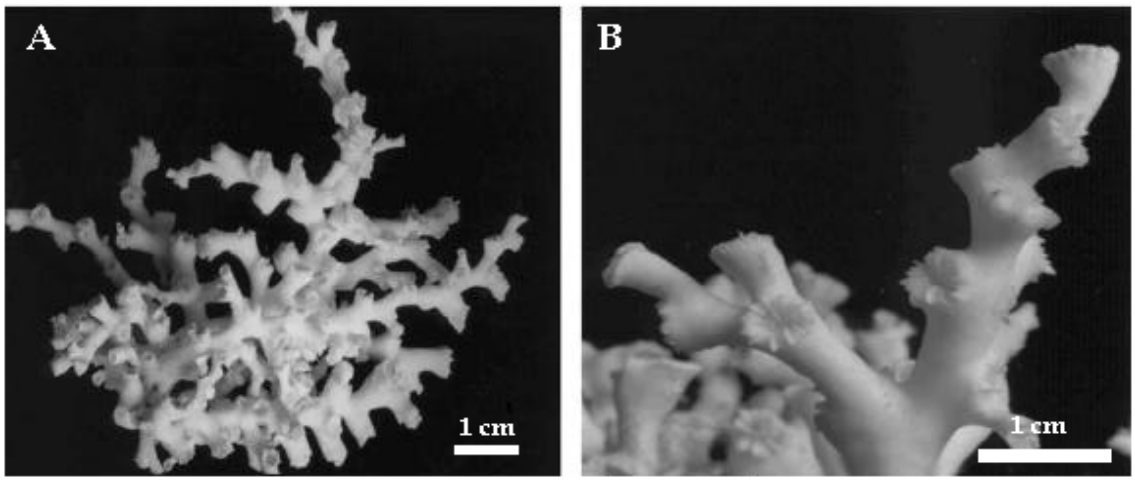

Figure 2.2. A Lophelia pertusa colony and **B** branch tip (From Reed, 2004).

One of the largest and well-known reefs along the coast of Norway is the Røst Reef, for location see figure 2.1b, it was discovered as recently as in May 2002 (Thorsnes 2003). The reef-complex is about 40 km long, up to 3 km wide and covers an area of about 100 km². *L.pertusa* has been found at the depths from 39 m on the Tautra Ridge in mid-Trondheimsfjord in Norway (Fig. 2.1a; Fosså et al. 2002), to 3383 m in the New England Seamount Chain, North Atlantic (Freiwald et al. 2004). Most commonly the reefs are formed at depths between 200 m and 800 m. Thus, unlike their tropical relatives, cold-water corals are found below the photic zone. Whereas tropical corals require light to survive, because they live symbiotically with photosynthetic algae, cold-water corals lack this relationship. Cold-water corals are filter-feeding and they extract food particles from the water column (Lumsden et al. 2007). Table 2.1 gives some general differences and similarities between tropic shallow-water and cold-water corals. The preferred temperature for cold-water corals seems to be between 6° and 8° C (Freiwald 1998), although some records from the Mediterranean suggest that cold-water corals can survive in waters as warm as 13 °C (Mortensen 2001). *L.pertusa* occurs mostly in waters with salinities of 35 -37 psu, but in the fjords they can also adapt to salinities as low as 32 psu (Rogers 1999; Mortensen et al. 2001). *Lophelia* requires hard substrate and fast currents for food supply and to keep the corals free of sediments (Wilson 1979; Rogers 1999).

Table 2.1. Differences and similarities between cold-water and tropical shallow-water structure-forming coral (Lumsden et al. 2007)

Parameter	Cold-water corals	Tropic shallow-water corals
Distribution	Potentially global (most common 56° S-71°N)	Tropical and subtropical seas (30°N-30°S)
Depth range	39 - 3383 m	0 - 100 m
Temperature	4 - 13 °C	18 - 31 °C
Salinity range	32 - 38.8 ‰	33 - 36 ‰
Growth rates	1-20 mm per year	• 1-10 mm per year for massive slow growing corals • 50-150 mm per year for faster growing branching corals
Symbiotic algae	No	Yes
Nutrition	Zooplankton and possibly suspended organic matter	Photosynthesis, zooplankton and suspended organic matter

2.1.3. ENVIRONMENTAL ASPECT

Coral reefs are among the most impressive ecosystems on the planet; they have rich biodiversity and high density of marine life, which gives them particular conservation interest (Ross 2007). Jensen and Fredriksen (1992) reported that biological diversity of *L.pertusa* reefs on the Faroe Shelf is as high as those in tropical areas. Generally, the diversity of species associated with *L.pertusa* reefs seems to be much higher than that of the surrounding sedimentary substrate (Freiward et al. 2004; Johsson 2006). Reefs provide a variety of niches for other organisms, within the coral matrix and dead coral fragments, but especially within the underlying sediment (Rogers 1999). Over 1300 species of invertebrates have been recorded during studies of several *Lophelia* reefs in the north-eastern Atlantic (Freiward et al. 2004). Mortensen and Fosså (2006) identified 361 species in 24 samples from *Lophelia* reefs off Norway. Reef communities have also been identified as important habitat for several commercially fished species. Recent investigations show high occurrence of tusk (*Brosme brosme*) redfish (*Sebastes* spp.), ling (*Molva molva)* and saithe (*Pollachius virens*) on the Norwegian *Lophelia* reefs (Husebø et al. 2002). Fish seem to be attracted to the reefs because of abundant hiding places, enhanced feeding possibilities (increased density of zooplankton) and superior nursery areas (Mortensen 2000).

Additionally, cold-water corals may serve as indicators of past climate because they are very long-lived; living cold-water reefs have grown up to 8,000 years old

(Hovland et al. 1998). Their banded skeletal structure and growth in concentric rings similar to tree-rings, make them good environmental archives by preserving information from past environmental conditions as ocean temperature and nutrient levels (Kerr 1998; Torok 2006). It is suggested that these data can enhance our current understanding of climate change. Cold-water corals may also be significant contributors to global calcium carbonate budget. Recent investigations suggest that they may account for at least 1% of global carbonate production (Lindberg and Mienert 2005a).

The high biodiversity associated with cold-water coral communities may provide numerous resources of natural products with enormous potential for developing pharmaceutical, nutritional supplements, enzymes, pesticides, cosmetics, and other commercial products (Bruckner 2002; Hourigan et al. 2007).

2.1.4. THREATS TO COLD WATER CORALS

Cold-water corals are slowly growing and fragile, which makes them vulnerable to human-induced impacts like fishing and oil and gas activities (Rogers 1999). *L.pertusa* is listed on the Norwegian Red List of Threatened Species in the endangered species category, which means *L.pertusa* is currently not threatened by extinction. However, it may become threatened in the near future (Oug and Mortensen 2006). *L.pertusa* is also listed under CITES (the Convention on International Trade in Endangered Species of Wild Fauna and Flora) Appendix II in January 18th 1990. The United Nations Environmental Programme recognized that this species are sensitive, especially to anthropogenic disturbance, and *Lophelia* species are considered to decline (CITES Appendix 1990).

The most widespread human threat to deep-sea coral communities is impact of fishing gear. The most destructive of all the fishing gears are bottom trawls because the forces on the seafloor are large and the area of seafloor contacted per haul is large (Hobday et al. 2006; Johansson 2006). Towed gear has long-lasting damaging effects on reefs, such as destroying patches of corals and flattening of the seafloor, leading to death of corals, and damaging or wiping out delicate species that live on reefs (Hall-Spencer 2002). Other bottom gear such as bottom longlines, gillnets, crab pots and lobster traps have also negative impacts (Gass 2002). Cold-water corals are sensitive to increased sedimentation, and even though a passing trawl may not physically damage them, the suspension of sediments in the water may hinder their

physiology (Jones 1992). Trawling damages are well documented on the continental shelves of Norway, Ireland, and Tasmania and in Alaskan waters (Fosså et al. 2000; Hall-Spencer 2002; Roberts 2002). Furthermore, Fosså et al. (2000) concluded that trawling had damaged 30-50% of the reefs on the Norwegian margin. Examples of trawling damages to coral reefs on the Norwegian margin are illustrated in figure 2.3.

Exploration and production of oil and gas has negatively affected corals in several ways. Potential threats from oil industry include the physical impact of drilling, placement of structures on the seafloor and intentional or accidental well discharges (WWF 2004). Of particular concern for *L.pertusa* has been the exposure to drill cuttings and suspended mud, because corals are suspension feeders and sensitive to the effects of sedimentation (Rogers 1990). Previous studies from Thompson et al. (1980) have shown direct mortality of tropical corals from effects of drill cutting. Other activities that have

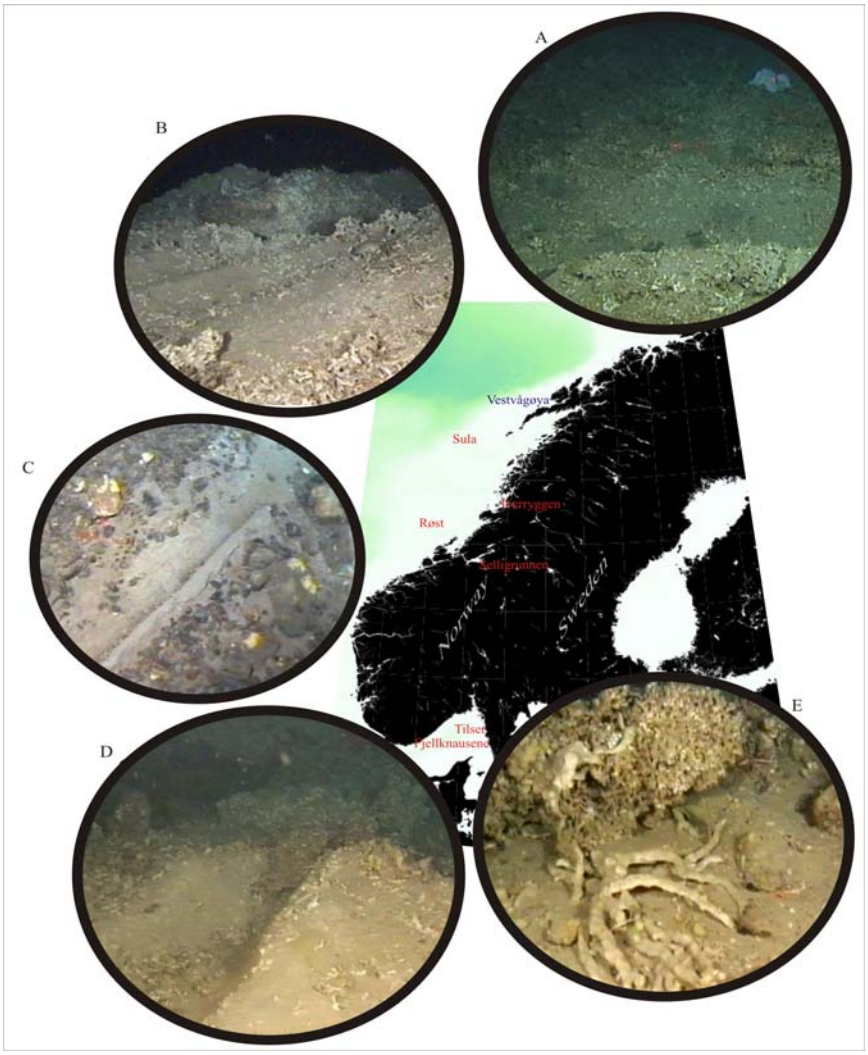

Figure 2.3. A Damaged coral reef near Vestvågøy (autumn 2008), **B** fragments and larger pieces of dead *L.pertusa* from a trawling ground near Iverryggen at the 190 m depth (17/05/99), **C** trawling scar in the seabed near Storegga at 220 m depth (16/05/98), **D** Fragments of dead *L.pertusa* from a trawling ground near Iverryggen at 190 m depth (17/05/99), and **E** dead *Lophelia* and gorgonians near Iverryggen (17/05/99). Pictures are from Havforskningsinstituttet and MAREANO-database. Protected coral reefs are marked with red colour.

negative effect on coral reefs are submarine cable or pipeline deployment (Brancato and Bowlby 2005) and seismic testing by using air guns in order to find hydrocarbon deposits (WWF 2004). Additional potential threats include discharges related to shipping activities and the disposal of waste onto the seabed in deep waters (Gass 2003).

Drastic water temperature change will influence physiology, calcification rates and biochemistry of cold water corals (Hobday et al. 2006). The Intergovernmental Panel on Climate Change (IPCC) 4th Assessment Report (IPCC 2007) concluded that the global ocean temperature has risen by 0.1 °C from the surface to a depth of 700 m since the industrial revolution; this is the depth where most cold-water corals are located. Moreover, coral reefs grow slowly and have developed long time in extremely stable environmental conditions and they are unlikely to be able to shift habitats with rapid climate change (Hobday et al. 2006). Another threat to corals is that of increased acidity of the oceans due to rising atmospheric CO_2 levels. The release of fossil fuel emissions to the atmosphere is changing seawater chemistry and the calcium carbonate saturation of the oceans (Guinotte et al. 2006). So as the atmospheric CO_2 levels increase, the depth of the aragonite saturation horizon will decrease. The pH of ocean surface has decreased 0.1 units since 1961 and will probably drop another 0.3 to 0.4 units by 2100 (Caldera and Wickett 2003). Experimental evidence has shown that the ability of deep-water corals to build skeletons will be impaired as the seawater becomes more acidic and they will grow slower (Raven et al. 2005; Guinotte et al. 2006).

2.2. PREVIOUS STUDIES IN FUGLØY REEFS AREA

The occurrence of high concentrations of coldwater corals (*Lophelia pertusa*) in the Fugløy area was first described by Hovland and Mortensen (1999). The Fugløy Reef was discovered accidentally by Statoil in the summer 1982, during a survey for a potential pipeline route from the Snøhvit gas field in the Barents Sea to the shore in the Lyngenfjord, northern Norway (Hovland and Risk 2003). The Fugløy Reef is named after the Fugløy island (in Norwegian “bird-island”), located southwest of the Fugløy island (70°14’N, 21°15’E). The reef was inspected by the use of a remotely operated vehicle (ROV). The ROV survey revealed structures consisting of large white bulbous forms of living coral colonies, known as *L.pertusa* (Linné). Additionally, the reef was

investigated by a single-beam, hull-mounted echosounder, and a towed instrument combining a side-scan sonar and, sub-bottom profiler (Hovland and Risk 2003). Reefs had also been recognised on single-channel airgun lines shot in 2002, when the reefs appear as cone-shaped, acoustically transparent features on seismic reflection data (Fosså et al. 2005). Because there were no plans to develop the Snøhvit field at that time, the Fugløy area did not have high priority and no additional studies were conducted by Statoil (Hovland et al. 2002).

Detailed studies of the Fugløy reefs were done later by Lindberg et al. (2005; 2007). Lindberg et al. (2007) made the first in-depth study of a cluster of cold-water reefs, by combining high-resolution seismic reflection data, side-scan sonar imagery, video-images, and oceanographic measurements in order to study the geological, geomorphologic and oceanographic settings in which reefs occur. Lindberg et al. (2007) reported that the reefs in Fugløy area consist mainly of *L.pertusa*. Together eight coral reefs were found and some of the reefs studied were among the highest *L.pertusa*-colonies along the Norwegian margin (Lindberg et al. 2007).

3. PHYSIOGRAPHIC AND GEOLOGIC SETTING

3.1. STUDY AREA

The study area is located on the continental shelf, off the coast of Troms County in northern Norway about 300 km north of the Arctic Circle (Fig. 3.1). It is approximately 20 km long and 18 km wide centred at 70°N and 20°E. The shelf bathymetry off northern Norway is generally dominated by several relatively small and well-defined banks separated by troughs (Nordby et al. 1999). The Fugløy Reef study area is located at the outlet of a fjord system incising the Norwegian mainland. The three large fjord systems are Ullsfjorden, Lyngenfjorden and Kvænangen; and they feed the wide and shallow south-western Barents Sea.

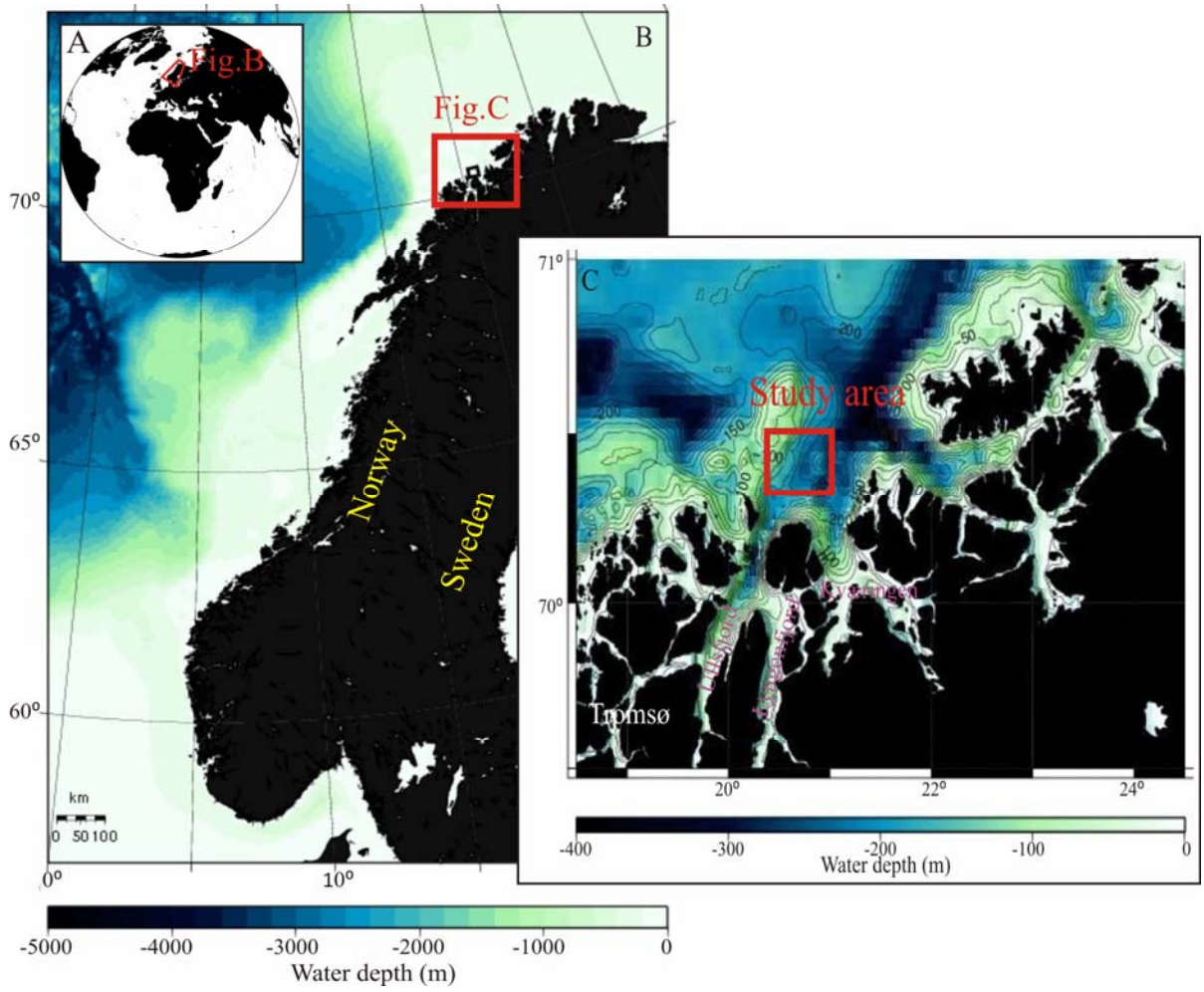

Figure 3.1. Maps showing location of study area **A** in global map, **B** overview map of the area, and **C** location of study area in northern Norway, contour interval is 10 m.

3.2. BEDROCK GEOLOGY

The geology in the northern part of Norway is characterized by the Precambrian basement. The Precambrian rocks were formed in the Achaean and Early Proterozoic, and were reshaped and deformed during several subsequent geological events (Ramberg et al. 2008). Precambrian rocks can be found about 25 km west from the study area on the island of Vanna (Fig. 3.2). The Caledonian rocks were pushed inn over the basement during Caledonian orogeny and consist mainly of long transported nappes (Andersen 1980). The nappes are divided into Lower, Middle, Upper and Uppermost Allochthons. The lineation pattern shows that nappes were transported in a south-easterly direction. The Uppermost Allochthon is represented in the Fugløy area and consists primarily of mica-schists. Those metasediments are dated to Cambrio-Silurian age (Sigmond 1992; Sollid and Nordgulen 2006). Sedimentary rocks of Mesozoic age occur about 20 km in the north of the study area. The boundary between crystalline and sedimentary rocks is indicated with a dashed line in figure 3.2.

3.3. GLACIAL HISTORY

Cyclic glaciations have taken place over a global scale because of a climatic variability that affected the Earth's atmospheric, oceanic and glacial systems during the Quaternary period. These glaciations and their associated formation of kilometres-thick ice sheets have had a large influence on the geomorphology on Scandinavia. The Fugløy area has repeatedly experienced glaciations (Andreassen et al. 2004). This section gives a general overview of the Last Glacial Maximum in the south-western Barents Sea and the advances and retreats of the glacial ice cap. Ice flow pattern along the coastal part of northern Norway and the extent of the ice sheet during Last Glacial Maximum (LGM) have been discussed widely (Vorren et al. 1986; Vorren et al. 1989; Landvik et al. 1998; Ottesen et al. 2008). In general, ice sheets were fed from the dispersal centre in northern Fennoscandia. The study area was traversed by ice flow from Ullsfjorden, Lyngenfjorden and Kvænangen (Fig. 3.2), which afterward converged with flow from Altafjorden and moved towards Fugløybanken. The ice flow continued further north–northeastwards into Ingøydjupet (Ottesen et al. 2008),

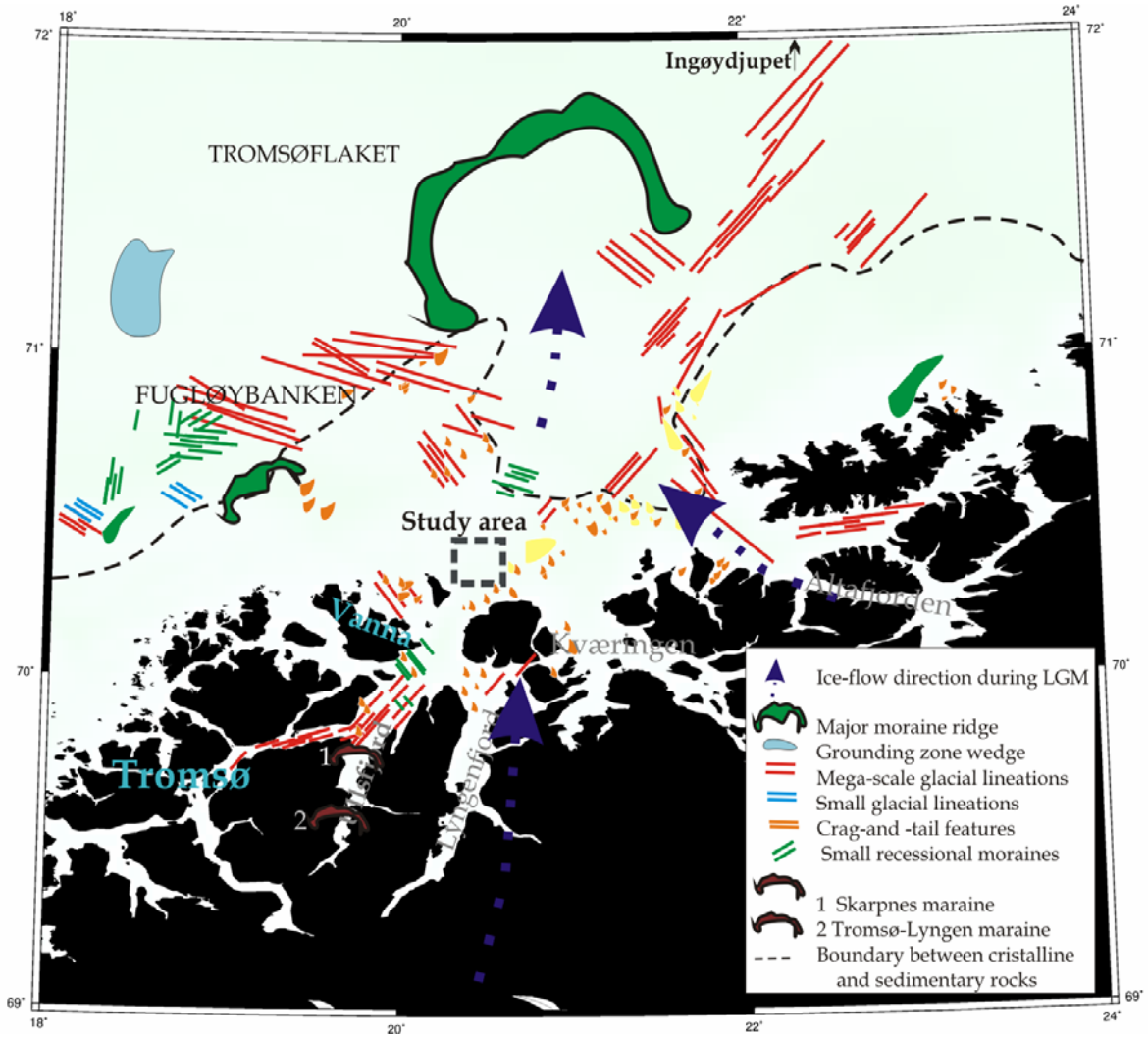

Figure 3.2. Geomorphological map of the study area showing the generalized distribution of glacial features on the continental shelf and fjord areas in northern Norway. Modified from Vorren and Kristoffersen 1986, Plassen and Vorren 2003 and Ottesen et al. 2008. Dark dashed line box showing study area.

where it met ice from the Barents Sea and converged towards the shelf edge (Landvik et al. 1998). Evidence of grounded ice is found approximately 70 km north of study area, on Fugløybanken (Fig. 3.2), where a large lobate moraine occurs. The moraine ridge has been described by Vorren and Kristoffersen (1986) and is dated to Late Weichselian age (13.3 ka). This suggests that the most recent ice flow over the study area was obviously directed towards the north. Moreover, during the Weichselian maximum, the ice sheet advanced more or less to the shelf edge covering the entire Barents Sea with ice (Landvik et al. 1998; Ramberg et al. 2008). Previous studies suggest that the LGM in the south-western Barents Sea took place in two phases: the first advance was until 22 ka, and the second after 19 ka (Landvik et al. 1998). The loading and moving of the ice sheets scoured sediments and transported glaciogenic

material beneath the ice-streams into the deep-sea and created big through mouth fan, such as the Bear Island Through Mouth Fan (BMF). The BMF is one of the world's largest depocentres about 215 000 km² (Vorren and Laberg 1997), and it has been estimated that during the last 0.8 Ma about 150 m of vertical erosion have been taken place in south-western Barents Sea (Vorren et al. 1990).

The ice recession from the LGM is characterized by several still-stands and smaller pauses that left behind recessional moraines. Vorren and Kristoffersen (1986) speculate that the south-western Barents Sea was deglaciated before 13.5 ka. Lindberg and Mienert (2005a) reported that there are several morainic highs in the Fugløy area that consist of diamictons, deposited approximately 12 ka ago. Nevertheless, no detailed studies have been done in Fugløy area, and it would require additional regional mapping to reconstruct the deglaciation history in this area. In order to estimate the approximate age when the Fugløy area became ice-free from last inland ice-sheet, one can use moraines or other deposits on land that could mark locations of the ice-front. Skarpnes moraine is located about 60 km south-west from Fugløy in Ullsfjorden (Fig. 3.2). In fact, this moraine represents Skarpnestrinnet in northern Norway, a significant glacial advance during the Older Dryas. The Skarpnes moraine is dated to about 12.2 ^{14}C ka BP (12.5-12.0 ka; Plassen and Vorren 2002). Thus, the Fugløy area lies outside of Skarpnes moraine, which means the Fugløy area was ice-free already by this time. More over, during the Younger Dryas the glacier re-advance continued, and deposited another well marked moraine called the Tromsø-Lyngen (Fig. 3.2; Plassen and Vorren 2002).

3.4. OCEANOGRAPHY

The shelf off northern Norwegian is influenced by two northward-flowing current systems; Norwegian Coastal Current (NCC) and the Norwegian Atlantic Current (NAC) (Nordby et al. 1999). These two water masses are characterized by relatively high salinity >34 ‰ and quite high temperature about +3° to +10°. The NAC enters the Norwegian Sea through the Faroe-Shetland Channel, and is containing Atlantic Water (AW). The NCC consists of Norwegian Coastal Water (NCW) and mixes with water masses from Skagerrak and low saline water from the Norwegian fjords. However, the NCC is somewhat fresher than the AW, and has a stronger seasonal temperature variation (Breen 1990).

Both the NAC and NCC are narrow, deep and strong, and are controlled by the bathymetry of the northern Norwegian shelf. NAC is topographically influenced north of the study area near Tromsøflaket (c. 71°30'N and 17°30'E) and continues along the Norwegian coast together with the NCC (Fig. 3.3). In the Barents Sea the, NAC current splits into two branches: the northern branch, which flows into the Hopen Trench and the southern branch follows along the coast eastwards towards Novaja Zemlya. In the northern part of the Barents Sea (Fig. 3.3), fresh and cold Arctic water flows from northeast to southwest. The warm Atlantic and cold Arctic water masses are separated by the Polar Front, which is characterized by strong temperature and salinity gradients (ICES 2007a).

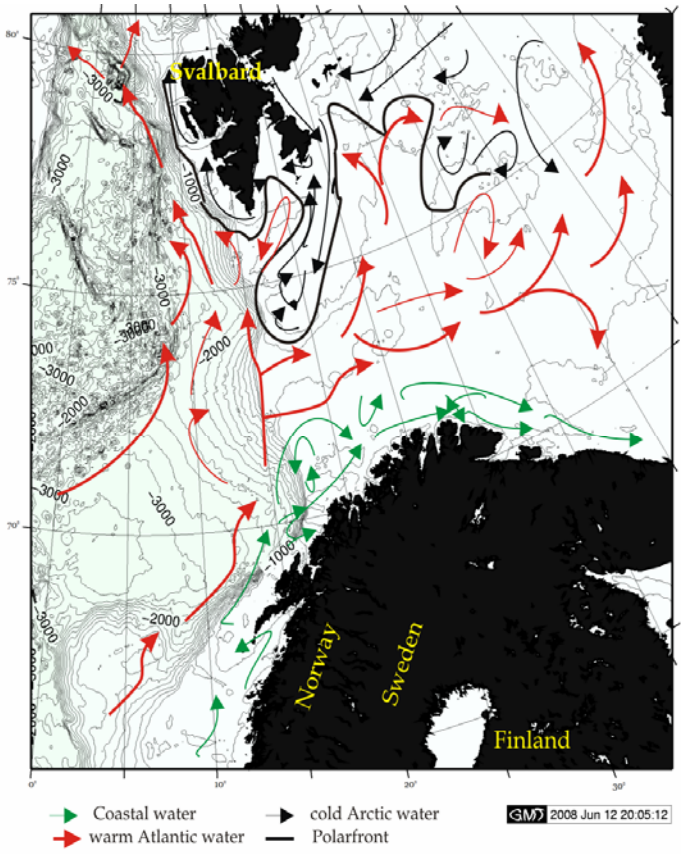

Figure 3.3. Current systems in the Norwegian and Barents Sea. Modified from Havforskiningsinstituttet (2008).

The current pattern along the banks off northern Norway is frequently a superposition of a shelf-edge current and mesoscale eddy fields (Orvik and Mork 1995). Several oceanographic studies along the coast of Norway have detected the formation of eddies, rings, and meanders. Sundby (1976) showed the presence of semi-permanent eddies over Tromsøflaket, whereas Eide (1979) reported an anticyclonic, topographically trapped vortex over Haltenbanken (Petersen et al. 2005).

The hydrographical regime in the northern fjords and sounds is generally controlled by tidal currents, which can reach velocities up to 168 cm/s in the Tromsøysund in Tromsø (Sætre 1972). Current measurements in March 2002 displayed a pronounced tidal signal in Fugløy area (Lindberg et al. 2007). The current direction is NNE - SSW, whereas the velocity varies through the water column. Lower velocities are typically close to the seabed (generally < 10 cm/s). The tides have higher

velocity and are warmer and more saline. Tidal waves have a period of 12 h 41 min and the tidal range 1.5 m (Lindberg et al. 2007).

The Barents Sea is characterized by large variability of temperature and salinity during the year (Ingvaldsen et al. 2008). The salinity and the temperature variations generally reflect the influence of the North Atlantic Oscillation (NAO) and are driven by the movement of AW into the Barents Sea and the ocean–atmosphere heat exchange (ICES 2007b). Nevertheless, the AW becomes colder and fresher with increasing latitude, as it mixes with colder and fresher NCW, and due to the decrease of solar irradiance at increasing latitudes. Temperature and salinity anomalies in Fugløy and Bear Island section are shown in figures 3.4. The water temperatures in this section have been relatively high during most of the 1990s (ICES 2007b). Figure 3.4b shows a continuous warming period from 1989 to 1995. During the years of 1996-1997, the temperature was just below the long-term average. At the end of the decade, the temperature started to increase again and it has stayed relatively high until the present. Surface salinity has also been rising in the recent years in Fugløy-Bear Island section (Fig. 3.4c). However, the salinity has continuously been rising since 1977 (ICES 2007a).

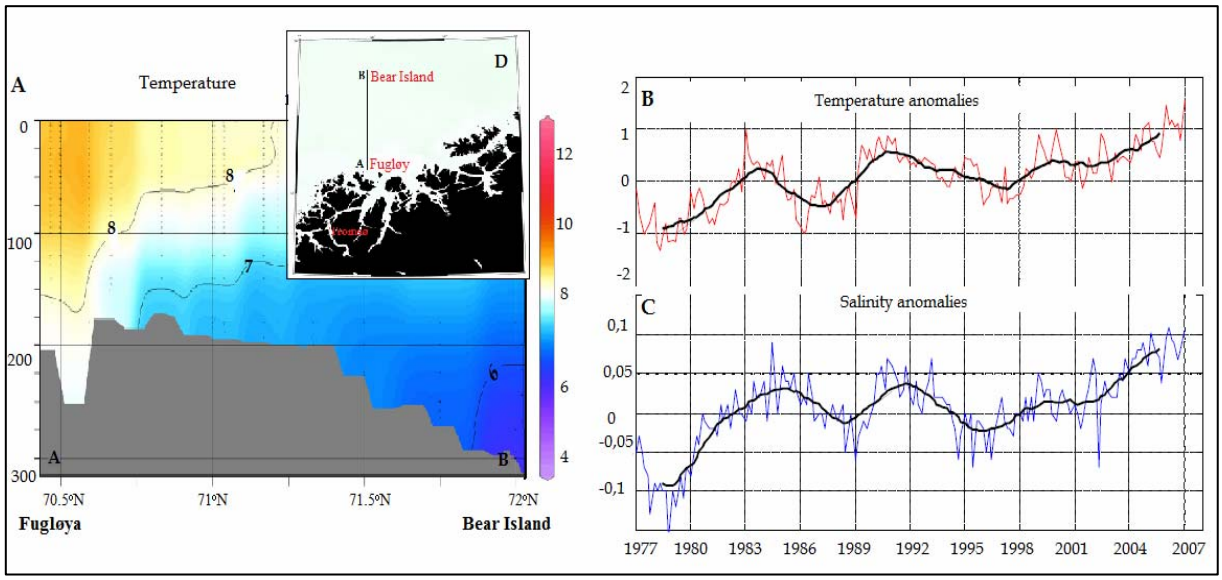

Figure 3.4. A Temperature change with depth and latitude between Fugløy and Bear Island section, from October to December in 1995 – 2004, based on data from ICES- Ocean Data View. Modified from Lunde,M.T (2006). **B** temperature & **C** salinity anomalies in the 50-200 m layer of the Fugløy-Bear Island section, and **D** location map of vertical profile in the Fugløy-Bear Island section. Modified from ICES Advice 2007 Book 3.

4. MATERIALS AND METHODS

4.1. MULTIBEAM BATHYMETRY AND BACKSCATTER DATA

4.1.1. DATA ACQUISITION

Mapping of the seafloor in the study area was carried out with a hull-mounted, motion-compensated Kongsberg Simrad EM300 system on R/V Jan Mayen (University of Tromsø). The first part of multibeam and backscatter data was collected in October 2007. Additional data from the northern part of the study area were acquired in March 2008. In total, c. 520 km of survey lines were collected during the two surveys, covering an area of approximately 20 x 18 km² (Fig. 4.1).

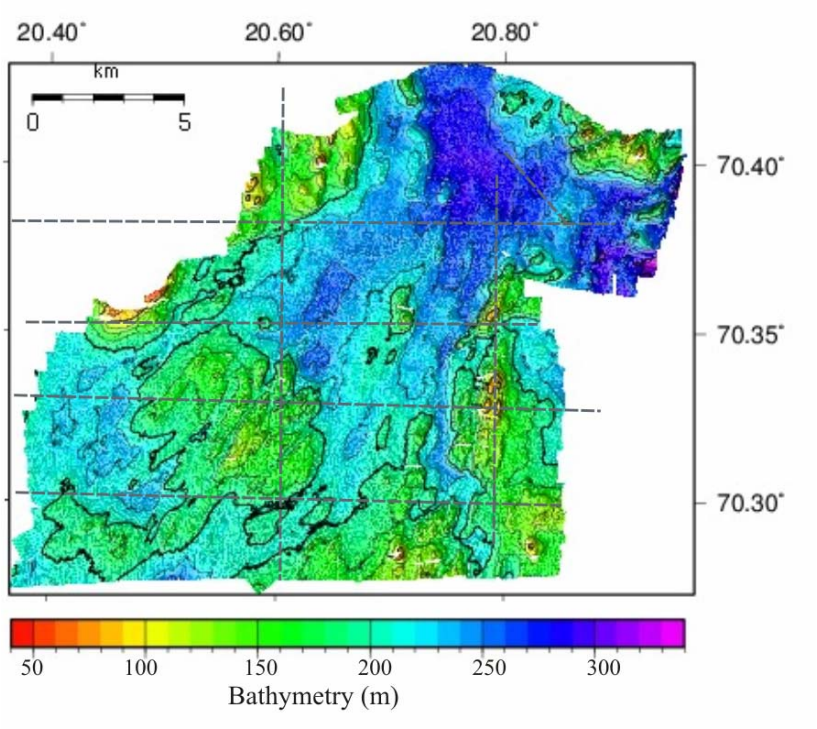

Figure 4.1. Bathymetric map of Fugløy and acquired seismic lines (showing with dark grey dashed lines).

The weather conditions were moderate during the data collection and the average ships speed was 4 - 5 knots.

The multibeam echo-sounder is designed for seabed mapping from 10 m to 5000 m depth; the optimal water depth is considered to be from 300 m and below (Kongsberg 2003). The EM300 system operates with 30-kHz multibeam sonar system with up to 135 electrically formed beams. The multibeam sonar transmits signals in a plane orthogonal to the direction of the ships movement, and the transmit beam is 1° in width. On the other hand, the receiver beams are 2°/cos (steering angle) wide athwart ships. The system can operate in either equal-angle or equal-distance mode. When

operating in the equal-distance mode, the system keeps the distance between beams equal when they hit the seabed. The equal-angle mode generates 135 1°x2° beams and is configured so that the angles between the beams are kept equal. Hence, the size of the area imaged by each beam gradually increases away from the nadir (Hughes-Clark et al. 1994). The basic principle of echo-sounding is that the transmitted beams bounce off the seafloor and are registered by the receiver. The time it takes for each beam to travel from the ship to the seafloor and back is recorded and converted to depth using a sound-velocity profile through water column.

The depth accuracy of the EM300 system is approximately 0.2% of water depth (Kongsberg 2003). The position of the depth measurements is determined using a DGPS receiver.

In order to get high quality bathymetric data, detailed sound speed information of the water column is essential. Water properties were measured using a standard Seabird SBE 9 CTD with a SBE 11+ deck unit. The sound velocity in water was calculated from measured conductivity and temperature versus depth (CTD). The sound-velocity profiles (SVP) data are fed directly into the Simrad EM300 processor for instantaneous raytracing calculations of the individual beams (Kongsberg 2003).

In addition to bathymetry, the EM300 system also records backscatter data. The backscatter strength is the intensity of the acoustic returns, and it corresponds to the relative amount of energy reflected back from the target. The backscatter strength is measured in decibels (dB) and it depends on the physical nature of the seafloor, the structure and the characteristics of the acoustic pulse (Fig. 4.2). However, received backscattered intensities need to be

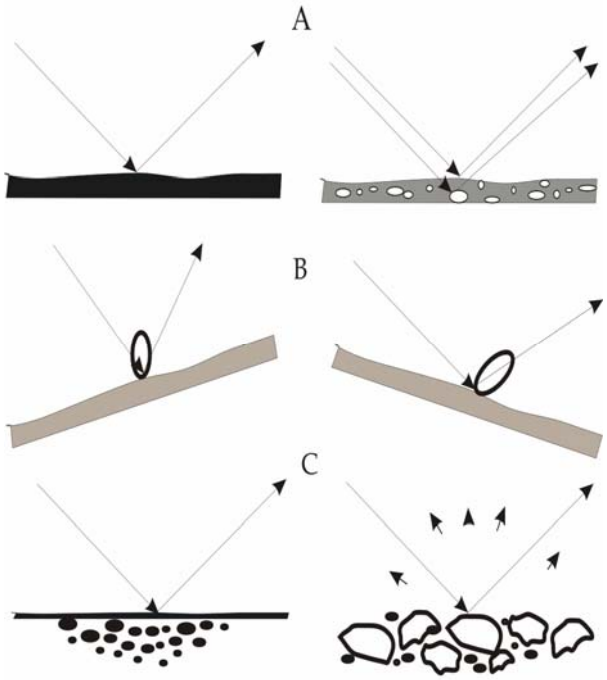

Figure 4.2. The backscatter strength from the seafloor is influenced by three factors: **A** properties of the seafloor, **B** local geometry of insonification and grazing angle. For the lower grazing angle data the difference in ray path between an ideal straight ray and the refracted ray path may be as much as 3 degrees (Hughes Clarke et al. 1996), and **C** roughness of the seafloor. Modified from Beyer 2006.

compensated for source power, grazing angle, bottom topography, receiver sensitivities, pulse characteristics, ensonified area, spherical spreading and attenuation (Hammerstad 1994). The corrected backscatter strength depends only on the sea bottom characteristics and is therefore useful for classifying the different substrate types (Lurton 2002; Christiansen 2006). For example, the pulse returning from the surface of soft sediments would have lower amplitude than a pulse reflected from a rocky surface, due to higher absorption and hence weaker reflection from the surface of the sediments as contrasted by the rocky surface (Fig. 4.2a).

4.1.2. PROCESSING OF BATHYMETRIC AND BACKSCATTER DATA

Kongsberg-Simrad Neptun software was used for post-processing of bathymetric data. Post-processing of bathymetric data consisted of the correction of erroneous position data and the elimination of erroneous depth measurements. Position and depth correction were applied line by line, whereas statistical data cleaning was done block by block. Moreover, raw data were also cleaned manually with the ping graphic editor to improve the accuracy on the depth data. Data were also adjusted for tidal variations (Kongsberg-Simrad 2000). Tidal correction was performed using water level measurements from the nearest tidal gauge located in Tromsø (69º39' N, 18º58'E; Norwegian Hydrographic Service). The tidal range was approximately one meter. The raw depth data had a good quality, only the outer beams had somewhat higher noise level.

After processing, the bathymetry data sets were exported from Neptun as a 3-column XYZ ASCII file (Easting, Northing, depth) with positive depth values based on a mean water datum. The XYZ bathymetry was gridded and examined in the interactive visualization system Fledermaus for geomorphic analysis. Several tests were done to create an optimal digital terrain model (DTM) from the multibeam data. The number of neighbouring soundings inside a given radius is important for surface modelling. By using a too small radius, remaining noise from processed data can not be reduced well enough. On the other hand by using a too large radius, it could smooth surface characteristics. Finally, a weighted-moving average gridding type was chosen with weight diameter set to 3 (Fledermaus- Reference manual 2007). The good density of measurement point allowed a grid cell size of 15 m x 15 m.

The cleaned datasets were also visualised using GMT (Generic Mapping Tools) for further geomorphic analysis. The data in GMT were gridded using near neighbour algorithm. GMT is a public suite of tools used to manipulate tabular, time-series, and gridded data sets, and to display these data in appropriate formats for data analysis (Wessel and Smith 2008). GMT was used to create different attribute maps such as slope map. A slope map provides a visual representation of the steepness of the terrain in the study area. The slope is calculated by determining the maximum slope value between an individual cell and its eight neighbours.

The backscatter data were post-processed using the Kongsberg-Simrad software suite Poseidon. Post-processing of backscatter data consists of the correction of variation in backscatter strength due to the beam angle. Data from beam angles higher than 67º were removed. Poseidon also offers histogram and contrast filters correction. Neither of these corrections was used, because several attempts failed to significantly improve the backscatter image (Kongsberg 2003).

After processing the bathymetry data sets were exported from Poseidon as a 3-column ASCII file (Easting, Northing, backscatter strength).

The same gridding procedure was applied to the backscatter data as previously described for bathymetric data, so that an integrated interpretation of sea-floor features could be conducted based on bathymetry and backscatter data.

4.1.3. VERTICAL AND HORIZONTAL RESOLUTION

An important issue in developing multibeam systems is vertical and horizontal resolution. Sheriff (1991) defines resolution as the ability to separate two features that are very close together; the minimum separation of two bodies before their individual identities are lost.

The horizontal resolution in multibeam sonar refers to the beam pattern and it is dependent first of all on the beam width along the two axes of the acoustic signal, secondly from bottom echo detection within the received beam footprint and finally from spatial sampling and positioning resolution. Thus, the area of ensonification of an acoustic beam is the area of a sphere ($\pi r_1 r_2$). The beam area for the vertical beams ($S1$) is a function of the water depth (H) and the beam angles in the along-track (φ) and cross-track (θ) orientations (Fig. 4.3), and can be calculated by following the equitation:

$$S1 = \pi H \tan(\varphi/2) \tan(\varphi/2) \quad \text{(Eq.4.1)}$$

The beam area out off the vertical (***S2***) is a function of the beam emission angle (***α***, from vertical) and the seabed grazing angle (***β***, from the seabed surface), approximated by:

$$S2 = \frac{\pi(H/\cos(\alpha,)) \tan(\varphi/2) \tan(\varphi/2)}{\sin(\beta)} \quad \text{(Eq.4.2)}$$

Both equations (Eq.4.1. and Eq.4.2.) show that the deeper the water or the more oblique the beam, the larger the ensonification area resulting in a lower spatial resolution. Furthermore, with increasing water depth, and increasing the footprint size, a fewer number of soundings will be received from a discrete-seafloor area (Rønhovde et al. 1999).

The vertical resolution of a multibeam echosounder is controlled by the length of pulse. That corresponds with bandwidth in the frequency domain. The EM300 system generally operates with one of two different pulse lengths: 2 and 10 ms. According to the relationship between frequency, velocity and wavelength (wavelength= velocity/frequency) one can calculate the vertical resolution (Badley 1985). These frequencies give a vertical resolution of approx. 1 m and 15 m (in water). The above mentioned factors control the depth estimate for the nadir beam, but the range of resolution for the oblique beams is much smaller than the physical beam footprint (O'Brien et al. 2005).

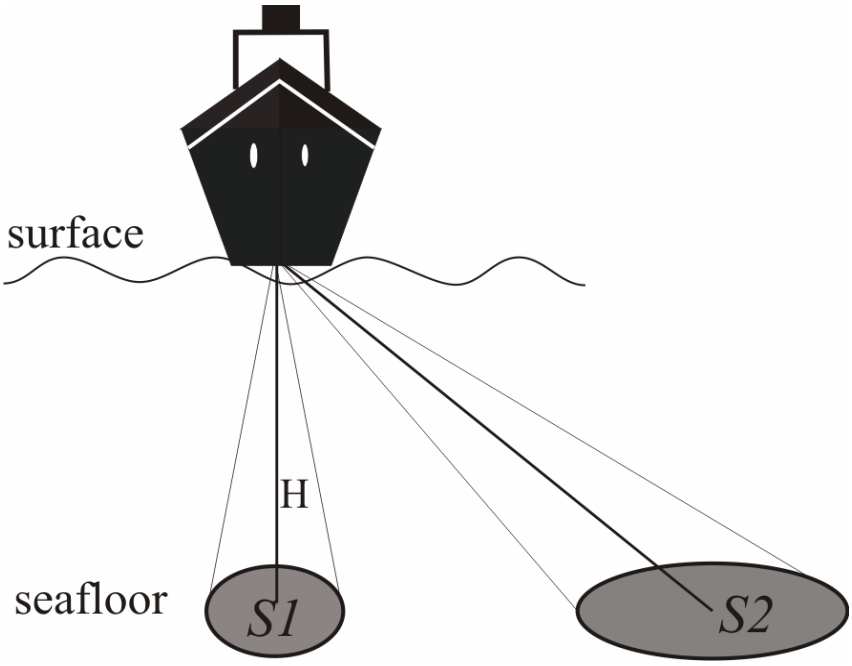

Figure 4.3. Schematic view of the area of ensonification from multibeam echo sounder. Modified from Mosher et al. 2006.

4.2. SUB-BOTTOM PROFILER SYSTEM (SBP)

4.2.1. SBP DATA

The sub-bottom profiler EdgeTech X-STAR system recoded data throughout both surveys. The EdgeTech X-STAR system can operate in up to 8,000 meters water depth and penetrate up to 80 meters in soft clay (EgdeTech 2005). X-STAR transmits a focused acoustic signal (an FM pulse) to the sea-bottom. Some of the energy is reflected by the bottom, and the remaining energy penetrates into the sediments. Each time the seismic signal meets a different material or a lithological boundary, a portion of the energy is reflected back, and the receiver records the reflected signal. Combining these reflections produces a cross-sectional image of the sub-bottom. A sub-bottom profiling system is used to obtain information about the sediments beneath the surface. In this study the EdgeTech X-STAR full spectrum digital sub-bottom profiler is primarily used to identify and investigate locations of coral reefs and pockmarks. The SBP data will also be used together with multibeam data for an integrated interpretation.

4.2.2. VERTICAL AND HORIZONTAL RESOLUTION

The horizontal resolution of the sub-bottom profile is given by the minimum value between the size of the first Fresnel zone and the resolution given by the beam pattern (Langli et al. 2004). The first Fresnel zone is defined as the surface whose points are separated by a phase difference that is less than $\lambda/4$ from the central point, or whose maximum total path length difference is $\lambda/2$ where λ is the acoustical wavelength (Langli et al. 2004). The size of the first Fresnel zone (Sf) can be written by following equation:

$$Sf = 2\sqrt{H\lambda/2 + \lambda^2/16} \approx 2\sqrt{H\lambda/2} \qquad \text{(Eq.4.3)}$$

While the size of the footprint can be calculated with:

$$Sb = 2H \tan(\varphi/2) \qquad \text{(Eq.4.4)}$$

Both equations (Eq.4.3. and Eq.4.4) show that the greater the water depth, the wider the beam, and the greater the number of potential returns arriving from different directions from the seafloor. In fact, for shallow water sites, the use of the narrower beam-width will then improve the horizontal resolution (Galway 2000). Also shooting

rate and vessel-speed influence the horizontal resolution, because the lower shooting rate and higher vessel speed increase trace distance (Fosså et al. 2004).

Typically SBP systems operate at frequencies between 2 and 16 kHz according to the relationship between frequency, velocity and wavelength one can calculate the vertical resolution for the SBP (Badley 1985). Taking a sound velocity in water of 1500 m/s and a frequency of SBP system of 3.5 kHz, it gives a vertical resolution less than one meter. Generally, higher frequencies provide higher resolution, but poorer penetration.

4.3. SEISMIC-REFLECTION DATA

Eight single-channel seismic profiles were acquired with R/V Jan Mayen (University of Tromsø) in 2002 (see location of seismic lines in figure 4.1). Two 40 cubic inch sleeve-guns were used as the source of the seismic survey, which provide a signal with typical frequencies between 40 and 200 Hz. The shooting interval was 10 seconds with a firing pressure of 130 - 140 bar, and the vessel had a speed of 3 to 5 kn. A single channel digital streamer with 11 hydrophones was used to receive the signal. The signals from each hydrophone are summed up to form the recorded seismic signal. The high resolution 2D seismic data were digitally recorded in SEG-Y format on hard disk using an Elics-Delph recording-processing unit on a Windows-based PC. The processing included bandbass frequency filtering, trace mixing and AGC-scaling (Lindberg et at. 2007).

5. RESULTS

5.1. GENERAL BATHYMETRY

The bathymetry data set analyzed in this study is shown in figure 5.1. The water depth ranges from 53 to 332 m. This chapter gives a general overview and presentation of morphological features; more detailed results are given in the subsequent sections. In general, the morphology of the investigated area consists of ridges and basins (Figs. 5.1 & 5.2a). The central part looks very irregular; the topographic high area consists of several ridges cut by northeast-southwest trending erosional channel-like features (Fig. 5.2b). On the top of these ridges we can observe several smaller cone-shaped features (Figs. 5.2b & c). A broad, low ridge extends across the eastern part of study area, and also here, some small cone-shaped features appear. The water depth increases to the northeast of the central ridge area and is deepest in the north-eastern edge of the study area. Here the water depth reaches down to 332 m, and the bathymetric low comprises of two relatively large basins (Fig. 5.1b). The first one is located straight NE of the central high, and the second one is located further NE. These basins are surrounded by ridges, with up to 150 m in relief. The seafloor in bathymetric lows is generally relatively smooth. However, several almost circular depressions can be observed there (Fig. 5.2d). The seafloor image also contains several white spots (Fig. 5.1), in those places data is missing because track lines did not overlap beams properly during surveying.

Using the seafloor grid, it is possible to create different attribute maps, which facilitate a better interpretation of features on the seafloor. Grid based attributes show variation between grid cells as azimuth, curvature or slope map. In order to illustrate this, a slope map was created (Fig. 5.3a). The slope map provides a visual representation of the steepness of the terrain in study area. Figure 5.3a illustrates that the steeper part or rougher terrains (having yellow colour) occur in the centre and around the edges of study area. The slope map could possibly be a good indicator of coral reefs because areas with high slope values are often associated with high relief.

A backscatter map analyzes the reflectivity of the seafloor. The Backscatter map (Fig. 5.3b) is a representation of the amount of acoustic energy that is scattered back to the receiver from the seafloor. The backscatter strength depends on the

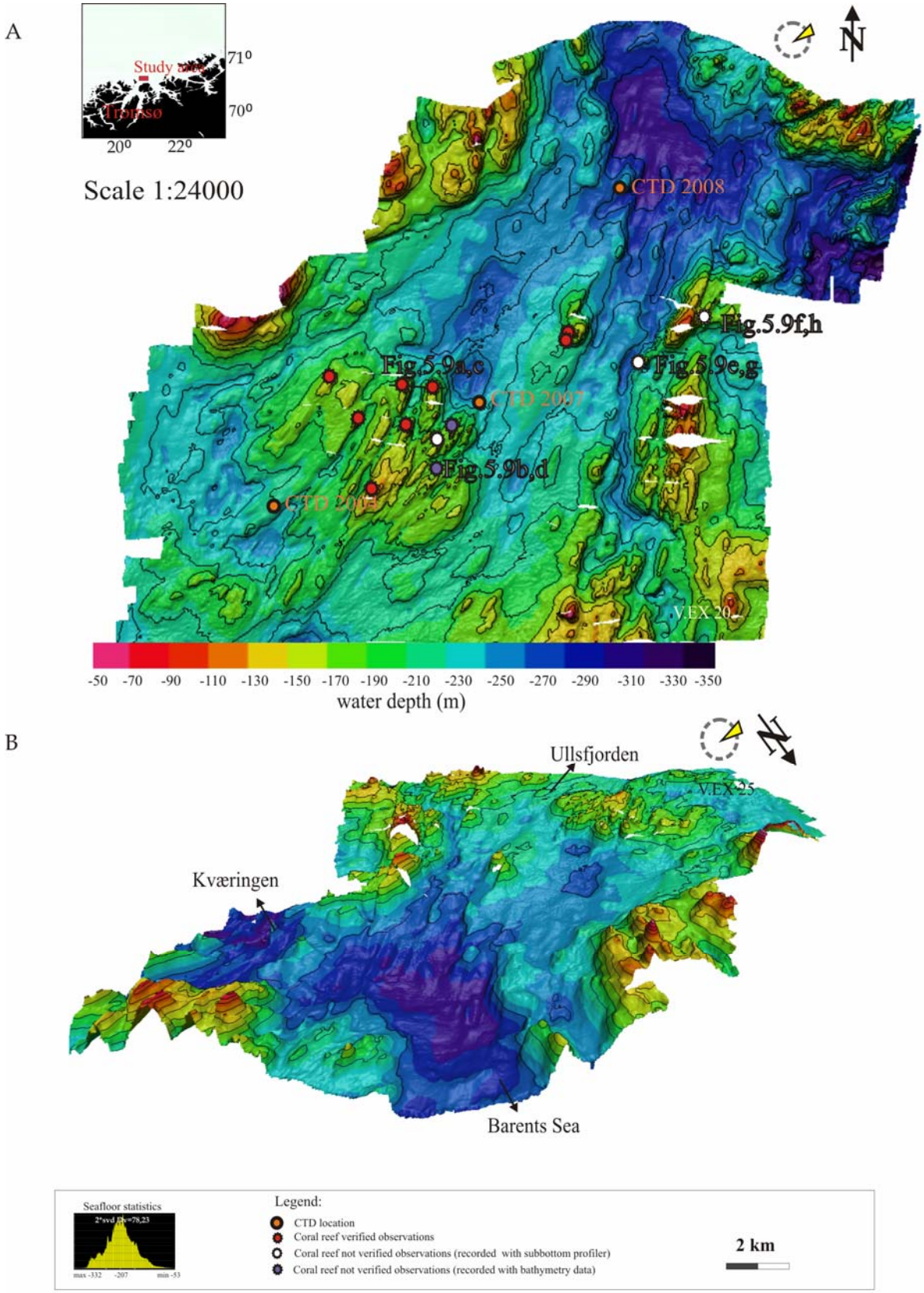

Figure 5.1. A and **B** 3D view of the multibeam bathymetry of the Fugløy Reefs area. Contour interval 20 m. Digital terrain models produced from multibeam bathymetric data, ordered arrays of depths for a number of sea-floor positions sampled at regularly spaced intervals. Yellow chart shows samples in range (-332 and -53 = -279 m): 1009724 (95%).

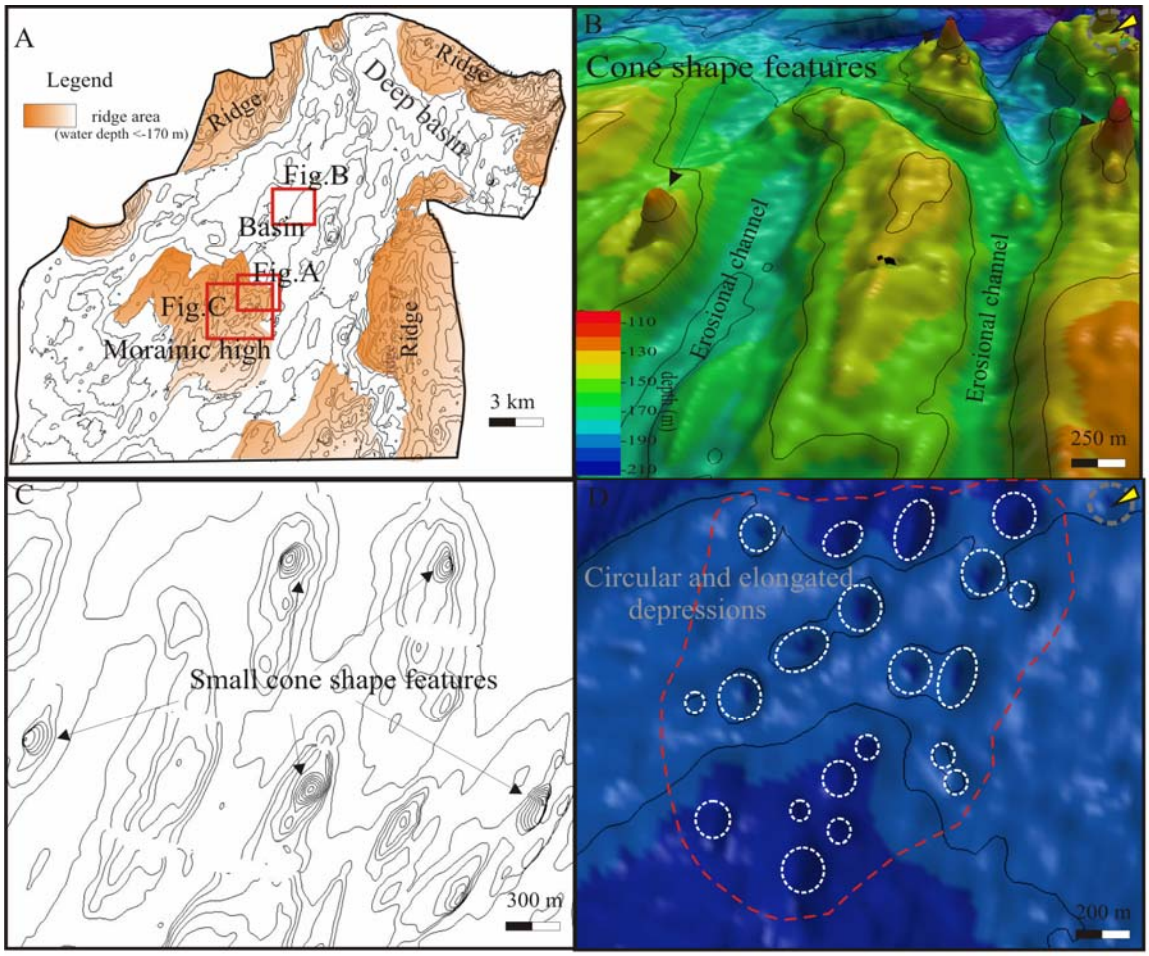

Figure 5.2. A Bathymetric map constructed by use of multibeam echosounder. Contour interval is 10 m between 50 and 160 m, and later on 20 m per interval. Interparetation of main ridges are coloured red, **B** 3D view of the central high and cutting channels, **C** detailed topographic map of the central part of the study area with 10 m isobaths. Note the appearance of cone shape features on morainic high, and **D** detailed interpretation of the area of circular and elongated depressions.

seafloor characteristic, and also on surface structure and sediment type such as grain size, porosity and density (Le Gonidec et al. 2003).

Low backscatter generally indicates lower energy conditions and finer grained sediments, for example backscatter values for fine-grained sand range between -40 and -60 dB (McMullen et al. 2007). High backscatter is usually associated with higher energy conditions and coarser grained sediments, such as gravelly surfaces. These typically have back-scatter values of -10 to -30 dB (McMullen et al. 2007). A backscatter image of the study area at Fugløy is given in figure 5.3b. The dominantly whitish and light-greyish areas indicate the presence of hard surface sediments and/or outcropping basement, covering about 64% of study area. Four areas show low backscatter (darker grey) and are interpreted as having smoother surface topography and soft surface sediments (Fig. 5.3c). These areas of low backscatter coincide with the

north-eastern basins that have been identified on the bathymetric data (Fig. 5.1). The backscatter image shows regularly spaced thick lines in east-west direction, which are related to acquisition artefacts.

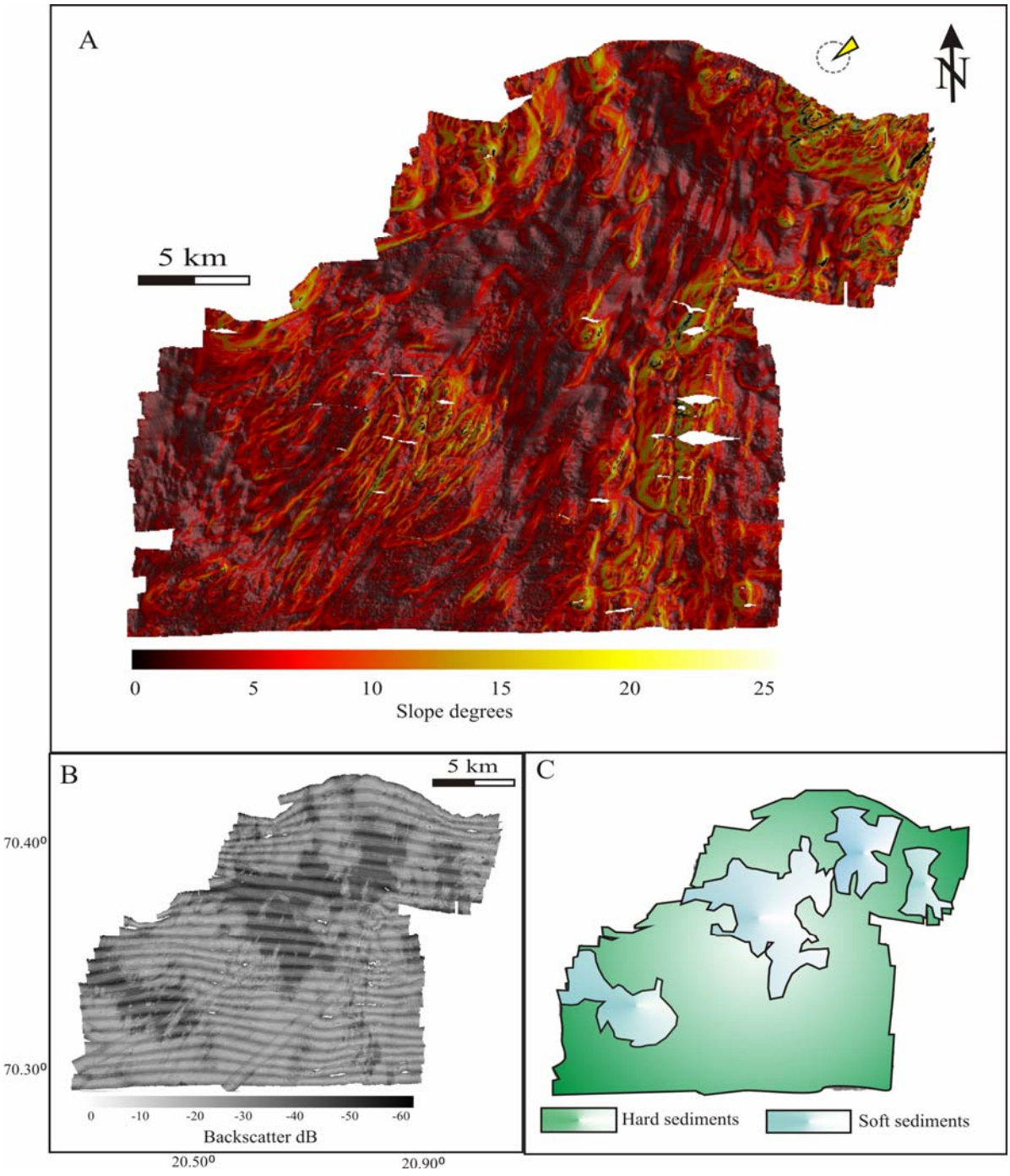

Figure 5.3. A Surface slope of the Fugløy Reefs area is overlain the multibeam bathymetry. Note that slope map is different than a shaded-relief map, in which topography is artificially illuminated from a specific direction and angle, **B** Backscatter map of study area. The backscatter varies from 0 (light) to -60 dB (dark), and **C** interpretation of soft and hard sediments area based on backscatter data.

5.2. CORAL REEFS

5.2.1. MULTIBEAM AND BACKSCATTER

Several elevated bathymetric features occur on the tops of moraine ridges in the central part of the study area. They in general appear to have cone- or dome-shaped forms and they appear as continues elongated ridges parallel to northeast-southwest trending channels (Figs 5.2b, c & 5.4.). The discovered features are interpreted to be coral reefs sitting atop topographic highs. This observation is in accordance with Hovland and Mortensen (1999) and Lindberg et al. (2005a & 2007) who reported the presence of

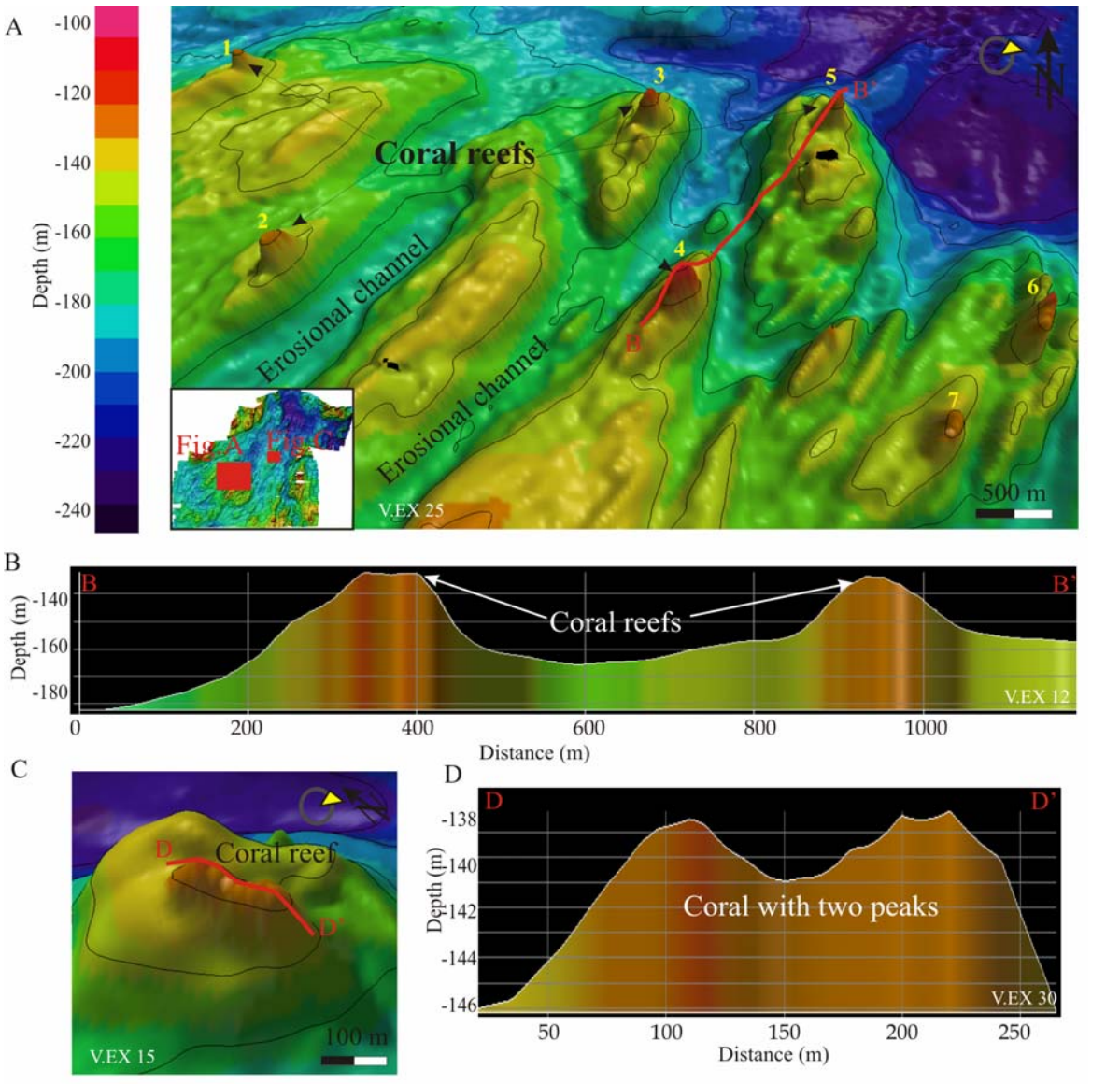

Figure 5.4. Occurrence of large, suspected coral reefs in the Fugløy: **A** 3D view of the spatial distribution of the coral reefs in the Fugløy. The morphology of dense located coral reefs varies locally and mostly follows the general seabed topography such as moraine ridges and contour channels, **B** a vertical profile through two coral reef, **C** 3D view of the coral reef with two peaks, and **D** vertical profile through double peak coral reef.

coral reefs on moraine ridges in Fugløy, based on observation from a remotely operated vehicle and side-scan sonar data. The present study shows the first multibeam data set acquired from this area and allows a more complete and integrated interpretation including existing backscatter and seismic data. Eight coral reefs could be identified on the central moraine ridges (Fig. 5.4a). Almost all reefs discovered here are located on the seaward side (the Barents Sea) of moraine ridges facing to a deeper basin, except for one reef that could be found on the fjord side. Characteristic of the latter reef is that it is approximately 50% smaller than the rest of the reefs. Two reefs were discovered 2 km northeast from the main ridge system (Fig. 5.4c). Additional two individual coral reefs were observed on moraine ridges in the eastern part of study area (for location see Fig. 5.1a).

The reefs coincide with a region of high backscatter, and *L.pertusa* reefs grow in the areas where surface sediments have been interpreted to form a hard bottom (Figs. 5.3b & c). However, on the backscatter image the reefs appear as sub-circular low backscatter patches, with backscatter strengths between -35 and -43 dB (Fig. 5.5a).

Furthermore, coral reefs are easily recognized on the slope map due to their very high slope angle (Fig. 5.5b).

The morphology of the reefs, their orientation and distribution are clearly revealed by the multibeam data, therefore it was possible to study the morphology of individual reefs in larger detail and make several statistical analyses. Together 12 coral reefs were mapped in the study area (Fig. 5.1) and the tabular summary of coral reef location, height and diameter is given in table 5.1. Only reefs 5 m or higher were interpreted as likely *L.pertusa* reefs in the study area, to be sure not to include mounds or smaller reefs of sponges and other organisms.

Mostly, reefs are orientated in SW-NE or NNE-SSW, the systematic change from these main directions is about 10°, and they are orientated similar to the moraine ridges and ridge cutting the erosional channels (Figs. 5.2b & 5.4a). The *L.pertusa* reefs longest and shortest axis was measured and it showed that the reefs are more or less elongated and that the longest axis was in SSW-NNE direction. Planar view of reef shape and orientation is sketched in Fig. 5.6b. With one exception, almost all coral reefs had one peak (Figs. 5.2c & d). This exception is a reef with a height of 10 m and it consists of two peaks. Both reef tops are over 4 m high (Fig. 5.2d). One-peak reefs mostly have a flat top, have a more or less cone shape, and are mainly symmetrical in a vertical profile (Figs. 5.4b & 5.6a).

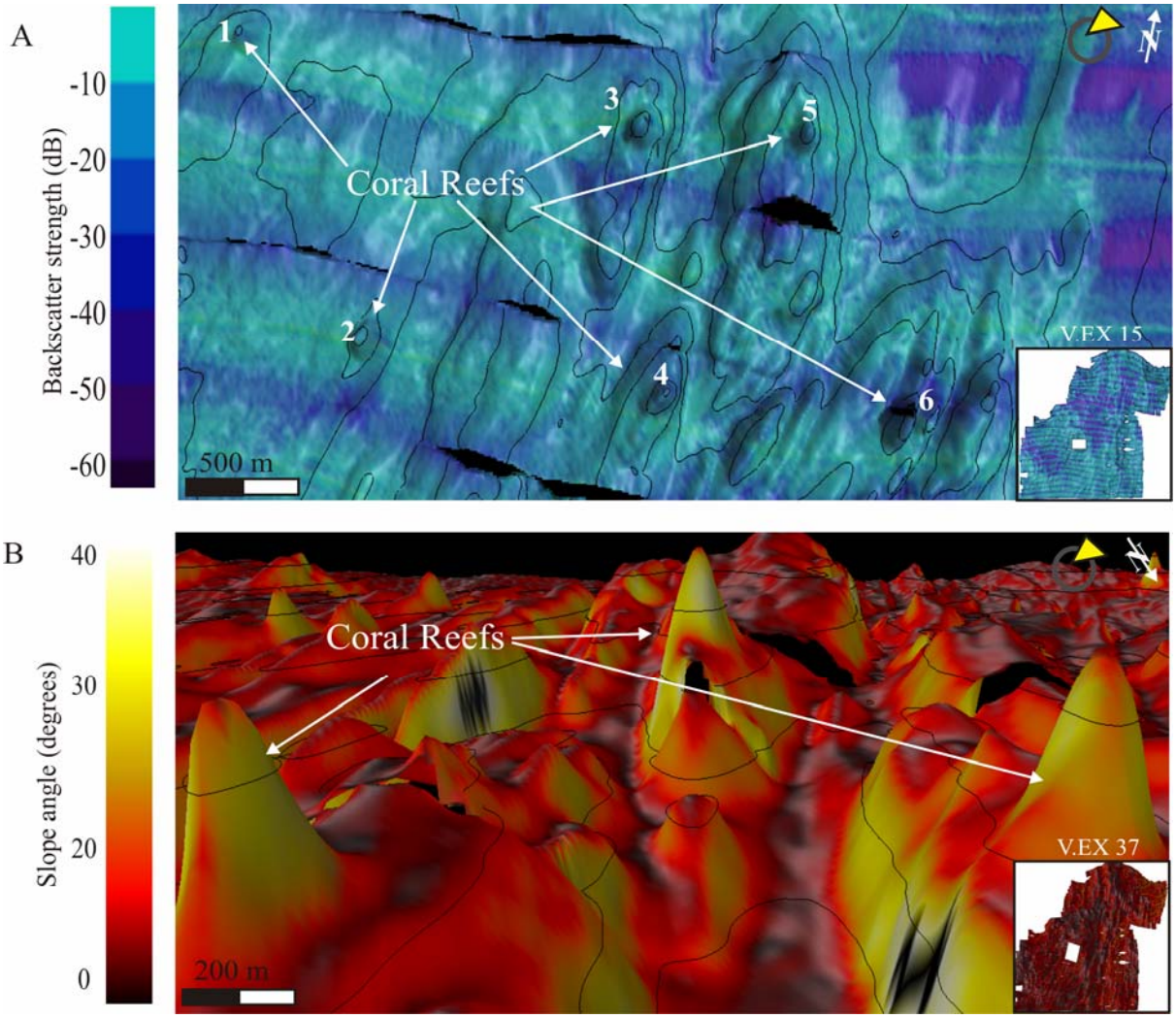

Figure 5.5. A 3D view of the multibeam bathymetry overlain with the color-coded backscatter data (20m isobaths), and **B** 3D view of the multibeam bathymetry overlain with the slope-map. Note coral reefs have a high slope angle value (from 20° to 35°).

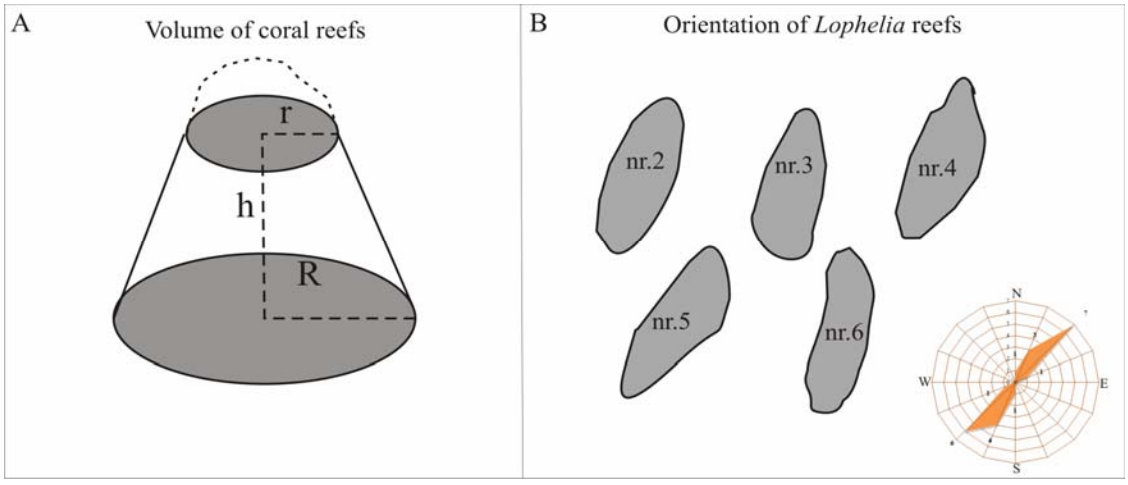

Figure 5.6. A The sketch of the coral reef volume, where h is height, R is radius of coral reef bases and r is radius of top of reef, and **B** planar view of the shape and orientation of coral reefs in Fugløy (not to real scale). Location given in figure 5.5a.

Table 5.1. Overview of location, depth to coral reef base, height and the longest axis diameter of discovered coral reefs in the Fugløy area. Method of discover include multibeam bathymetry data (MB), sub-bottom profiler (SBP) and seismic data.

L.pertusa reef nr.	Positions		Depth to base (m)	Height (m)	Longest axe (m)	Shortest axe (m)	Area (m^2)	Volume (m^3)	Source of discover
1	70°32.52'N	20°32.17'E	-148	11.5	102	78.2	24966	26903	MB
2	70°19.87'N	20°33.10'E	-158	21.5	178.5	103.4	57770	124293	MB
3	70°20.33'N	20°35.29'E	-152	24.3	163.8	109.3	56037	131872	MB. SBP
4	70°19.75'N	20°35.48'E	-145	27.1	202.9	102.8	49712	96143	MB. Seismic line69A
5	70°20.31'N	20°36.59'E	-150	20	154.5	126.7	80464	214089	MB. SBP
6	70°19.17'N	20°38.38'E	-153	20.5	241	88	66381	160965	MB
7	70°19.47'N	20°36.69'E	-150	16.7	183.2	83.5	47880	86356	MB. SBP. Seismic line67
8	70°18.93'N	20°36.41'E	-147	11.2	89	64.3	23265	26461	MB
9	70°18.57'N	20°33.55'E	-144	5.4	238	65.5	18246	9377	MB
10	70°21.20'N	20°42.78'E	-147	14.6	238	98	73004	119276	MB
11	70°20.78'N	20°45.80'E	-163	15.4	104.6	64.4	21084	32062	MB. SBP
12	70°21.45'N	20°48.34'E	-141	13.7	127.2	72	28665	39646	MB. SBP

Their axis ranged between 89.5 and 241 m in SW-NE direction, and between 64.3 and 126.7 m in NW-SE direction. The individual area of the 12 mapped reefs varies between 18246 and 80464 m^2, and the total area that the reefs cover is 508147 m^2, using an elliptic area formula. Eight reefs are closely located on a moraine ridge in the central part of the study area, where the average density has been calculated to 1.39 reefs per km^2. Coral reefs peaks have been identified in a water depth interval between 115 and 149 m (Fig. 5.7a).

The height of reefs was estimated from the bathymetric map. The base of coral reefs is characterized with a raped decrease of slope angle and this change was easily recognized on the respective attribute map (Fig. 5.5b). The average height of the reefs is 16.84 m with standard deviation (StDev) of 6.15 m (Fig. 5.7b). In fact, the highest reef crest is 27.1 m higher than the adjacent seafloor. There was a significant positive correlation between coral reef height and longest axis diameter. This means that higher reefs have also longer diameter. The linear regression analysis showed that a relationship between coral reefs height and diameter follows the equation (Fig. 5.7c):

$$\boldsymbol{Height = 5.16 + 0.08 \times d1} \qquad \text{(Eq.5.1)}$$

In equation 5.1. ***d1*** is the longest axis diameter in meters. The calculated diameter to height ratios fell between 3:1 and 7:1. The reefs have sides with slope angles of 10 to 36°. The average slope was approx. 15° (StDev.6.8) and there is a good correlation between slope angle and the height and size of coral reefs (R=71%). The steepest slopes at the reefs were mostly on the western and the north-western side.

In order to obtain the best fitting estimate for the volume of coral reefs one needs to find the best fitting model. As mentioned earlier coral reefs are cone-shaped with a flat top. Therefore, one could use the formula of a frustum of a right circular cone (Eq.5.2) to calculate the reef volume (table 5.1). A frustum of a right circular cone is that part of a right circular cone between the base of the cone and a plane which intersects the cone parallel to the base (Fig. 5.6a). The formula for this geometric body is:

$$V = \pi(R^2+rR+r^2)h/3 \qquad \text{(Eq.5.2)}$$

Where ***R*** is the radius of the reef's base and ***r*** is radius of the top in meters. An average coral reef in Fugløy has a volume of 8.89×10^4 m³ (for average R= 61.6 m, r = 56.16 m and h = 16.84 m) and the total volume for 12 coral reefs is 1.06×10^5 m³.

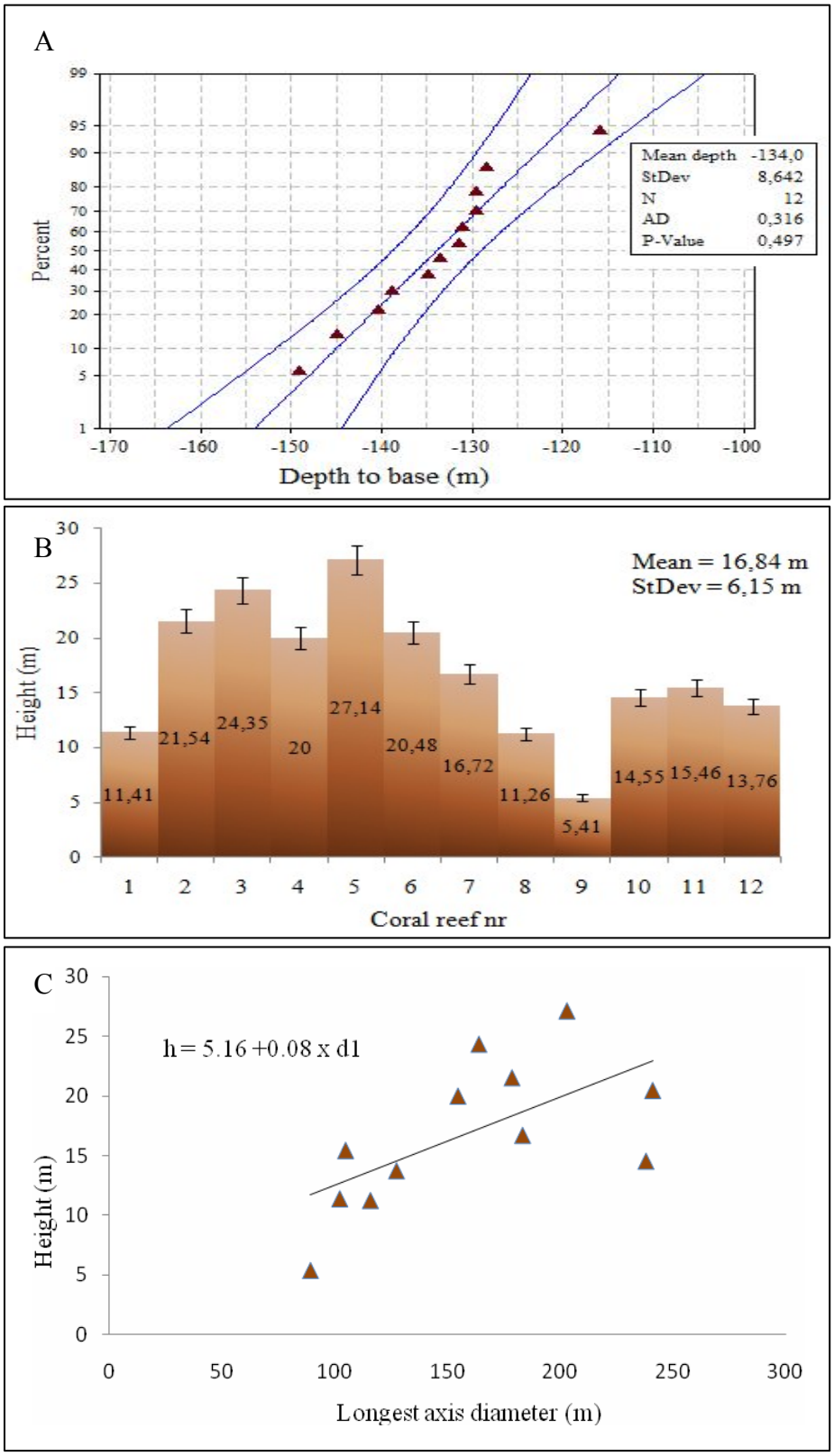

Figure 5.7. A Probability plot of coral reefs peak depth, **B** histogram of coral reefs height versus coral reefs in Fugløy area, and **C** fitted line plot between reef height and longest axis diameter in NW-SE (correlation was 56%).

5.2.2. SEISMIC DATA

The ability to identify coral reefs with seismic data depends on the size of the reefs and the acquisition parameters of the seismic system. Two seismic profiles cross the coral reef area (Figs. 4.1 & 5.8b). Coincidentally both lines were crossing a coral reef, whereby seismic line 69A was running directly over a large reef, and seismic line 67 just touches the north-eastern corner of a smaller reef. In both cases, coral reef appears as cone-shaped, acoustically semi-transparent features on the sleeve-gun seismic data (Figs. 5.8c & e). The seismic signature shows no abrupt internal variations of seismic impedance. The subsurface the coral reefs are situated on, have a chaotic seismic pattern. The intensity of reflection strength from coral reefs is lower than the surrounding seafloor, part of the energy has been scattered probably due to the rough and steep morphologic expression of these features. To calculate the height of a coral reef, the speed of sound was taken a bit higher (1600m/s) than in salt water, because the coral skeleton consists of aragonite with a density of 2.94 g/cm². This means that the reef in Fig. 5.8c is about 26.5 m high.

A large number of sub-bottom profiles crossed coral reefs. Examples of sub-bottom profiles and some interpretations are shown in Figs. 5.9. Line 6 (Fig. 5.9a) images two coral reefs and a NNW-SSE striking erosional channel between them. The coral reefs seem to have a flat top, and a ‘cauliflower’ or dome shaped morphology in the vertical section. SBP data of coral reefs shows weak acoustical reflections, while the seafloor beneath and adjacent to the reefs reveal strong reflection amplitudes (Fig. 5.9). The intensity of reflections from coral reefs is lower than the surrounding seafloor sediments and only the surface reflects the acoustic pulse. The indubitable identification of coral reefs on the SBP data corroborates the interpretation of these features on the bathymetric data (Figs. 5.9c, d, g & h).

The height of coral reefs was estimated from the bathymetric data, but for five reefs the SBP was running directly across the reef. This allowed determining the base of the coral reef with better confidence, and therefore, probably gives a better estimate.

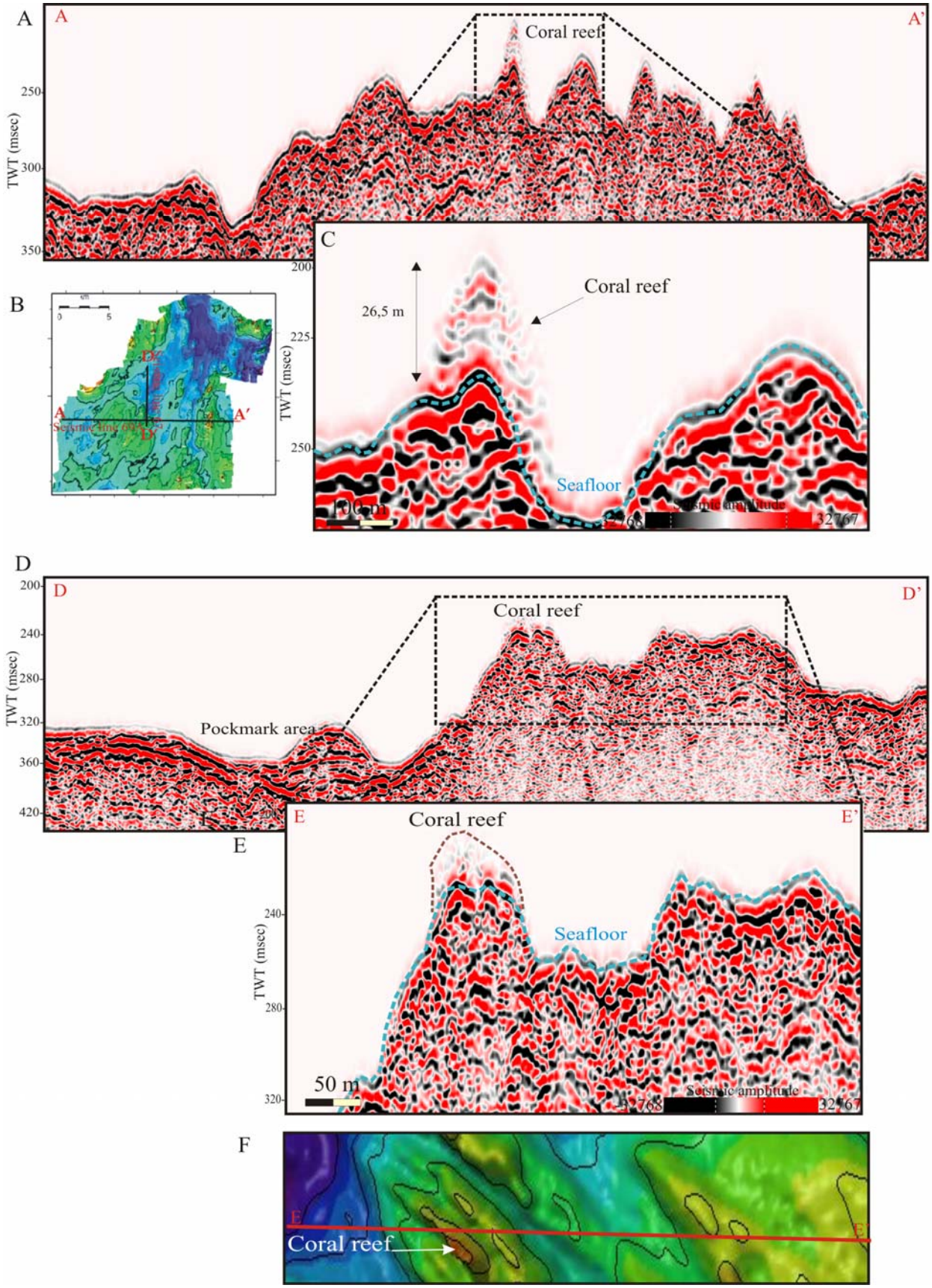

Figure 5.8. A Seismic line 69A over a large reef, **B** location map, **C** enlarged seismic section of coral reef. The seafloor is marked with the light blue dashed line, **D** seismic line 67 crossing a large reef, **E** enlarged seismic section of coral reef, and **F** showing the respective bathymetry (20 m contour interval).

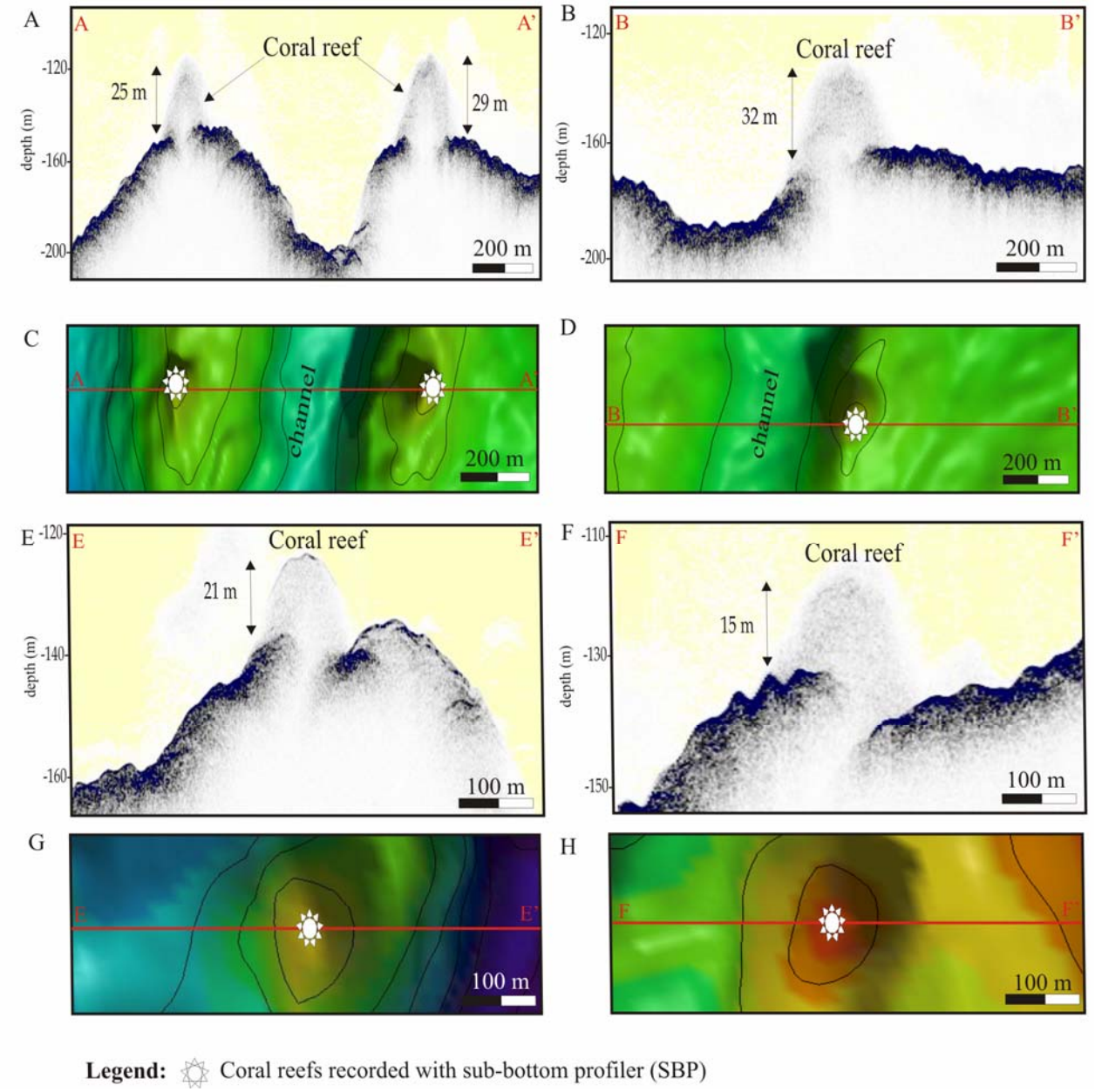

Figure 5.9. A Sub-bottom profile record (Line 6/2007) across cold-water coral reefs in the study area, **B** sub-bottom profile record (Line 7/2007) across coral reef. **C** & **D** maps showing the respective bathymetry (20 m contour interval), **E** sub-bottom profile record (Line 1/2008) across cold-water coral reef, **F** sub-bottom profile record (Line 2/2007) across cold-water coral reef, **G** & **H** maps showing the respective bathymetry (20 m contour interval). Location of profiles is shown in figure 5.1a.

5.3. THE OCEANOGRAPHIC CONDITIONS AROUND FUGLØY CORAL REEFS AREA

Figures 5.10 and 5.11 show temperature and salinity profile in Fugløy derived from CTD casts performed in October 2004, October 2007 and March 2008, representatively (for the location of the CTD stations see Fig. 5.1a).

5.3.1. TEMPERATURE

The temperature profiles for the autumn in 2004 and 2007 were relatively similar close to 8 °C in upper 110 m (Fig. 5.10). Below the surface layer the water temperature degreases approx. 0.03 °C per m. The CTD measurements taken in the spring 2008 shows a different temperature pattern. The surface temperature is characterized by a cold water temperature at 4.75 °C. It increases gradually to 6.09 °C at 250 m. The sea surface temperatures differed more than 3 °C from the March and October measurements, respectively. This is most probably the result of seasonal differences, i.e. that the temperature profile in spring 2008 is characteristic by winter cooled water and thus colder water.

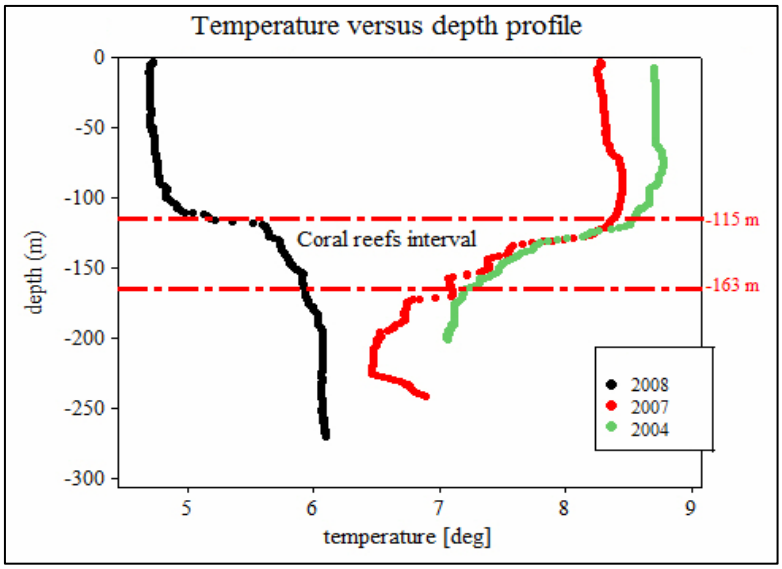

Figure 5.10. Temperature/depth profiles from the three CDT measurements conducted in October 2004, October 2007 and March 2008.

L.pertusa reefs in Fugløy are located at depth between 115 and 163 m, with a mean depth of 143 m. In figure 5.10 two red lines are marking the coral reefs interval and show that corals occur in a temperature range from 5.2 to 8.5 °C. Thus, the CTD data indicate that coral reefs are located at a water depth with quite significant temperature changes. However, the largest reef crest (measured coral reef height 27.1 m) is located at the most shallow depth and seems to have the largest temperature variations.

5.3.2. SALINITY

The salinity plot (Fig. 5.11) shows that the surface water has quite strong seasonal fluctuations. The salinities generally increase with water depth. The lowest surface salinities between 34.0 and 34.2 psu were measured in autumn, where salinity increased steadily through the water column and gave bottom water salinity about 34.9 psu. The salinity depth plot (Fig. 5.11) indicates a halocline, at around 115 to 150 m water depth. In this interval salinity increases more than 0.3 psu, respectively.

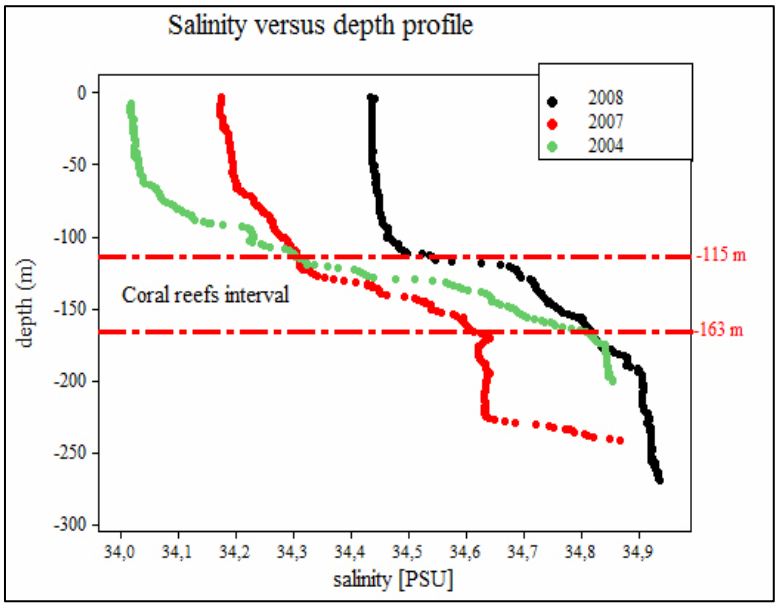

Figure 5.11. Salinity/depth profiles from the three CTD measurements conducted in October 2004, October 2007 and March 2008.

The coral reef interval is marked (red lines) in the salinity plot (Fig. 5.11). It shows that the salinity at a shallower level around coral reefs lies at 34.82 psu and at the deeper level it is at 34.52 psu (an average 34.67 psu). However, the salinity data shows small seasonal variations, approx. 0.2 psu in the *L.pertusa* reef interval.

The plot of the potential temperature versus salinity (Fig. 5.12) allows distinguishing between different water masses. A description of different water masses identified here is given by Petersen et al. (2005). As expected, the two main water masses are identified: Norwegian Coastal Water (NCW) and Atlantic Water (AW). NCW is originating from the NCC (Norwegian Coastal Current) and is commonly recognized by low salinity and lower temperatures ($S < 35$ psu; $4 < T > 12$ °C). AW is originating from the NAC, and contains warmer water and increased salinity ($S > 34.5$ psu; $5 < T > 10$ °C; Nordby et al. 1999).

An additional water mass was identified at the CTD2008 location at Fugløy (Fig. 5.1). This water mass is characterized by salinities between 34 and 34.5 psu and

temperatures in the range 4 and 4.8 °C, slightly colder than the NCW and the AW. Pedersen et al. (2005) classified this water mass as Norwegian Deep Fjord Water (NDFW).

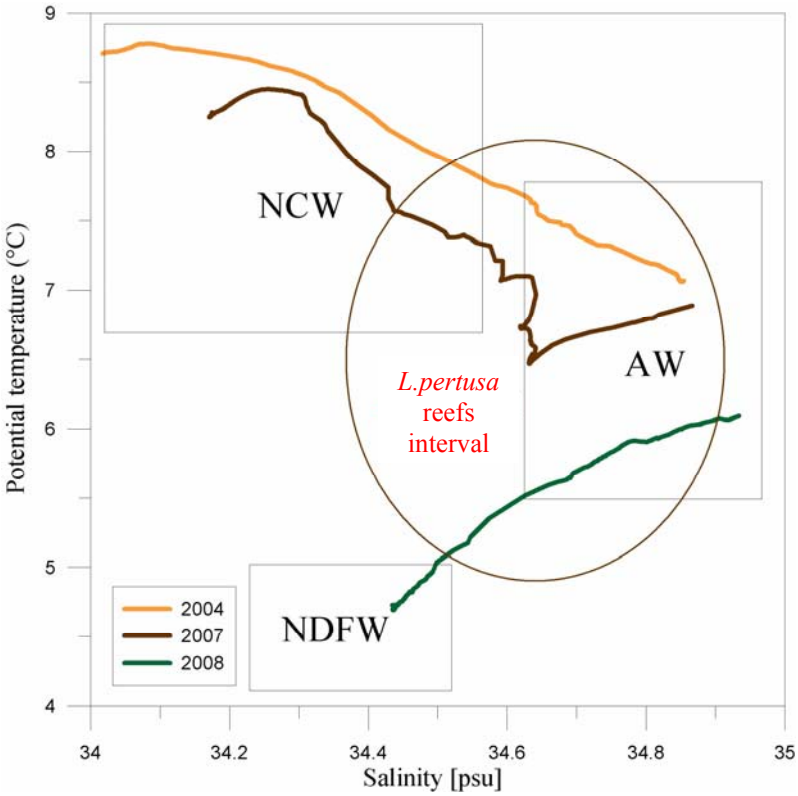

Figure 5.12. Temperature-salinity-diagram for data collected in 2004, 2007 and 2008. The upper left box indicates typical coastal water masses (NCW) being fresh and cold, the right box indicates typical Atlantic water masses (AW) being warm and saline. Norwegian Deep Fjord Water (NDFW) was recognized at CTD2008 location (Pedersen et al. 2005). Coral reefs interval marked with brawn circle. *L.pertusa* reefs interval is drawn with circle.

5.3.3. DENSITY

The contour plot of density versus temperature and salinity for autumn 2004 and 2007 is illustrated in figure 5.13. The density anomaly or sigma/theta is calculated with the following equation:

$$\sigma(s,t,p) = \rho(s,t,p) - 1000\ kg/m^3 \qquad \text{(Eq.5.3)}$$

where *s* is salinity, *t* potential temperature and *p* pressure. The plot shows that the density decreases with increasing temperature and increases with increasing salinity. We can observe that coral reefs occur within the density envelope of sigma-theta from 26.99 to 27.14 kg/m³. The bottoms of coral reefs are normally located at a higher density interval. The maximum recorded value at the bottom was 27.41 kg/m³. Difference between the spring and autumn measurements was about 0.25 kg/m³.

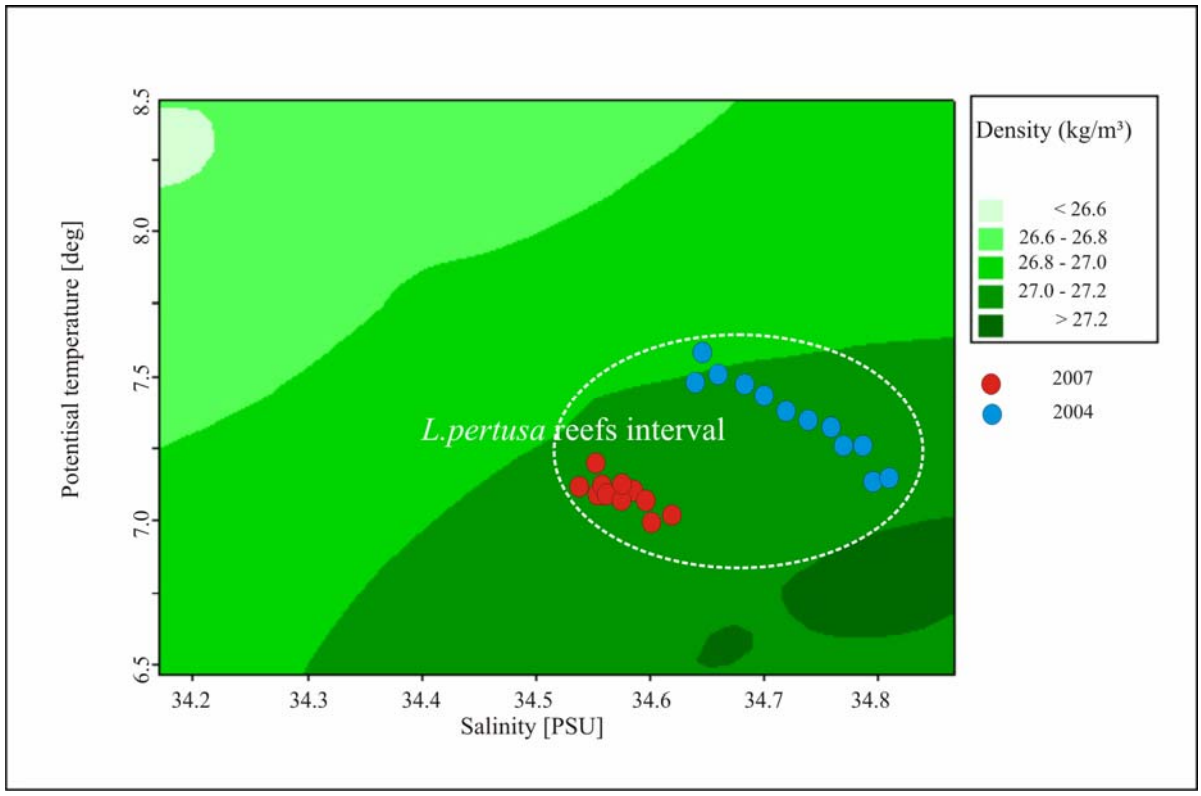

Figure 5.13. Temperature–salinity (T-S) diagram of CTD data collected in Fugløy area in October 2007 and 2004. The red dots indicate the location of the reefs. Density anomaly or sigma/theta is calculated with σ (*s,t,p*) = ρ (*s,t,p*) - 1000 kg/m^3, where *s* =salinity, *t* =potential temperature and *p* = pressure.

5.4. POCKMARKS

5.4.1. MULTIBEAM AND BACKSCATTER

The bathymetric data reveal numerous almost circular depressions in the sediment basin in the central part of study area, where the water depth is greater than 200 m (Figs. 5.2d & 5.14.). The same features were observed by Lindberg et al. (2007) based on high-resolution side-scan sonar data. He interpreted these features as pockmarks. The term pockmark was first used by King and MacLean (1970) to describe craterlike depressions on the muddy seafloor on the shelf of Nova Scotia, Canada. They suggested that the pockmarks were formed by escaping gas and porewater. In the sedimentary basin of this study pockmarks occur packed densely together, in other places pockmarks are more scattered. In one place pockmarks are linearly aligned (Fig. 14a). Figure 5.14b is a vertical profile over those linearly aligned pockmarks. The line direction is from NE to SW, and all pockmarks are deeper than 1.5 m. The high-density occurrence of pockmarks covers an area of approximately 1.2 x 1.8 km (Fig. 5.14b). This area contains 49 pockmarks, which results in a density of about 22.7 pockmarks per km².

As shown in figure 5.3b the pockmark area is associated with a region of low backscatter strength. Pockmarks occur in the areas where the surface sediments have been interpreted to be soft (Fig. 5.3c). It is difficult to distinguish pockmarks from surrounding sediments on backscatter data, but at some places pockmarks appear as indistinct circular targets with backscatter strength between -37 and -45 dB.

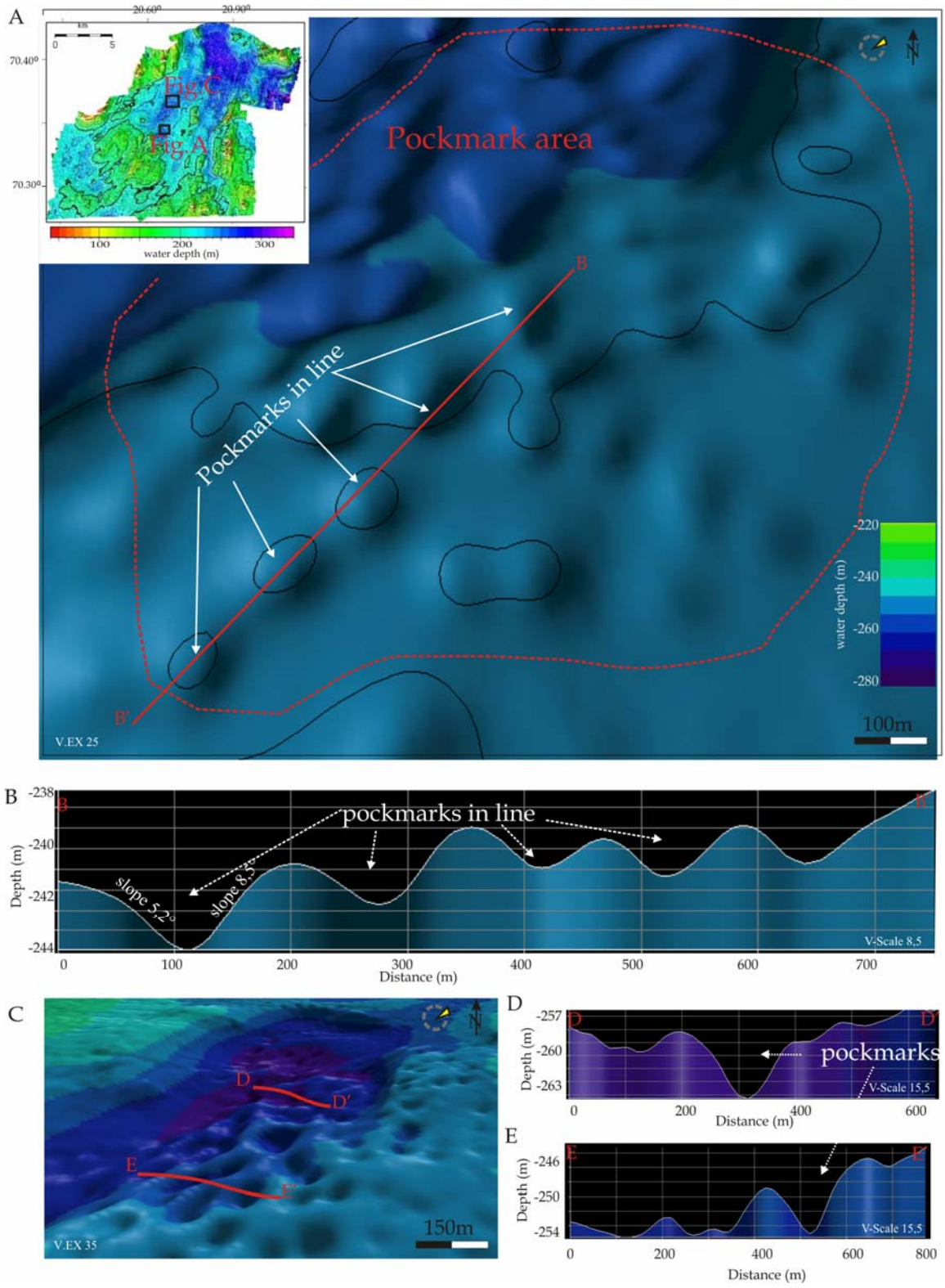

Figure 5.14. A 3D view of pockmark area. High density pockmark area is located in postglacial sedimentary basin, **B** vertical profiles through 5 pockmarks in line, **C** 3D view of the pockmarks, **D** and **E** vertical profiles through pockmarks.

About 25 pockmarks had sharp and distinct boundaries. These pockmarks were used to derive statistical measurements for the Fugløy pockmark province.

The size of individual pockmarks varies between 30 and 120 m in diameter. Their mean diameter is 74 m (StDev 30 m). The pockmark diameter was measured in two directions, from south to north and from east to west. A histogram of frequency versus diameter (Fig. 5.15a) shows that the distribution of pockmark size is skewed towards large pockmarks. The average pockmark depth is 4.06 m and the median depth is 4.26 m (StDev 1.49 m). However, the bottoms of some of the pockmarks are as much as 6.5 m below the surrounding seafloor. The relationship between depth and diameter follows the linear equation (correlation is 78 %):

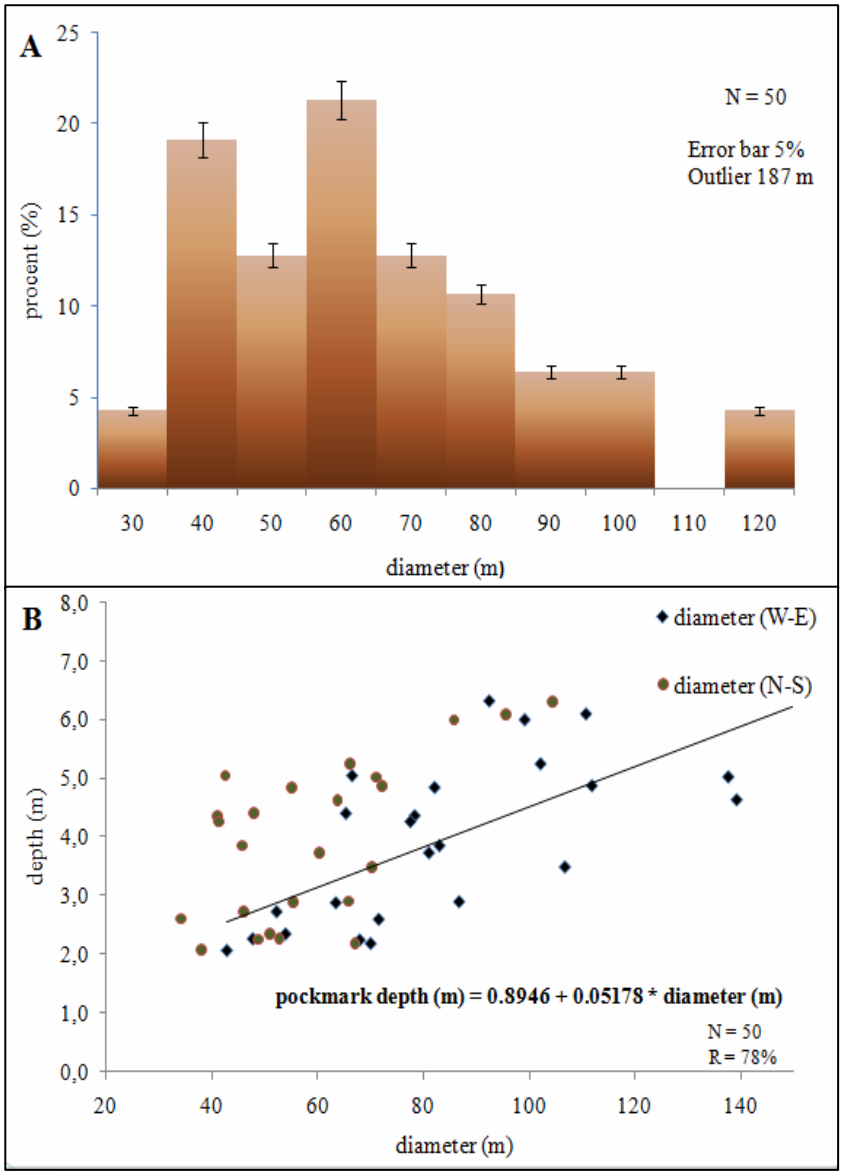

Figure 5.15. A Histogram of pockmarks diameter versus frequency in Fugløy area. The error bar displays 5% of diameter. **B** Scattplot between depth and diameter. Note that pockmarks had longer axes in N-S direction. Depth and diameter correlation was 78%.

$$Depth = 0.8946 + 0.05178 \times diameter \qquad \text{(Eq.5.4)}$$

We can notice that when the pockmark depth increases, also the diameter increases (Fig. 5.15b). The calculated diameter to depth ratios are between 6:1 and 11:1.

Pockmarks have considerable variations of shape in the Fugløy area. Almost 57% of the studied pockmarks are so-called normal pockmarks (see the sketch on figure 5.16c). Those pockmarks are circular depressions, where measured N-S diameters to W-E diameter ratios are between 0.95 and 1.15. Approx. 35% of the pockmarks are elongated, where one axis was much longer than the other, and mostly the longest axis seems to be in NNE-SSW direction. There are also composed pockmarks, i.e two or more pockmarks are connected together. The study showed that smaller pockmarks have a circular shape and larger pockmarks are elongated in NNE-SSW or NE-SW direction. There are 5 pockmarks, aligned in NE-SW direction where the pockmark shape follows the alignment (see Fig. 5.14a).

The pockmarks have an average slope of 6.05 degrees with a standard deviation of 1.76 degree. Pockmarks with a diameter larger than 50 m have lower slope angles than smaller ones. The pockmarks are well identified on the slope map (Fig. 5.16.) due to their circular form and varying slope angle.

It is interesting to calculate the volume of muddy sediments and pore water removed by pockmark processes. Pockmarks have a shape similar to a part of a sphere cut off by a plane (Fig. 5.14c). The volume can be calculated by using a mathematical formula for a segment of a sphere of the following form (Gulliksen 1998);

$$V = 1/6\,\pi h\,(3r^2+h^2) \qquad \text{(Eq.5.5)}$$

In equation 5.5. V is volume, h is depth of the pockmark, and r is the pockmark-radius. This results in an average pockmark volume of 8.7×10^3 m³, which may seem to be a large number, but if it would be spread over the pockmark area it would amount to an increase in thickness of 0.62 m.

5.4.2. SEISMIC DATA

Three seismic lines crossed the pockmark area (for location see Fig. 4.1). The seismic data shows that the sedimentary basin is acoustically well-stratified about 25 – 60 m thick, and overlying a highly reflective basement. No fractures and faults were identified in the seismic sections. Lindberg and Mienert (2005a) reported that the basin contains post-glacial deposits. Only two pockmarks were determined by low frequency seismic data (Figs. 5.17b & 5.18a). The reason for this is the small depth dimensions of pockmarks.

The seismic records (Fig. 5.17b) provide evidence that most subsurface layers in the sedimentary basin could be gas-charged, and that there may be hydrocarbon migration to the surface (Fig. 5.17b). Unfortunately, no clear fluid-migration pathways were identified on the seismic sections.

To obtain a better visualization and to try to identify the presence of gas on the vertical seismic sections, the reflection amplitude was regulated so that the strong negative amplitude has a yellow colour and the strong positive amplitude has a green colour (Fig. 5.18). In case free gas is present in the sediment pore space, it causes a dramatic reduction of P-wave velocity, which would result in anomalously high reflection amplitudes from the top of the gas (Badley 1985). Figure 5.18a shows a seismic profile through a pockmark structure with high-amplitude reflections and polarity reversals in the subsurface.

Most pockmarks that were identified on the multibeam data correspond to subtle or shallow depressions or hyperbolic echoes on sub-bottom profiles (Figs. 5.19b & f). Although the seafloor in the high-density pockmark area is quite flat and it was difficult to detect pockmarks due to a high noise level on the SBP data. In general, pockmarks look morphologically fresh and show no evidence of sediment infill.

On the SBP profile it was observed a pockmark that is similar to “eyed” pockmark (Fig. 5.19f). Hovland et al. (2002) described “eyed” or single pockmarks as pockmarks that have a central part with an acoustically highly reflective object. A sketch of “eyed” pockmarks is drawn in figure 5.19h. The slope map of this pockmark is provided in figure 5.19g. This pockmark has a diameter up to 84 m and slope angle of 8 degrees. Furthermore, the seismic data indicates few places with buried pockmarks. They cause hyperbolic echoes further down in the stratigraphy. They are

not out-of-plane images of pockmarks that have not been crossed directly, because the multibeam data assures exact positioning.

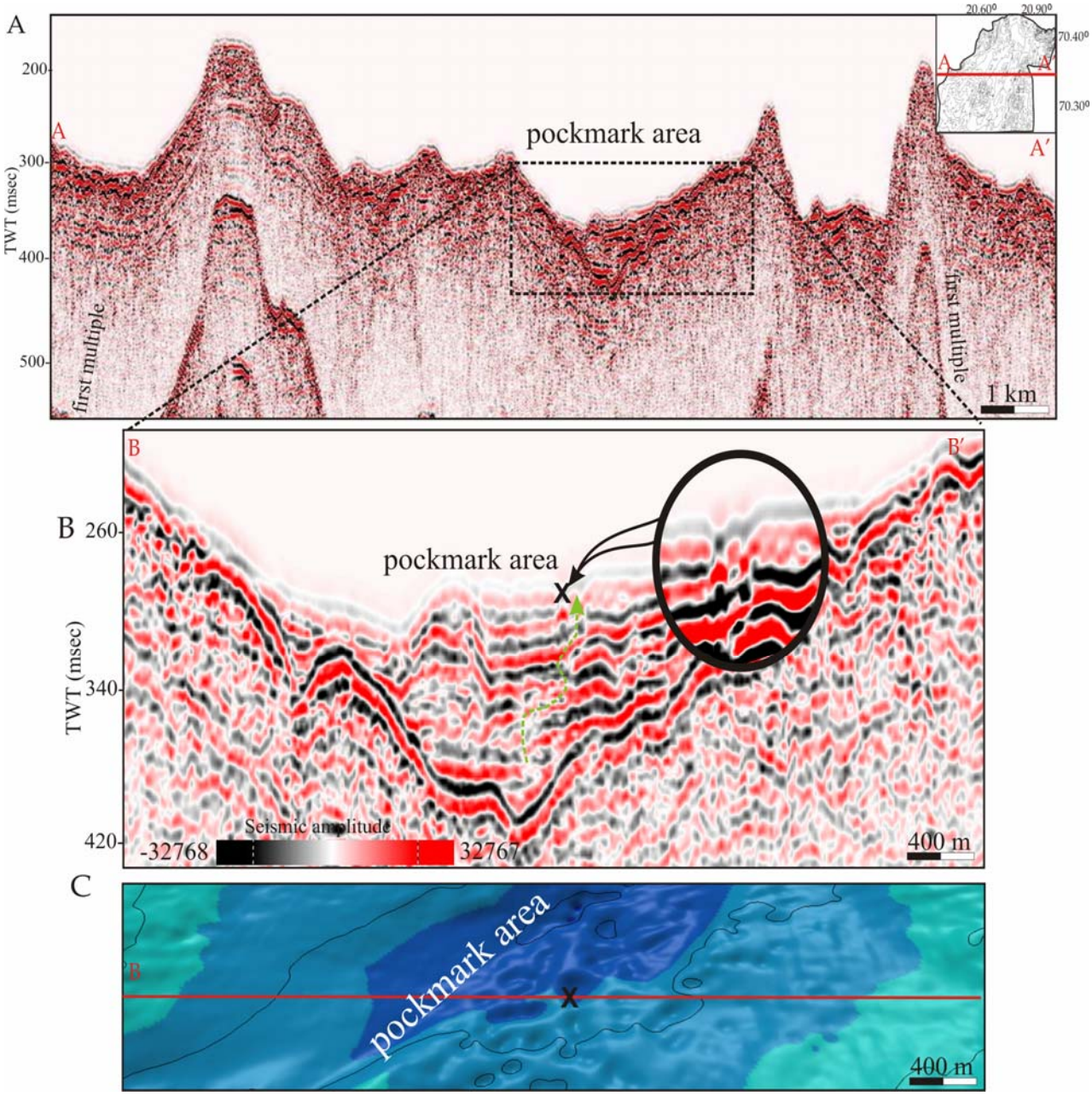

Figure 5.17. A Representative seismic profile (line 73) through the pockmark area, **B** enlarged seismic section of pockmark area, location of pockmark is marked with cross (X), and **C** showing the respective bathymetry (20 m contour interval).

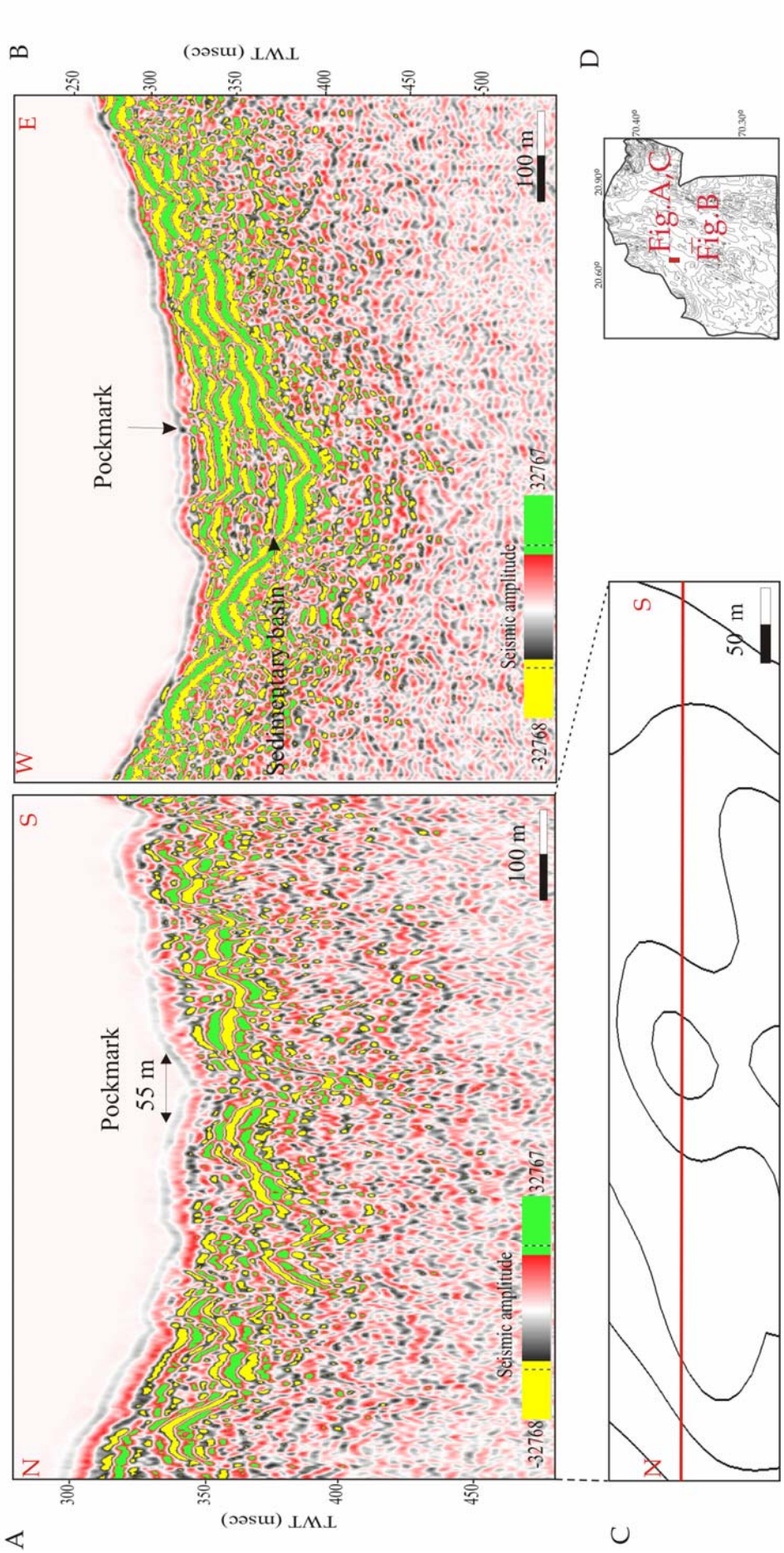

Figure 5.18. A Representative seismic profile (line 69) through pockmark, **B** representative seismic profile (line 73) through pockmark in the sedimentary basin, **C** showing the respective bathymetry (contour interval 2 m), and **D** location map of the Fugløy area.

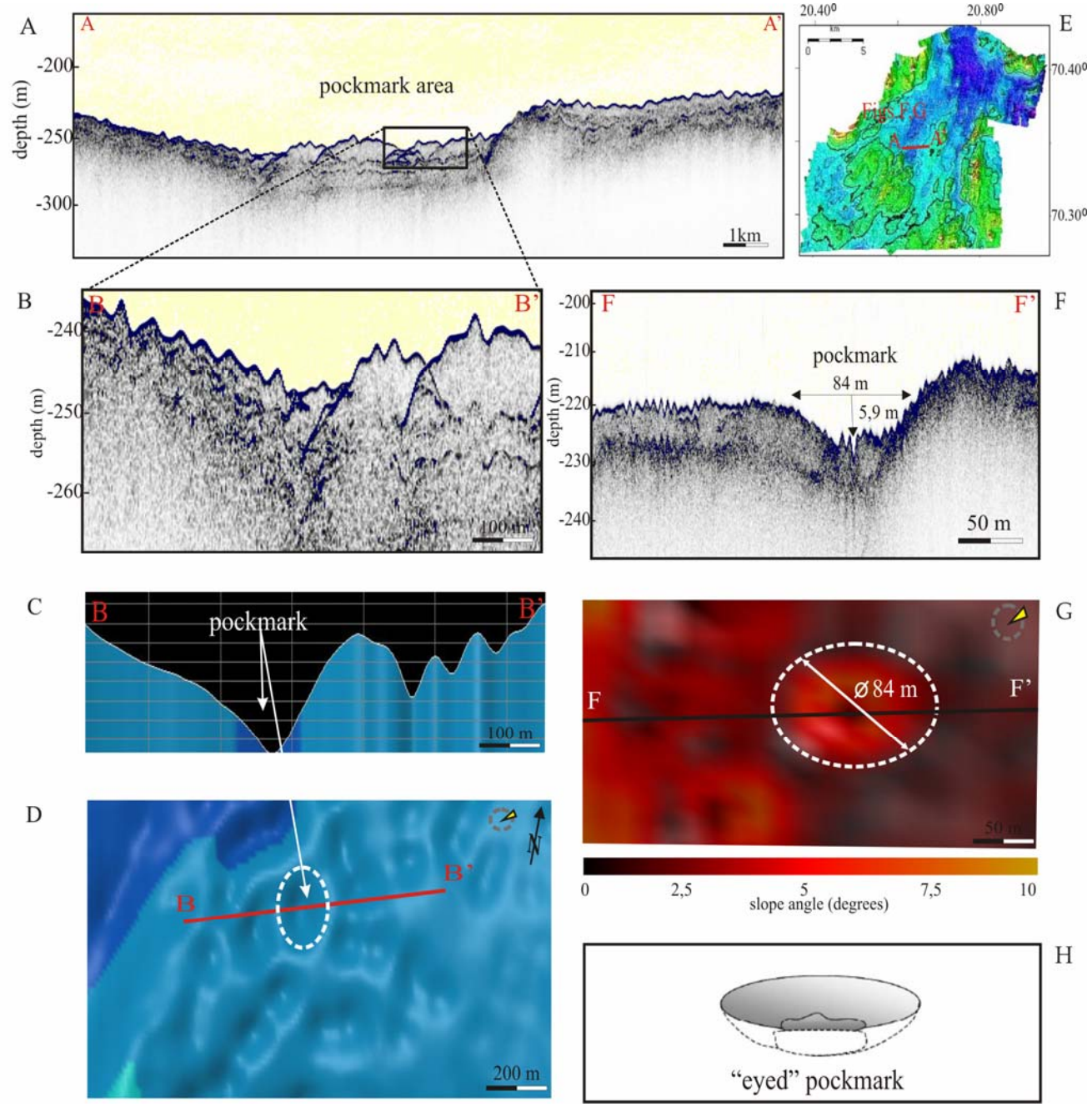

Figure 5.19. A Sub-bottom profile record (line 8/2007) across pockmark area, **B** enlarged SBP profile (line 8/2007) across pockmark area, **C** vertical profile from C-C'(Fledermaus) and **D** showing the respective bathymetry (20 m contour interval), **E** location map, **F** SBP record (line 9/2007) across a large pockmark, probably an "eyed" pockmark, **G** an interprateted pockmark on the slope map, and **H** a sketch shape of an "eyed" pockmark (from Hovland et al. 2002).

5.5. ICEBERG PLOUGHMARKS

More or less linear and sinuous features are observed in several places on the seafloor image (Figs. 5.20a & b). They are furrows with small rise on both sides. The furrows are up to 1.5 km long and up 92 m wide, but most of furrows are 200-600 m long and 15-35 m wide. They have a U-shape in a vertical profile and their shape is slightly smooth. Their depths range between 1 and 3 m (Figs. 5.20c & d). The best developed furrows are commonly present in the south-western part of the study area, where water-depth is between 150 and 190 m (Fig. 5.20). The dominant furrow orientation is southwest-northeast, but the direction varies greatly. In some cases, the furrows cross-cut each other and at the end point, the furrows create a headwall (see Fig. 5.20b).

Their morphology and previous studies from Lindberg and Mienert (2005a) and Lindberg et al. (2007) in the same area suggest that those features are iceberg ploughmarks. Iceberg ploughmarks caused are formed when the keel of an iceberg is exceeding the water depth and erodes soft sediments (Lien 1983; Andreassen et al. 2007). The iceberg ploughmark marked with a red dotted line in figure 5.20b was the longest at approximately 1420 m. The vertical profile across the ploughmark (Fig. 5.20d) shows that it has a depth of 1.54 m and a width of about 73 m. Ploughmarks indicate that the region has been influenced by glacial processes and are evidence of iceberg activity.

Iceberg ploughmarks are common features in front of marine glaciers and are well known features from the Norwegian continental margin, especially from the south-western Barents Sea (Vorren et al. 1983; Solheim 1997; Rafaelsen et al. 2002; Andreassen et al. 2007; Ottesen et al. 2007). The shape of the ploughmarks may indicate the direction of ice stream flow. Grounded ice streams appear to have flown from the southwest towards the Barents Sea.

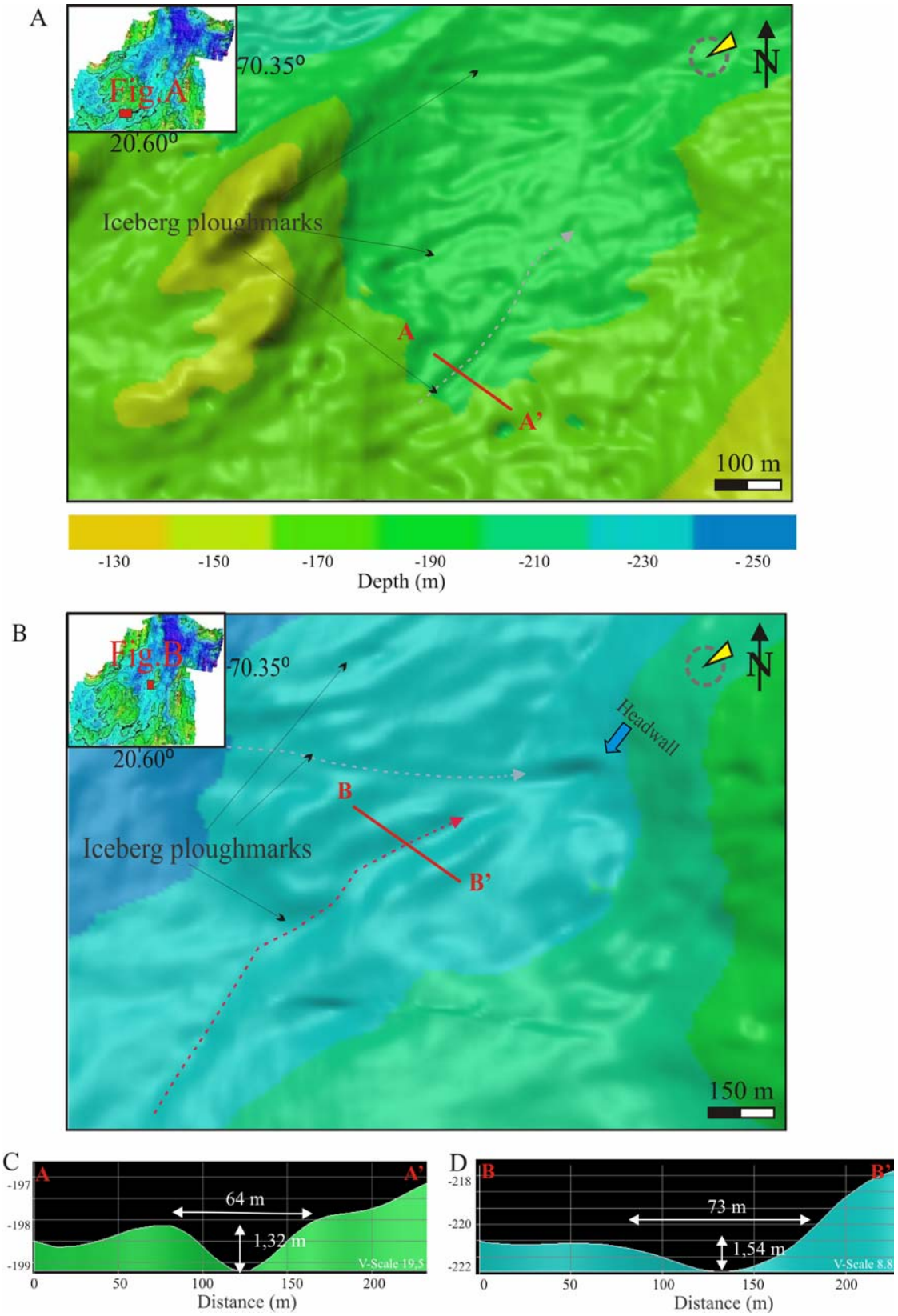

Figure 5.20. A and **B** 3D view of iceberg ploughmarks, **C** and **D** vertical profiles through iceberg ploughmarks in Fugløy.

5.6. EROSIONAL CHANNELS

The bathymetric high in the central area is cut by several NNE-SSW trending erosional channels (Figs. 5.2a, 5.4a & 5.21a). The largest erosional channel is about 4.2 km long, the width varies between 150 and 400 m and in the cross-section it is mostly U-shaped (Figs. 5.21b & c). The mean depth is about 15 m whereby the depth of the channel is measured from the bottom of the channel to the top of the flank rise. The channel bottoms have a relatively smooth morphology and show a slightly SSW to NNE dominant sea floor orientation. In several places coral reefs are located adjacent to the channels (Fig. 5.21a).

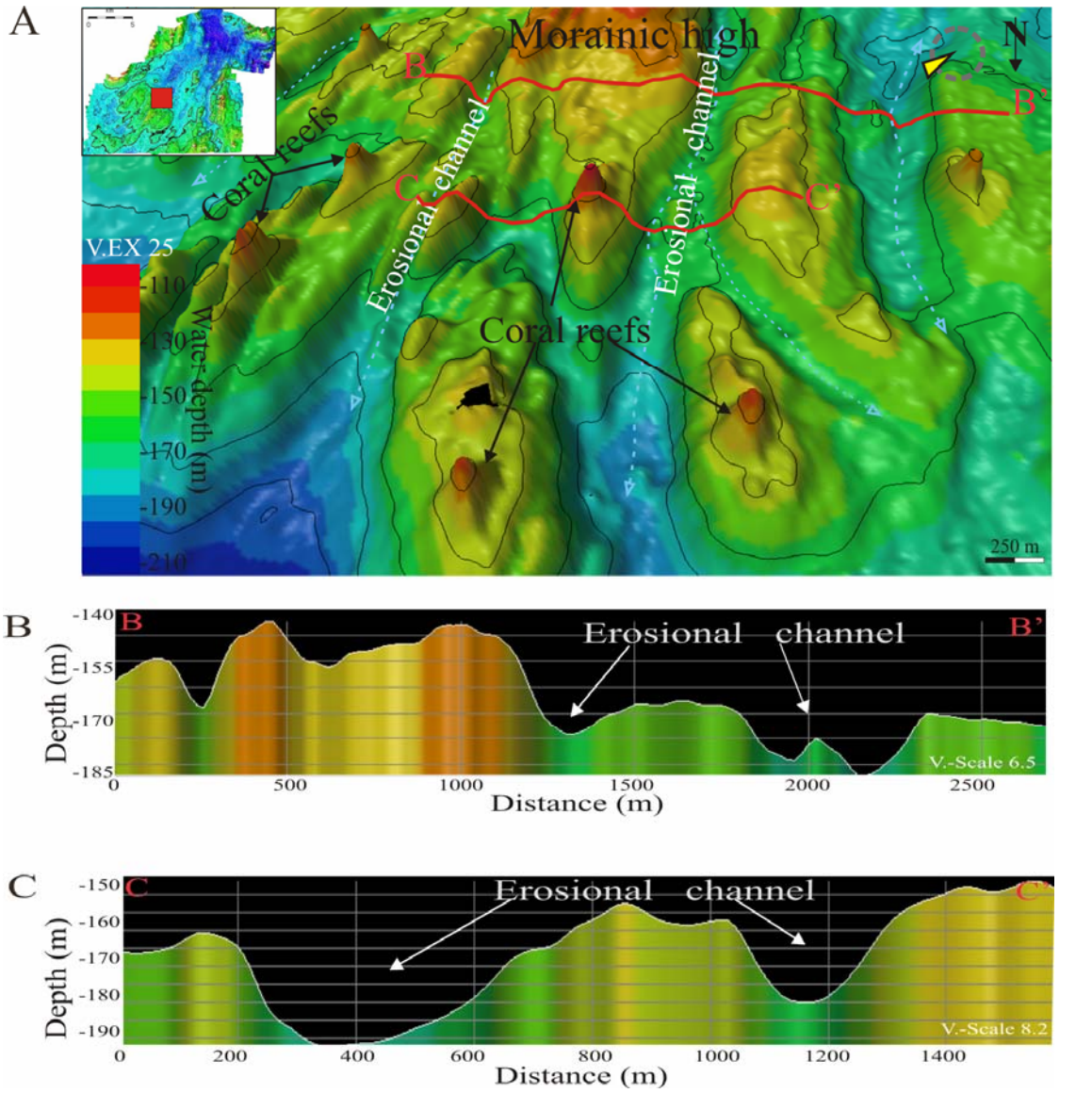

Figure 5.21. A 3D bathymetry map showing NNE-SSW trending erosional channels, **B** and **C** vertical profiles through erosional channel in Fugløy.

6. DISCUSSION

6.1. DISTRIBUTION OF CORAL REEFS

L.pertusa needs specific environmental conditions for their live and growth. Various studies (Freiwald 1998; Rogers 1999; Fosså et al. 2000; Mortensen et al. 2001; Hovland and Risk 2003; Wheeler et al. 2007) have shown that there are several factors that are controlling the distribution of coral reefs. Examples are the presence of suitable seabed substratum, seabed topography, temperature and salinity intervals, organic particulate supply, pH, as well as seepage of hydrocarbons. The bathymetric and backscatter data indicate the presence of 12 coral reefs in the Fugløy area (Figs. 5.1 & 5.4). They have a density of approximately 1.39 reefs per km². This is a relatively high density compared to other areas on the Norwegian margin. For example, over 70 *L.pertusa* reefs with a density of 1.2 reefs per km², have been mapped in the Haltenpipe Reef cluster (Mortensen et al. 2001; Hovland and Risk 2003). The highest known density of *L.pertusa* reefs in Norwegian waters occurs in the Trænadjupet Reef Complex, where 265 individual coral reefs with a density of about 10 reefs per km², have been mapped (Hovland and Risk 2003).

In this chapter, the influence of some of the above mentioned factors on the distribution of the coral reefs in the Fugløy area is discussed.

6.1.1. SEABED MORPHOLOGY

The multibeam data reveals that the most suitable terrain for coral reefs is the topographic highs, indicating the preference of local elevations (Figs. 5.4 & 5.21a). Various studies from the continental margin in the Northeast Atlantic, off the western coast of Ireland, on the Scotian Margin in Canada and in the Gulf of Mexico in the United States document that *L.pertusa* colonies favour elevated features, such as morainic ridges, glacial flutes, sills and iceberg ploughmark levees (Hovland and Risk 2003; Lundälv 2004; Beuck and Freiwald 2005; Hovland et al. 2005; Scott 2005; Tyler-Walters 2005). A reason for this could be that the increased current velocity increases the encounter rate of food particles, or creates turbulence and eddies which concentrate the food particles (Mortensen et al. 2001).

The detailed study of coral reefs in the Fugløy area shows that they have an elliptical and elongated shape in the horizontal plan, they are up to 241 m long and up to 126.7 m wide (Figs. 5.6b & 5.7c). The shape of coral reefs often seems to be determined by the topography of the underlying seabed (Mortensen et al. 2001; Hovland et al. 2005; Jonsson 2006; Dolan et al. 2008). For instance, Wheeler et al. (2007) defined two types of gross carbonate mound morphologies: inherited and developed coral forms. The inherited reefs have a strong substrate control, so that the reefs take the same gross morphology as the objects (bodies) that corals have colonised. It is therefore suggested that the seafloor morphology influences/pre-determines the distribution of the coral reefs in the study area, because they have the same orientations and shapes as the morainic ridges. It was observed that several coral reefs have almost the same width as moraine ridges. It is therefore suggested that they cannot grow wider and that the width of the reefs seems to be controlled by the width of the moraine ridges. As a consequence, reefs can only expand laterally along their longest axis and/or vertically upwards. Similar observations have been made at the Sula Ridge and the Pelagia Mound province. Individual coral reefs on the Sula Ridge align along the ridge crest escarpment, flutes or iceberg ploughmarks, and have the same geometry as the underlying seabed (Mortensen et al. 2001; Hovland et al. 2005). Coral mounds growing on scarps in the Pelagia Mound province seem to have a scarp shape (Wheeler et al. 2007). On the other hand, reef forms may develop independently of the topography of the *L.pertusa* original colonization site due to the hydrodynamical conditions. For example, in the Hovland mound province the mounds have elongated, elliptical and conical shapes and do not follow the seafloor morphology (Kiriakoulakis et al. 2003; Wheeler et al. 2007).

6.1.2. BOTTOM SUBSTRATE

A controlling factor on the distribution of *L.pertusa* is the bottom type. This is because of the fact that *L.pertusa* colonises a site as larvae (Rogers 1999). The coral larva needs a hard surface where it can settle and create a strong attachment point for a new colony. The backscatter data presented in this study indicates the presence of two different seabed environments in the Fugløy area; the hard and soft surface sediments (Fig.5.3). The results show that cold-water coral reefs occur only in the areas where surface sediments have been interpreted to form a hard bottom (Fig. 5.3 & 5.5a). The

steep sloping moraine ridges in the study area with an average slope angle of 8° are normally associated with hard substrate (Fig. 5.5b). The gravity core (Lindberg and Mienert 2005a & 2005b) take near coral reefs showed the presence of large clasts up to 10 cm. It is therefore suggested that morainic highs that contain clasts are a preferred substratum for colonization by *L.pertusa* in the study area. This result is supported by studies from Rogers (1999) and Freiwald et al. (2002). Those authors noted that corals require a hard substrate for initial settlement. Such substrates can be rock outcrops, gravelly or shell-hash beds, submarine moraines and ridges, as well as artificial objects like oil rigs or submarine cables (Rogers 1999). However, *L.pertusa* is also found on soft sediment beds or sand ripples, although the settling larvae is probably found small shells, pebbles, worm tubes or dead coral to settle on (Mortensen et al. 1995; Rogers 1999; Jonsson 2006).

About 64% of the Fugløy study area is covered by hard substrate, whereas only 12 reefs were discovered. This suggests that the distribution of *L.pertusa* reefs in the Fugløy is also determined by other factors.

Several iceberg ploughmarks were observed on the seafloor in the study area (Fig. 5.20). Boulder levees of ploughmarks seem to be common substratum for coral attachment (Freiwald et al. 1999; Wheeler et al. 2007). Such observations, where individual *L.pertusa* reefs are situated on ploughmark levees, have been made from the Sula Ridge and the Trænadjupet area (Freiwald et al. 2002; Hovland and Risk 2003). However, no coral reefs were observed on the ploughmarks in the Fugløy area. One reason for the absence of reefs could be the fact that observed ploughmarks in the Fugløy are relatively small and do not have well deformed levees. However, the main reason for the absence of coral reefs on ploughmark levees is probably that the ploughmarks occur in water depth between 150 and 190 m and therefore below the limit of the general distribution of the reefs in the study area (reefs interval 115-163 m).

6.1.3. HYDRAULIC CONDITIONS

The study area is located at the outlet of a fjord system where three large fjords (Ullsfjorden, Lyngenfjorden and Kvænangen) feed into the Barents Sea (Fig. 3.1). The multibeam data reveal the high concentration of *L.pertusa* reefs on the NE- or NNE-facing edges of the moraine ridges. These moraine ridges are cut by erosional channels

and have mostly NE-SW or NNE-SSW striking orientation (Figs. 5.4 & 5.21a). The high concentration of exposed coral reefs in this area could be related to the hydrographic conditions such as current velocity and direction. Current measurements, done by Lindberg et al. (2007), showed that the water is flowing southward into the fjords (Ullsfjorden and Lyngenfjorden) during the high tide and the water flowing out during low tides through these erosional channels. The water flow in these channels was continuous and current velocity as high as 0.3 m/s was registered. Measured temperature and salinity (S > 34.5 psu and 5 < T > 10 °C) indicate the presence of Atlantic water. Moreover, Vikebø and Ådlansvik (2005) used a current model (ROMS) to calculate the current direction at 50 m depth in northern Norway. They reported that the dominant bottom current direction in the Fugløy area is from NE to SW. Those oceanographic observations suggest that the *L.pertusa* reefs are closely related to high current regimes. The strong tidal current (Lindberg et al. 2007) in combination with local runoff probably produces an almost constant flow of saline and deep cold water into study area and creating the link between the location of reefs and current velocity. These high energy regimes are important for corals, because the higher current speed increases food supply. The diurnal current variations provide continues supply of fresh organic material to corals. Furthermore, strong currents prevent sedimentation and keep the corals from silting over. Corals are filter-feeders and increased particulates could clog their filter apparatus (Fricke and Hotting 1983; Fredriksen et al. 1992; Rogers 1999; De Mol et al. 2002; Jonsson 2006). Nevertheless, current velocity can not be too high otherwise *L.pertusa* colonies can dip over and/or break the corals (Wilson 1979).

6.1.4. OCEANOGRAPHY PARAMETERS

In the Fugløy area, *L.pertusa* reefs occur in the depth interval between 115 and 163 m (Fig. 5.11), indicating a shallower upper and lower limit for *L.pertusa* than the rest of the north-eastern Atlantic reefs, where *L.pertusa* occur at the depth between 250 and 450 m (Freiwald 1997; Fosså 2003). The shallowest *L.pertusa* occurrences have been recorded from oil platforms in the northern North Sea and from Norwegian fjords such as for instance the Tautra Ridge in mid-Trondheimsfjord at 39 m depth (Roberts et al. 2003). The results show also that in local scale *L.pertusa* is found on a much narrower depth range than that of their global distribution, where *L.pertusa* is observed in the

depth interval from 39 to 3383 m (Fosså et al. 2002; Freiwald et al. 2004). Therefore it is suggested that the environmental factors such as temperature and salinity combined with food availability and topographic conditions are more important for distribution than water depth. The upper depth limit (115 m) of coral reefs indicates that reefs in the Fugløya are located in the water depth out of wave action. In general, the coral reefs occur beneath the photic zone. The reason that *L.pertusa* can live so deep is that they do not live in symbiosis with photosynthetic algae and do not depend on sunlight. Instead they receive nutrients from plankton and other organic matter they can capture with their tentacles from the surrounding water (Freiwald 2002). Moreover, Dodds et al. (2007) suggested that the deepest limit of corals location may coincided the oxygen minimum zone.

In the Fugløy area, *L.pertusa* reefs occur in the temperature interval between 5.2 and 8.5 °C (Fig. 5.10). The measured data show that there is a significant annual temperature fluctuation and the *L.pertusa* reefs in the study area tolerate temperature variations up to 3 °C. Existing information suggests that in general *L.pertusa* is restricted to a temperature range from 4 to 12 C° (Fredriksen et al. 1992; Freiwald 1988; Roberts et al. 2003). In the northeast Atlantic, *L.pertusa* rarely occurs at temperatures below 4 °C (Roberts et al. 2003). Thus, the temperatures in Fugløy are in the middle part of the range in which *L.pertusa* is known to occur.

The salinity interval at which *L.pertusa* is found in the Fugløy area ranges from 34.83 to 34.53 psu (Figs. 5.11 & 5.13). The study shows that there are small annual and vertical salinity variations in the water column, providing stable growth conditions for *L.pertusa* and their associated fauna. This small-scale salinity variability is probably related to the seasonal vertical mixing processes or due to seasonal variation of fresh water input from mainland. Small variation in salinity profiles indicates that this parameter is important for the distribution of corals in the study area. The upper salinity limit for cold-water corals is measured at 38.8 psu in the Ionian Sea (Taviani et al. 2005) and the lower limit varies around 32 psu in Norwegian fjords (Freiwald 1998), indicating that *L.pertusa* tolerates a wide range of salinity values (Freiwald 1998; Roberts 2002). Mortensen et al. (1992) suggested that in shallow fjordic water *L.pertusa* salinity may be an important factor determining the location of *L.pertusa* reefs. In these places a pycnocline is created between lower salinity coastal/surface waters and cooler oceanic water resultin in more stable conditions within the fjords,

and a strong influx of oceanic waters. In such places, the *L.pertusa* and their community may be vulnerable to the change of salinity.

The variations in temperature and salinity influence water density. Potential density analysis shows that minimum values of 26.99 kg/m³ occur at the top of *L.pertusa* reefs, while this value slightly increases to 27.14 - 27.41 kg/m³ in the lower water column (Fig. 5.12). In a recent study conducted on the Celtic and Norwegian shelves, Dullo et al. (2008) noted that living cold-water coral reefs occur within the density envelope of sigma-theta = 27.35 – 27.65 kg/m³. Compared to those areas, the Fugløy reef area has a lower potential density value. One reason for this disparity could be that the Dullo et al. (2008) study was conducted only in shelf areas, no fjord systems were included in their study. The Fugløy area is located at the outlet of a fjord system were oceanic water is probably mixing with freshwater from the mainland and this affects the density value.

6.1.5. MODEL

A conceptual model of the Fugløy is illustrated in figure 6.1. This model is developed from the present study and previous works (Hovland and Risk 2003; Lindberg and Mienert 2005a & 2005b; Lindberg et al. 2007). The model summarizes the findings and suggests that a greater prominence of cold-water coral reefs on the morainic highs compared with adjacent areas can be explained by differing environmental conditions, such as 1) hard substrate, 2) local elevation, 3) current direction and 4) moderate current velocity. It is

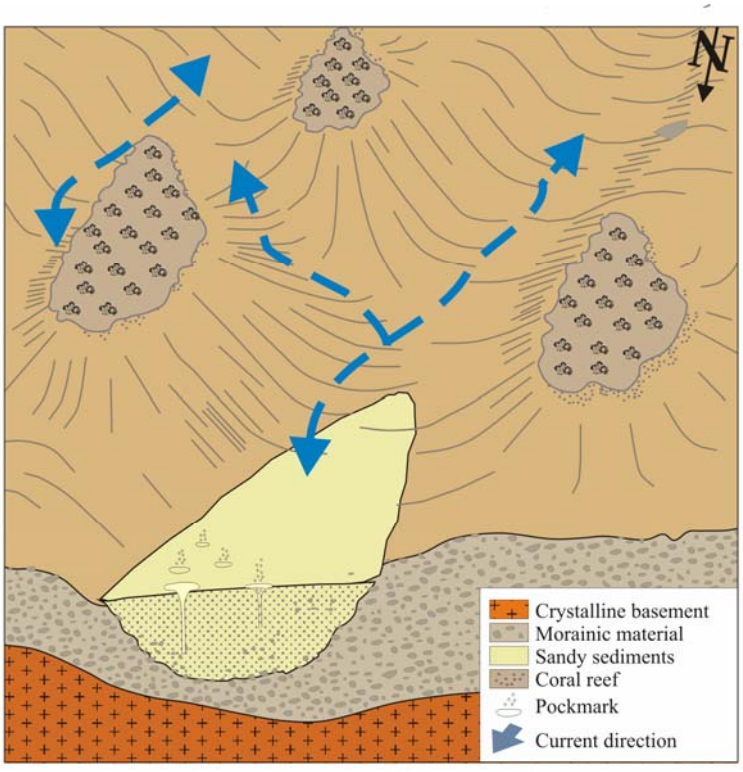

Figure 6.1. Conceptual model of distribution of *L.pertusa* reefs in the Fugløy area.

suggested that the local environmental conditions govern the shape and size of the individual *L.pertusa* reefs. The conceptual model does not exclude a hypothetical link between reefs and pockmarks (see next sub-section 6.1.5).

6.1.6. POCKMARKS AND CORAL REEFS

Numerous pockmarks were observed in the sedimentary basin north and northeast of the main *L.pertusa* reef area (Fig. 5.14). Previous studies have shown direct relationship of cold-water coral reefs with pockmarks, such as the Kristin Reef Cluster (Hovland and Risk 2003), the Haltenpipe Reef Cluster (Hovland and Risk 2003), reefs in the Gulf of Mexico, in the Porcupine Basin off Ireland (Hovland et al. 1994; Hovland 2005; Huvenne et al. 2007), off Brazil (Sumida et al. 2004), off Mauritania (Colman et al. 2005) and the Darwin Mounds located in the Rockall Trough (Masson et al. 2003). It is therefore possible that venting fluids in the pockmark area also affect *L.pertusa* growth in the Fugløy area.

Pockmarks are formed by episodic removal of fine-grained sediments during the expulsion of gas and porewater (Hovland and Judd 1988; Judd and Hovland 2007). The release of pressurized pore fluids excavates a crater to a depth that is limited by the supply of the pore fluid, local sedimentology and stratigraphy. Pockmarks in the Fugløy area are mostly circular in plan view and semicircular in cross section; and currents and slumping seems to deform their morphology. Pockmarks could affect the marine environment in different ways including increased turbidity and reduced water density in the water column. The biologic activity may benefit from an easily accessible source of carbon. The bacteria and microorganisms feeding on dissolved carbon from hydrocarbon seeps may establish a co-called chemosynthetic food chain, which in turn supports *L.pertusa* corals (Hovland and Thomsen 1997; Judd and Hovland 2007). In addition, turbidity can also adversely affect filter-feeding organisms by inhibiting feeding processes, like fine-grained material can clog the filtering mechanisms and starve the organism (Mortensen 2001).

The potential link between hydrocarbon seeps and reef growth in the Fugløy area was suggested by Hovland and Mortensen (1999). They hypothesized that active growth of coral reefs and reef location may be linked to areas on the seabed where light hydrocarbons seep from sediments. Another aspect is that organic matter may accumulate in the pockmarks craters while they are inactive and the near-bottom

currents, such as the south-westward flowing NCC in the Fugløy area may easily transport organic matter to the coral reefs (Lindberg et al. 2007). Our detailed mapping of coral reefs and pockmarks at Fugløy supports this hypothesis by a number of key observations:

- Almost all reefs are located on the seaward side of moraine ridges, so that *L.pertusa* reefs face towards the deeper basin where numerous pockmarks occur (Fig. 5.1).
- The high density area of pockmarks occur within a distance of less than 1500 m north or northeast of the main reef concentration
- Pockmarks look fresh and have mostly circular shape. There is a lack of sediment infill. These observations might indicate that pockmarks were recently active or are still active, so that they still escape fluid from the seafloor at the present day (Figs. 5.14 & 5.19).
- Some pockmarks appear to be modified by near bottom current actions. The circular form have modified to an ellipse with a major axis of NNE-SSW direction (Fig. 5.14a).

However, many authors disagree with the hydrocarbon seepage and reef link theory. For example Roberts and Aharon (1994) argued that if *L.pertusa* growth is supported by a food supply from hydrocarbon seep, coral tissues would have a low $^{13}\delta C/^{12}\delta C$ value. Analyses of skeleton material from *L.pertusa* show the $^{13}\delta C$ values within the range of ahermatypic carbon isotope fractionation (Mortensen and Rapp 1998; Spiro et al. 2000; Tyler-Walters 2005). Also, a preliminary biochemical study could not find evidence to support the hypothesis of *L.pertusa* feeding on bacteria from hydrocarbon seeps (Kiriakoulakis el at. 2005). In general, there is absence of *L.pertusa* in pockmarks areas, except the Kristin field in the North Sea where numerous up to 3 m high *L.pertusa* reefs are observed inside pockmarks (Hovland and Risk 2003). One reason for the absence of reefs in pockmarks is that pockmarks are found in soft sediment substrate and have episodic or continuous escape of gas or porewater, which causes resuspension of sediments. This is neither a suitable substrate nor an environmental condition for filter-feeding organisms (Hovland et al. 1998). In summary, the research on the relationship of hydrocarbon seepage and reef occurrence is scarce. However, there are several indirect and circumstantial evidence suggesting that this relationship exists.

6.2. AGE OF CORAL REEFS

The reported growth rates of *L.pertusa* range between 5 and 25 mm per year (Mortensen and Rapp 1998), the growth rates from colonies on oil platforms in the North Sea is estimated from 26 mm up to 33 mm per year (Freiwald et al. 2004, Gass and Roberts 2006). Additionally, Mortensen (2000) noted that because of bioerosion the total reef growth rate is about 1.3 m per 1000 years, which is much slower than individual colonies. Based on the investigations of the Sula Reef in mid-Norway, Freiwald et al. (1999) suggest that total growth rate is about 2 to 3 m per 1000 years. The entire study area was glaciated until the Late Pleistocene and the colonization and evolution of the Fugløy reef area must have happened after the last retreat of the ice-sheet, dated to about 13.5 BP (Vorren and Kristoffersen 1986). As the entire Norwegian shelf up to Svalbard was glaciated the migration of corals could only happen from south to north. The North Atlantic Current was well established after the last glaciation at about 8000 years BP (Andresen and Borns 1994). Accordingly, the possible pathway for coral larvae to reach to the Fugløya area in northern Norway is due to development and transport of relatively warm Atlantic waters onto the north-Norwegian shelf.

Thus, assuming that the largest reef was the first to be colonized and assuming a growth rate of 25 mm per year then the highest reef is 10 856 years old and the lowest reef in Fugløy is approximately 2164 years old. The calculated age of most of the reefs (95 %) are between 4504 and 8616 years old, which coincides well with the climate optimum phase of the Holocene (8000 to 3000 years BP; Andresen and Borns 1994; Alm et al. 1996). The age of *L.pertusa* reefs in other places are dated to the late glacial or post-glacial age, for example the *L.pertusa* reefs of the Sula Ridge were estimated to be 8600 years old (Mortensen et al. 2001) and the Haltenpipe Reef Cluster age is dated 8620±70 years (Judd and Hovland 2007).

Comparing the coral reef heights of the Fugløy area (up to 27 m) with reefs on the mid-Norway shelf, e.g. the Sula Ridge and the Haltenpipe Reef Cluster (up to 30 m), indicates that the reefs at Fugløy seem to have the same optimal condition. Higher growth rates are related to colonies living in even better oceanographic conditions and food supply.

6.3. MAPPING OF CORAL REEFS: INSIGHTS FROM SURVEY METHODS

6.3.1 BACKSCATTER DATA

Examination of backscatter data shows the reefs appear as sub-circular low backscatter patches on the backscatter image, with backscatter strength between -35 and -43 dB, while surrounding seafloor has much higher backscatter (Fig. 5.5).

Fosså et al. (2005) also reported the possibility to distinguish coral reefs on multibeam backscatter data. They studied backscatter intensity from the Sula Reef Complex and the Røst reef, and noted the association of coral reefs with very high backscatter intensity. Also Masson et al. (2003) described that the Darwin carbonate mounds appear as high backscatter objects on side-scan sonar data. In this study and in previous studies from Roberts et al. (2003), Conway et al. (2005) and Beyer (2006) provide evidence that coral reefs appear as low backscatter patches on backscatter records. It is known that coral reefs have a complex surface morphology. The reef surface is uneven and rough, causing the acoustic energy to scatter and giving a weak acoustic return. In this study both, the backscatter and the sub-bottom profiler data (SBP; see next section) showed coral reefs in the Fugløy area as less acoustically reflective and as diffuse reflectors. The cause of the difference in backscatter records is currently unknown, but the high backscatter intensity observed elsewhere could have two explanations. First, coral reefs in the Sula and Røst reefs complexes could occur on soft seafloor. Since coral reefs are made of calcium carbonate, they provide a much harder surface reflection than a sandy sea bottom. Second, coral reefs may have high acoustic return due to a consolidated and hard reef surface. *L.pertusa* reefs on the Sula Ridge are dated to an age older than 8600 years. Over such a long period, the surface could be well consolidated (Mortensen et al. 2001). However, it is possible that reefs in the Fugløy are related to dense accumulation of other suspension feeders or contain more coral debris.

6.3.2 SEISMIC DATA

Coral reefs appear as cone-shaped, acoustically semi-transparent features on the low frequency seismic data (Fig. 5.8). The reflection strength from coral reefs is lower than the surrounding seafloor, because part of energy has been scattered due to the complex

morphology of the reefs. Comparing seismic characteristics of reefs in the Fugløy area with other coral reefs and mound systems found in the North Atlantic and elsewhere, shows that they have the same seismic pattern, i.e. that these structures are represented as a poor discontinuous seismic reflector (De Mol et al. 2002; van Wheeling et al. 2003; De Mol et al. 2007).

Five coral reefs were crossed directly with a sub-bottom profiler (SBP). The coral reefs seem to have a flat top, and a 'cauliflower' or dome shaped morphology in the vertical section (Fig. 5.9). SBP data from coral reefs showed diffuse reflectivity, while the seafloor beneath the reefs shows as a strong and coherent reflector. The "cauliflower" shape in SBP data is caused first of all because of varying sizes of single *L.pertusa* colonies that cover a coral reef and provide an uneven surface (Freiwald 2002). Also, the large reefs have three characteristic zones: the living, dead and rubble zone, which most likely have different reflection characteristics (Mortensen 1998). Previous studies from Wheeler et al. (2005) concluded that based on SBP data it is possible to indentify if coral reefs are active or retired. Accordingly, a diffuse reflection especially from the top of a coral reef indicates that reefs are active at present time and retired coral reefs generally have a solid seabed reflector. The solid reflector is caused due to a hard and consolidated upper reef layer. All the five directly crossed coral reefs have a diffuse reflector implying that reefs are active. Active reefs are characterised with rich faunal community with living coral (Mortensen et al. 1995; Huvenne et al. 2005).

6.4. STATUS OF COLD-WATER CORALS IN THE FUGLØY

The Fugløy Reef area is an important spawning area of Norwegian-Arctic cod and capelin, and nursing area of herring and tusk (Stiansen et al. 2005). In general, reefs are known as good fishing places, but unfortunately all fishing methods affect coral reefs. The Fugløy Reef area is located outside of main active trawling areas (see Fig. 6.2a) and so far damages of bottom trawling or other anthropogenic activity has not been reported. However, the Norwegian Institute of Marine research in Bergen documented that *L.pertusa* reefs are very sensitive to bottom trawling, and they estimated that between 30 and 50% of the cold-water coral reefs in Norwegians waters had been partly or totally damaged (Fig. 2.3; Fosså et al. 2002). Most of the cold-water coral reefs on the Norwegian margin are not protected from bottom trawling. So far, Norway

has banned bottom trawling on just 6 cold-water coral reef systems (Norwegian Directorate of Fisheries 2004). Those reefs are the Sula Reef (1999), the Iverryggen Reef (2000), the Selligrunnen Reef (2000), the Røst Reef (2003), the Fjellknausene Reef and Tisler Reef (2003; for location see the map 6.2b), although more areas are proposed for protection (Langaas 2008). On the other hand, all potential threats to the study area are not known. The possible threats to this area might be the development of new petroleum fields in the Barents Sea, such as the Shtokman field or the Snøhvit field. The Snøhvit field is located only 130 km north of the Fugløy reef area. Additional threats are increasing transport especially transport dominated by Russian oil tankers (Sawhill et al. 2006). Production and transport of oil at sea will always include a risk for oil spills and discharges. The study area is located about 300 km north of the Arctic Circle, this means that the area has a

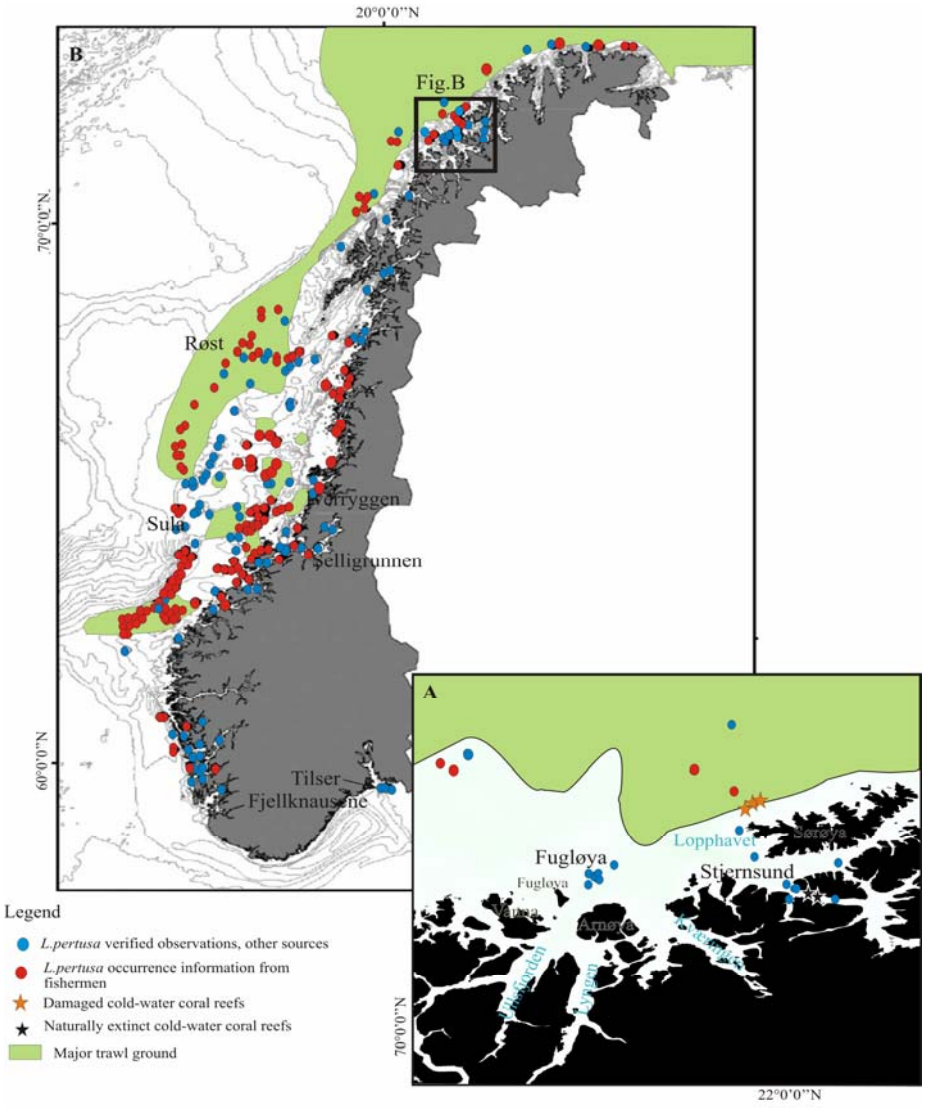

Figure 6.2. A Distribution of verified and not verified observations of *L.pertusa* reefs and major trawl ground (green) in Norwegian waters. Map is showing the degree of overlap between coral and trawling distribution, **B** Distribution of *L.pertusa* reefs and trawling ground in northern Norway. After *L.pertusa* corals die the structures they built still provide a home for many groups of animals. Modified from Fosså 2002, Føyn et al. 2002, Thiem et al. 2006 and MAREANO-maps, Coral reefs and oil (2008).

harsh climate and long winter period with very little daylight; all this increases the possibility for accidents for oil spills (WWF 2003 & 2007). Various studies have shown that oil persists longer in arctic conditions, because the evaporation is very slow in cold climate and oil may be trapped in or under ice, which makes it less accessible to bacterial degradation (Peterson et al. 2003). Environmental risk analysis made for areas around Fugløy, Arnøya and Sørøya (for location see Fig.6.2a) shows that the region has a high vulnerability for acute oil pollution (Brude 2005). Mostly because those areas are important locations of coral reefs, spawning and nursing areas for the most important fish species, and also, there is high occurrence of seabirds and marine mammals (Brude 2005; WWF 2007). *L.pertusa* reefs might be protected from the acute and short term effects of oil spills by their depth. However, it is reported that oil contamination is reducing corals growth, damaging tissues and feeding behaviour, disrupting cell structures, and even resulting reproduction failures (Rogers 1999; Tyler-Walters 2005). In conclusion, cold-water reefs in the Fugløy area are one of the northernmost reefs and they have high ecological value Due to their environmental settings they are endangered by a number of potential threats (Fig. 6.3).

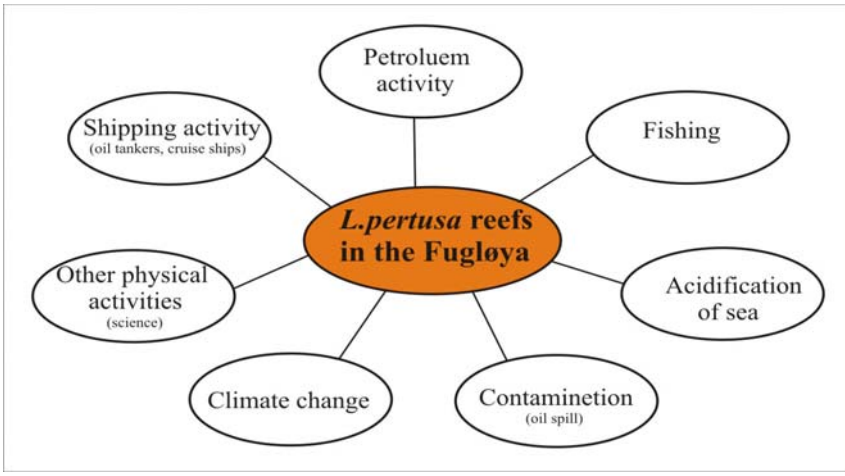

Figure 6.3. Potential threats to *L.pertusa* reefs in the Fugløy.

7. CONCLUSION

The present study has shown that newly acquired multibeam data integrated with backscatter and seismic data provides a better understanding of *L.pertusa* reef occurrences in their environmental setting in the Fugløy area in northern Norway.

Based on the geological and geophysical analyses and the integrated interpretation the following conclusions can be drawn for the occurrence of cold-water corals in the Fugløy area.

- Altogether 12 individual coral reefs were identified in the study area. The density of reefs within the area is very high, compared to other areas on the Norwegian Margin, and consists of about 1.2 reefs per km². The reefs cover an area of about 508147 m², respectively.
- Detailed analysis of the multibeam bathymetry data clearly shows that coral reefs mostly have an elongated shape, ranging in length from 89 to 241 m and in width from 64 to 127 m. The orientation of the longest axis of the reefs runs approximately in NE or NNE direction.
- The height of the coral reefs in the Fugløy has been determined between 5.41 and 27.14 m and the corals were calculated to be between 4504 and 8616 years old.
- *L.pertusa* in the Fugløy area occurs at a water depth ranging from 115 to 163 m, and thrives under fully-marine conditions, with temperature fluctuations between 5.2 and 8.5 °C and salinity variation between 34.83 and 34.53 psu. Coral reefs occur within the density envelope of sigma-theta = 26.99 – 27.41 kg/m³. These physical oceanographic conditions match well with the conditions found at *L.pertusa* sites along the north-western European continental margin.
- There is a clear relationship between coral reef occurrence and substrate composition. Coral reefs are located on the top of morainic highs and prefer to grow on hard bottom sediments.
- The presence of a warm and nutrient-rich current, the Atlantic drift, and eddy currents stimulate the formation of large cold-water reefs in the Fugløy area.
- Possibly venting fluids in the pockmark area could also affect *L.pertusa* growth in the Fugløy area.

REFERENCES

ANDREASSEN,K., NILSSEN,L.C. & RAFAELSEN,B. (2004) Three-dimentional seismic data from the Barents Sea margin reveal evidence of past ice streams and their dynamics. Geology 32:729-732

ANDREASSEN,K., LABERG,J.S., & VORREN,T.O. (2007) Seafloor geomorphology of the SW Barents Sea and its glaci-dynamic implications. Geomorphology

ANDERSEN,A. (1980) The age of the Precambrian basement in western Troms, Norway, Geologiska foreningens i Stockholm Forhandlingar 101(4):291-298

ANDRESEN,B.G., & BORNS,H.W.Jr (1994) The Ice Age World- An Introduction to Quaternary History and Research with Empahasis on North-America and Nortern Europe during the last 2.5 Million Years. Scandinavian University Press, Oxford, p.208

BADLEY,M.E. (1985) Practical Seismic Interpretation. Boston, MA: D. Reichel

BRANCATO,MS. & BOWLBY,CE. (2005) Survey of fishing gear and fiber optic cable impacts to benthic habitats in the Olympic Coast National Marine Sanctuary. Pages 629–630 in Barnes PW, Thomas JP (eds.), Benthic habitats and the effects of fishing. American Fisheries Society Symposium 41, Bethesda, Maryland

BIRD,K.J., CHARPENTIER,R.R., GAUTIER,D.L., HOUSEKNECHT,D.W., KLETT,T.R., PITMAN,J.K., MOORE,T.E., SCHENK,C.J., TENNYSON,M.E. & WANDREY,C.J. (2008) Circum-Arctic Resource Appraisal: Estimates of Undiscovered Oil and Gas North of the Arctic Circle. U.S. Geological Survey Fact Sheet 2008-3049

BRUCKNER,A.W. (2002) Life-saving products from coral reefs. Issues in Science and Technology Online

BLINDHEIM,J. (1990) Arctic intermediate water in the Norwegian Sea. Deep-Sea Research, 37:1475-1489

BREEN,O. (1990) Oseanografi. Gyldendal norsk forlag, Oslo. p.179

BRUDE,O.W. (2005) Areas vulnerable to acute oil pollution in the Norwegian Barents Sea. Report for WWF Norway. Report No: 2005-0456

CAIRNS,S.D. (1982) Antartic and subantartic Sceractinia. Antartic Research Series 34:74

CALDEIRA,K. & WICKETT,M.E. (2003) Anthropogenic carbon and ocean pH. Nature 425: 365

CHRISTENSEN,O. (2006) SUSHIMAP Survey strategy and methodology for marine habitat mapping. Doctoral thesis for the degree of doktor ingeniør. Norwegian University of Science and Technology

CITES species database (1990) Convention on International Trade in Endangered Species of Wild Fauna and Flora. Available at < http://www.cites.org> Last updates 1/08/2008

COLMAN,J.G., GORDON,D.M., LANE,A.P., FORDE,M.J. & FITZPATRICK,J.J. (2005) Carbonate mounds off Mauritania, Northwest Africa: status of deep-water corals and implications for manaement of fishing and oil exploration activities. In Cold-water Corals and ecosystems, eds Freiwald A, Roberts JM, Springer Publishing House, Heidelberg, Germany

CONWAY,K.W., BARRIE,J.V. & KRAUTTER,M. (2005) Geomorphology of unique reefs on the western Canadian shelf: sponge reefs mapped by multibeam bathymetry. - Geo-Marine Letters, 25/4:205-213

CÔTÉ,I.M.& REYNOLDS,J.D (2006) Coral Reef Conservation (Conservation Biology) Cambridge University Press p.589

COPLEY,J., TYLER,P.A., SCHEADER,M., MURTON,J. & GERMAN,C.R. (1996) Megafauna from sublittoral to abyssal depth along the Mid-Atlantic Ridge south of Iceland. Oecologica Acta 19:549-559

DE MOL, HENRIET.J-P. & CANALS,M. (2005) Development of coral banks in Porcupine Seabight: do they have Mediterranean ancestors. Friewald, A. and Roberts, J.M. (eds.) Cold-water corals and ecosystems. Berlin, Germany, Springer, p.515-533

DE MOL,B., KOZACHENKO,M., WHEELER,A., ALVARES,H. HENRIET,J.P. & OLU-LE ROY,K. (2007) Thérèse Mound: a case study of coral bank development in the Belgica Mound Province, Porcupine Seabight. International Journal of Earth Sciences. Vol 96 No1:103-120

DODDS,L.A., ROBERTS,J.M, TAYLOR,A.C. & MARUBINI,F. (2007) Metabolic tolerance of cold-water coral *Lophelia pertusa* (Scleractinia) to temperature and dissolved oxygen change. Journal of Experimental Marine Biology and Ecology 349:205-214

DONS,C. (1944) Norges korallrev. Det kongelige norske videnskabers selskabers forhandlinger 16, p.37–81

DULLO,W.C., FLÖGEL,S. & RŰGGEBERG,A. (2008) Cold-water coral growth in relation to the hydrography of the Celtic and Nordic European continental margin. News Updates. Hermes. Hotspot Ecosystem research on the Margins of European Seas. Vol 13:13

EDGETECH 2005 Sub-bottom profiling systems Available at < http://www.edgetech.com/subbottom.html > Accessed on: August 12, 2008

EIDE,L.I. (1979) Evidence of a topographically trapped vortex on the Norwegian continental shelf. Deep-Sea Research, 26:601-621

FLEDERMAUS. Reference manual Vesion 6.3 (2007) Interactive Visualization Systems

FOSSÅ,J.H., MORTENSEN,P.B. & FUREVIK,D.M. (2000) *Lophelia*-korallrev langs norskekysten, forekomst and tilstand. Fisken og Havet 2:1-94

FOSSÅ,J.H., MORTENSEN,P.B. & FUREVIK,D.M. (2002) The deep-water coral *Lophelia pertusa* in Norwegian waters: distribution and fishery impacts. Hydrobiologia 471:1-12

FOSSÅ,J.H., ALVSVÅG,J. & MORTENSEN,P.B. (2004) Protection and management of deep-water coral reefs in Norway. International Council for the Exploration of the Sea, CM AA, 08

FOSSÅ,J.H., LINDBERG,B., CHRISTENSEN,O., LUNDÄLV,T., SVELLINGEN,I., MORTENSEN,P.B. & ALVSVÅG,J. (2005) Mapping of *Lophelia* reefs in Norway: experiences and survey methods. In Cold-water Corals and Ecosystems, eds: Freiwald A, Roberts JM, Springer Publishing House, Heidelberg, Germany

FREIWALD,A. HENRICK,L. & PÄTZOLD,J. (1997) "Anatomy of a deep-water coral reef mound from Stjernsund, West-Finnmark, Northern Norway." SEPM, Special Publication. 56: 141-161

FREIWALD,A. (1998) Geobiology of *Lophelia* pertusa (Sclerctinia) reefs in the North Atlantic. Habilitationsschrift zur Erlangung der venia legendi am Fachbereich Geowissenschaften der Universität Bremen, Universitat Bremen, p.116

FREIWALD,A., WILSON,JB. & HENRICH,R. (1999) Grounding Pleictocene iceberg shape recent deep-water coral reefs. Sediment Geology 125:1-8

FREIWALD,A. (2002) Reef-Forming Cold-Water Corals. In Ocean Margin Systems (ed.G.Wefer, D. Billett, D. Hebbeln, B. B. Jørgensen, M. Schlüter, and T. v.Weering), p.365-385

FREIWALD,A., HUEHNERBACH,V., LINDBERG,B., WILSON,J.B. & CAMPBELL,J. (2002) The Sula Reef Complex, Norwegian Shelf. Facies 47:179-200.

FREIWALD,A., FOSSÅ,J.H., GREHAN,A., KOSLOW,T. & ROBERTS,J.M. (2004) Cold-water coral reefs. UNEP-WCMC, Cambridge, UK

FRICKE,H.& HOTTINGER,L. (1983) Coral bioherms below the euphotic zone in the Red Sea. Marine Ecology-Progress Series Vol 11:113-117

FØYN,L., QUILLFELDT,C.H & OLSEN,E. (red.) (2002) Miljø- og ressursbeskrivelse av området Lofoten – Barentshavet. Fisken og havet No 6:58

GALWAY,R.S (2000) The Integration of Multibeam Sonar Data with Huntec Sub-bottom Profile Data into a Marine GIS, Masters of Science in Engineering, University of British Columbia

GASS,S.E. (2002) An assessment of deep sea corals in the Atlantic Canada using both scientific and local forms of knowledge. MES Thesis, School for Resource and Environmental Studies, Faculty of Management, Dalhousie University. p.186.

GASS,S.E., & ROBERTS,J.M (2006) The occurrence of the cold-water coral *Lophelia pertusa* (Scleractinia) on oil and gas platforms in the North Sea: colony growth, recruitment and environmental controls on distribution. Marine Pollution Bulletin 52: 549-559

GUINOTTE,J.M., ORR,J., CAIRNS,S., FREIWALD,A., MORGAN,L. & GEORGE,G. (2006) Will human-induced changes in seawater chemistry alter the distribution of deep-sea scleractinian corals? The Ecological Society of America Vol 4 No1

GULLIKSEN,T. (1998) Matematikk i praksis, (4. utgave, 3. opplag). Universitetsforlaget p.220

HALL-SPENCER,J., ALLAIN,V. & FOSSÅ,J.H (2002) Trawling damage to Northeast Atlantic ancient coral reefs, Royal Society Publishing, No 1490/March 7, 269:507-511

HALLYDAY,E.J., BARRIE,J.V., CHAPMAN,N.R. & ROHR,K.M.M. (2008) Structurally controlled hydrocarbon seeps on a glaciated continental margin, Hecate Strait, offshore British Columbia. Marine Geology 252:193–206

HAMMERSTAD,E. (1994) Backscattering and Sonar Image Reflectivity: EM12/950/1000 Technical Note, p.10

HEINRICH,R. & BAUMANN,K.-H. (1994) Evolution of Norwegian Current and Scandinavian Ice Sheets during the past 2.6 m.y.: evidence from ODP Leg 104 biogenic carbonate and terrigenous records. Palaeography, Paleoclimatology, Paleoecology 108, p.75-94

HOBDAY,A.J., OKEY,T.A., POLOCZANSKA,E.S., KUNZ,T.J. & RICHARDSON,A.J. (2006) Impacts of climate change on Australian marine life: Part C. Literature Review. Report to the Australian Greenhouse Office, Canberra, Australia. September 2006

HOVLAND,M. (1981) Characteristics of pockmarks in the Norwegian Trench Marine Geology 39:103-117

HOVLAND,M., TALBOT,M., QVALE,H., OLAUSSEN,S. & AASBERG,L. (1987) Methane-related carbonate cements in pockmarks of the North Sea. Journal Sedof sedimantary Petrology 57:881-892

HOVLAND,M. & JUDD,A.G. (1988) Seabed Pockmarks and Seepages. Graham and Trotman, London, p.293

HOVLAND,M., CROKER,P.F. & MARTIN,M. (1994) Fault-associated seabed mounds (carbonate knolls?) off western Ireland and north-west Australia. Marine Pet. Geolology 11:232-246

HOVLAND,M. &THOMSEN,E. (1997) Cold-water corals – are they hydrocarbon seep related? Marine Geology 137:159–164

HOVLAND,M., MORTENSEN,P.B., THOMSEN,E. & BRATTEGARD,T. (1997) "Substratum-related ahermatypic coral banks on the Norwegian Continental Shelf." Proceedings of the 8th International Coral Reef Symposium, Panama City, 2: 1203-1206

HOVLAND,M., MORTENSEN,P.B., BRATTEGARD,T., STRASS,P. & ROKOENGEN,K. (1998). Ahermatypic coral banks off Mid-Norway: Evidence for a link with seepage of light hydrocarbons. Palaios 13:189-200

HOVLAND,M. & MORTENSEN,P.B. (1999) Norske korallrev og prosesser i havbunnen. - John Grieg forlag, Bergen p.155

HOVLAND,M. (2002) On the self-sealing nature of marine seeps. Cont Shelf Res 22: 2387-2394

HOVLAND,M., VASSHUS,S., INDREEIDE,A., AUSTDAL,L. & NILSEN,Ø. (2002) Mapping and imaging deep-sea coral reefs off Norway, 1982–2000, Hydrobiologia 471: 13–17

HOVLAND,M. & RISK,M. (2003) Do Norwegian deep-water coral reefs rely on seeping fluids? Marine Geology 198:83-96

HOVLAND,M. (2005) Pockmark-associated coral reefs at the Kristin field off Mid-Norway. In: Cold-water corals and ecosystems. Freiwald, A. and Roberts, J.M. (eds.) Springer-Verlag, Berlin, p.623-632.

HOVLAND,M., OTTESEN,D., THORSNES,T., FOSSÅ J.H. & BRYN,P. (2005) Occurrence and implications of large *Lophelia*-reefs offshore Mid Norway. In: Wandas, B. et al. (Eds.): Onshore – offshore relationships on the North Atlantic margin. Elsevier B.V., Amsterdam, Norwegian Petroleum Soc. (NPF), Special Publ. 12:265-270

HOURIGAN,TF., LUMSDEN,SE., DORR,G., BRUCKNER,AW., BROOKE,S. & STONE,RP. (2007) Deep Coral Ecosystems of the United States: Introduction and National Overview. Pages 1-65 in Lumsden SE, Hourigan TF, Bruckner AW, Dorr G (eds.), The State of Deep Coral Ecosystems of the United States. NOAA Technical Memorandum CRCP-3, Silver Spring, Maryland

HUGHES CLARKE,J.E. (1994) Toward remote seafloor classification using the angular response of acoustic backscattering: a case study from multiple overlapping GLORIA data. IEEE Journal of Oceanic Engineering 19, No1:112-127

HUGHES CLARKE,J.E., MAYER,L.A. & WELLS,D.E. (1996) Shallow-water imaging multibeam sonars: A new tool for investigating seafloor processes in the coastal zone and on the continental shelf: MGR, 18:607-629

HUSEBØ,A., NØTTESTAD,L., FOSSÅ,J.H., FULVIK,DM. & JØRGENSEN,SB. (2002) Distribution and abundance of fish in deep+sea coral habitats. Hydrobiologia 471:91-99

HUVENNE,V.A.I., BEYER,A., DE HAAS,H., DEKINDT,K., HENRIET,P., KOZACHENKO,M., OLU-LE ROY,K. & WHEELER,A. and the TOBI/Pelagia 197 and CARACOLE cruise participants (2005). The seabed appearance of different coral bank provinces in the Porcupine Seabight, NE Atlantic: results from sidescan sonar and ROV seabed mapping. In: A. Freiwald & J.M. Roberts (eds). Cold-water corals and Ecosystems, Springer-Verlag, p.535-569

HUVENNE,V.A.I., BAILEY,W.R., SHANNON,P.M., NAETH,J., DI PRIMIO,R., HENRIET,J.P., HORSFIELD,B., DE HAAS,H., WHEELER,A. & OLU-LE ROY,K. (2007) The Magellan mound province in the Porcupine Basin International Journal of Earth Sciences 96(1): 85-101

ICES 2007a (2007) Report of the ICES Advisory Committee on Fishery Management, Advisory Committee on the Marine Environment and Advisory Committee on Ecosystems, 2007. ICES Advice. Book 3 – p.103

ICES 2007b (2007) Report of the ICES Advisory Committee on Fishery Management, Advisory Committee on the Marine Environment and Advisory Committee on Ecosystems, 2007. ICES Advice. Book 6 – p.249

IPCC 2007 (2007) Climate Change 2007: Synthesis Report. An Assessment of the Intergovernmental Panel on Climate Change

JENSEN,A. & FREDRIKSEN,R. (1992) The fauna associated with the bank-forming deepwater coral *Lophelia pertusa* (Scleractinia) on the Faroe shelf. Sarsia 77:53-64

JONSSON,L. (2006) Ecology of three coastal cold-water cnidarians, in particular the scleractinian *Lophelia pertusa* Department of Marine Ecology Göteborg University

JUDD,A. & HOVLAND,M. (2007) Seabed Fluid Flow. The Impact on Geology, Biology, and the marine Environment p.475

KERR,R.A. (1998) Deep-Sea Coral Records Quick Response to Climate SCIENCE 1 May 1998: Vol 280 No5364:679

KIRIAKOULAKIS,K., FISHER,E., WOLFF,G.A., FREIWALD,A., GREHAN,A. & ROBERTS,J.M. (2005) Lipids and nitrogen isotopes of two deep-water corals from the North-East Atlantic: initial results and implications for their nutrition. In Cold-water Corals and Ecosystems, eds: Freiwald A, Roberts JM, Springer Publishing House, Heidelberg, Germany

KONGSBERG (2003) EM300 Multibeam echosounder. Operator manual

LANDVIK,J.Y., BONDEVIK,S., ELVERHØI,A., FJELDSKAAR,W., MANGERUD,J., SALVIGSEN,O., SIEGERT,M.J., SVENDSEN,J.I. & VORREN, T.O. (1998). The Last Glacial Maximum of Svalbard and the Barents Sea: ice sheet extent and configuration. Quaternary Science Reviews 17:43–75

LANGAAS,A. (2008) Kartlegging og verdisetting av naturtyper. MAREANO forbrukerkonferanse 2008

LANGLI,B. & LE GAC,J.-C. (2004) The first results with a new multibeam subbottom profiler OCEANS '04. MTTS/IEEE TECHNO-OCEAN '04 Vol 2:1147-1153

LASTRAS,G., CANALS,M. URGELES,R. HUGHES-CLARKE,J.E. & ACOSTA,J. (2004) Shallow slides and pockmark swarms in the Eivissia Channel, western Mediterranean Sea. Sedimentology 51:1-14

LE GONIDEC,Y., LAMARCHE,G. & WRIGHT,I. (2003) Using sound waves to sort out seafloor sediment types. NIWE Science. Water & Atmosphere Vol 11 No4

LIEN,R (1983) Iceberg scouring on the Norwegian continental shelf. Continental Shelf Institute, Norway, Publication 109

LINDBERG,B. & MIENERT,J. (2005a) Sedimentological and geochemical environment of the Fugløy Reef off northern Norway; In A. Freiwald and J.M. Roberts (eds.): Deep-water corals and ecosystems; Springer-Verlag, Berlin-Heidelberg, p.635-650.

LINDBERG,B. & MIENERT,J. (2005b) Postglacial carbonate production by cold-water corals on the Norwegian Shelf and their role in the global carbonate budget. Geology, Vol 33 No7:537

LINDBERG,B., BERNDT,C. & MIENERT,J (2005) The Fugløy Reefs on the Norwegian-Barents Continental Margin. Geology 33:7

LINDBERG,B., BERNDT,C. & MIENERT,J. (2007) The Fugløy Reef at 70°N; acoustic signature, geologic, geomorphologic and oceanographic setting. International Journal of Earth Sciences, 96 (1):201-213

LJØEN,R. (1962) The waters of the western and northern coast of Norway in July–August 1957. Fiskeridir Skr Ser Havunders 13:1–39

LOENG,H. (1991) Features of the physical oceanographic conditions of the Barents Sea. Polar research 10:5-18

LUNDÄLV,T. **(**2004) Local physical forcing factors and particle dynamics at a Kosterfjord DWC site. ACES, deliverable 11–2

LURTON,X. (2002) An introduction to underwater acoustics, principles and applications. Springer, Praxis Publishing.

LUMSDEN,E., HOURIGAN,T.F., BRUCKNER.A.W. & DORR,G (2007) The State of Deep Coral Ecosystems of the United States NOAA Technical Memorandum CRCP 3, National Oceanic and Atmospheric administration

LUNDE,T.M. (2006) Studie av kysttorskbestander i Troms og Finnmark basert på tråldata, 1995-2004: Statistiske analyser av mengdeutvikling, geografiske sammenhenger, lengdefrekvensfordeling og feilkilder i trålmetodikk. Mastergradsoppgave (M. Sc) i Water Resources and Coastal Management ved Universitetet i Bergen, p.109

MAREANOa, MAREANO maps depth and topography, sediment composition, contaminants, biotopes and habitats in Norwegian waters. Programme co-ordinator Lene Buhl-Mortensen, Institute of Marine Research (IMR) Available at <http://www.mareano.no/> Accessed on August 12, 2008

MAREANO News, Existing observations in 2007. Available at <http://www.mareano.no/> Last updates at April 23, 2008

MASSON,D., BETT,B.J., BILLETT,D.S.M., JACOBS,C.L., WHEELER,A.J. & WYNN,R.B. (2003) The origin of deep-water, coral-topped mounds in the northern Rockall Trough, Northeast Atlantic. Marine Geology 194:159-180

MCMULLEN,K.Y., POPPE,L.J, DENNY.,J.F., HAUPT,T.A & CROCKER,J.M. (2007) Sidescan-Sonar Imagert and Surficial Geologic Interpertation of the See Floor in Central Rhode Island Sound. USGS. Report Series 2007-1366

MIENERT,J. & BŰNZ,S (2006) Cruise Report "Gas hydrates of the NBS-margin " Vestnesa ridge (3D-pcable and multicomponent seismic. Petromaks-gans project. UiTø

MORTENSEN,P.B., HOVLAND,M., BRATTEGAARD,T. & FARESTVEIT,R. (1995) Deep water biotherms of the scleractinian coral *Lophelia pertusa* (L.) at 64° N on the Norwegian shelf: structure and associated megafauna. – Sarsia 80:145-158. Bergen

MORTENSEN,P.B. & RAPP,T. (1998) Oxygen and carbon isotope ratios related to growth line patterns in skeletons of *Lophelia pertusa* (L.) (Anthozoa, Scleractinia): implications for determination of linear extension rates. Sarsia 83:433–446

MORTENSEN,P.B. (2000). *Lophelia pertusa* (Scleractinia) in Norwegian waters; distribution, growth, and associated fauna. Dr scient. thesis. Department of Fisheries and Marine Biology, University of Bergen

MORTENSEN,P.B. (2001) Aquarium observations on the deep-water coral *Lophelia pertusa* (L. 1758) (Scleractinia) and selected associated invertebrates. Ophelia 54 (2): 83-104

MORTENSEN,P.B & FOSSÅ,J.H. (2001) Korallrev og andre bunnhabitater på Tautraryggen i Trondheimsfjorden. Fisken og havet 7, p.34

MORTENSEN,P.B., HOVLAND,M.T., FOSSÅ,J.H. & FUREVIK,D.M. (2001) Distribution, abundance and size of *Lophelia pertusa* coral reefs in mid-Norway in relation to seabed characteristics. Journal of the marine Biological Association of the UK 81: 581–597

MORTENSEN,P.B. & BUHL-MORTENSEN,L. (2005) Deep-water corals and their habitats in The Gully, a submarine canyon off Atlantic Canada. In: Cold-water corals and ecosystems. Freiwald, A. and Roberts, J.M. (eds.) Springer-Verlag, Berlin, p.849-879.

MORTENSEN,PB. & FOSSÅ,J.H. (2006) Species diversity and spatial distribution of invertebrates on *Lophelia* reefs in Norway. Pages 1849-1868 in Proceeding of the 10th International Coral Reef Symposium. Okinawa, Japan

NORDBY,E., TANDE,KS., SVENDSEN,H. & SLAGSTAD,D. (1999) Oceanography and fluorescence at the shelf break off the north Norwegian coast (69°20'N-70°30'N) during the main productive period in 1994. Sarsia 84:175-189

NORWEGIAN DIRECTORATE OF FISHERIES (2004) Forskrift om utøvelse av fisket i sjøen FOR 2004-12-22 nr 1878: Kapittel XIII. Beskyttelse av korallrev § 66. Forbud mot å drive fiske i nærheten av korallrev. Available at < http://www.lovdata.no/cgi-wift/ldles?doc=/sf/sf/sf-20041222-1878.html#66 > Accessed on: November 12, 2008

NORWEGIAN HYDROTROPIC SERVICE NORWEGIAN. Tidal and Sea Level Data. Tromsø tide gauge. Available at <http://vannstand.statkart.no/Engelsk/main.php> Accessed on: August 12, 2008

O'BRIEN,J., BERROW,S. & WALL,D. (2005) The impact of Multibeam on cetaceans: A review of best practice, the Irish Whale and Dolphin Group

OLSEN,E., GJØSÆTER,H., RØTTINGEN,I., DOMMASNES,A., FOSSUM,P., & SANDBERG,P. (2007) The Norwegian ecosystem-based management plan for the Barents Sea – ICES Journal of Marine Science, 64

ORVIK,K.A. & MORK,M. (1995) A case study of Doppler-shifted inertial oscillations in the Norwegian Coastal Current. Continental Shelf Research, 15: 1369-1379

OTTESEN,D., DOWDESWELL,J.A., LANDVIK,J.Y. & MIENERT,J. (2007) Dynamics of the Late Weichselian ice sheet on Svalbard inferred from high-resolution sea-floor morphology. Boreas, Vol 36:286-306

OTTESEN,D., STOKES,C.R., RISE,L. & OLSEN,L. (2008) Ice-sheet dynamics and ice streaming along the coastal parts of northern Norway. Quaternary Science Reviews

OUG,E. & MORTENSEN,P.B. (2006) Koralldyr. Anthozoa – I: Kålås, J.A., Viken, Å. og Bakken, T. (red.). Norsk Rødliste 2006– *2006 Norwegian Red List*. Artsdatabanken, Norway

PETERSON,C.H., RICE,S.D., SHORT,J.W., ESLER,D., BODKIN,J-L., BALLACHEY,B.E. & IRONS,D.B. (2003) Long-term ecosystem response to the Exxon Valdez oil spill. Science 302. 19 December.

PEDERSEN,O.P., ZHOU,M., TANDE,K.S. & EDVARDSEN,A. (2005) Eddy formation on the coast of North Norway - evidenced by synoptic sampling. ICES Journal of Marine Science, 62: 615-628

PAPATHEODOROU,G., LAVRENTAKI,M., MOURELATOS.P., VOUTSINAS.K. & XENOS,K. (2001) Pockmarks on the seabed of the Aetoliko Lagoon, Greece (in Greek). Alieftika Nea (Fishing News), 238:73–87

PAULL,C.K., NEUMANN,A.C., AM ENDE,B., USSLER,W. & RODRIGUEZ,N. (2000) Lithoherms on the Florida-Hatteras slope. Marine Geology 166: 83–101

PICKRILL,R.A. (1993) Shallow seismic stratigraphy and pockmarks of a hydrothermally influenced lake, Lake Rotoiti, New Zealand. Sedimentology 40:813–28.

PLASSEN,L. & VORREN,T.O. (2002) Sedimentary processes and the environment during deglaciation of a fjord basin in Ullsfjorden, North Norway. Norwegian Journal of Geology, Vol 83:23-36

RAMBERG,I.B., BRYHNI,I., NØTTVEDT,A. (2008) The making of a land geology of Norway. Norsk geologisk forening p.624

RAFAELSEN,B., ANDREASSEN,K., KUILMAN,L.W., LESESBYE,E., HOGSTAD,K. & MIDTBØ,M. (2002) morphology of buried glaciogenic horizons in the Barents Sea from three dimensional seismic data. Geological Society 203:259-276

RAVEN,J.A., FINKEL,Z.V. & IRWIN,A.J. (2005) Picophytoplankton: bottom-up and top-down controls on ecology and evolution. Vie et Milieu 55 (3-4):209-215

REED,J.K. (2004) Deep-water coral reefs of Florida, Georgia and South Carolina: Summary of the distribution, habitat, and associated fauna. Harbor Branch Oceanographic Institution, p. 71

Roberts,H.H. & Aharon,P. (1994) Hydrocarbon-derived build-ups of the northern Gulf of Mexico continental slope: a review of submersible investigations. Geo-marine Letters 14(2-3):135-148

ROBERTS,J.M. (2002) The occurrence of the coral *Lophelia pertusa* and other conspicuous epifauna around an oil platform in the North Sea. Journal for the Society for Underwater Technology, 25:83-91

ROBERTS,S. & HIRSHFIELD,M. (2002) Deep sea corals: out of sight, but no longer out of mind. Protecting the world's oceans. Available at <www.oceana.org> Last update: at August 17, 2008

ROBERTS, J.M., LONG, D., WILSON, J.B., MORTENSEN, P.B. & GAGE, J.D. (2003) The cold-water coral *Lophelia pertusa* (Scleractinia) and enigmatic seabed mounds along the north-east Atlantic margin: are they related? Marine Pollution Bulletin 46:7-20

ROBERTS,JM., WHEELER,AJ. & FREIWALD,A. (2006) Reefs of the deep: the biology and geology of cold-water coral ecosystems. Science 312:543–547

ROGERS,AD. (1990) Responses of coral-reefs and reefs organisms to sedimentation. Marine Ecology Process Series 62:185-202

ROGERS,AD. (1999) The biology of *Lophelia pertusa* (Linnaeus 1758) and other deep-water reef-forming corals and impacts from human activity. International Review of Hydrobiology 84:315–410

ROGERS,J.N. (1999) Mapping of subaqueous, gas-related pockmarks in Belfast Bay, Maine using GIS and remote sensing techniques. Unpublished MS Thesis, University of Maine, Orono, ME, p.139

ROKOENGEN,K & ØSTMO,S.R. (1985) Shallow geology off Fedje, western Norway.- IKU Report, 24.1459/01/85

ROSS,S.W. (2007) Unique deep-water ecosystems off the southeastern United States. Oceanography 20(4): 130-139

RØNHOVDE,A., YANG,L., TAXT,T. & HOLM,S. (1999) "High-resolution beamforming for multibeam echo sounders using raw EM3000 data," Proc. IEEE Oceans'99, Vol. II:923-930

SAWHILL,S.G., THOMMESSEN,Ø.B., VIK,J.K. & ØSTRENG,W. (2006) Focus North: Ten thematic studies about the Barents Sea and the northern areas. Ocean Futures

SHERIFF,R.E. (1991) Encyclopedic Dictionary of Exploration Geophysics, Third Edition: Society of Exploration Geophysicists, p.384

SIGMOND,E.M.O. (1992) Bedrock map of Norway and adjacent ocean areas. Scale 1:3 million. Geological Survey of Norway

SOLHEIM,A. (1997) Depth-Dependent Iceberg Plough Marks in the Barents Sea. In Davies, T.A., Bell, T., Cooper, A.K., Josenhans, H., Polyak, L., Solheim, A., Stoker, M.S. & Stravers, J.A. (eds.): Glaciated Continental Margins: An Atlas of Acoustic Images. 138-139. Chapman & Hall, London

SPIRO,B., ROBERTS,J.M., GAGE,J. & CHENERY,S. (2000) 18O/16O and 13C/12C in an ahermatypic deep-water coral *Lophelia pertusa* from the North Atlantic: a case of disequilibrium isotope fractionation. Rapid Communication in Mass Spectrometry 14:1332–1336

STIANSEN,J.E., AGLEN,A. ,BOGSTAD,B., BUDGELL,P., DALPADADO,P., DOLGOV,A.V., DOMMASNES,A., FILIN,A.A., GJØSÆTER,H., HAUGE,K.H., HØINES,Å., INGVALDSEN,R., JOHANNESEN,E., JØRGENSEN,L.L., KARSAKOV,A.L., KLUNGSØYR,J., KNUTSEN,T., LIEN,V., LOENG,T., MEHL,S., MORTENSEN,R.B., MUCHINA,N.V., NESTEROVA,V.N., OLSEN,E., ORLOVA,E.L., OZHIGIN,V.K., PEDCHENKO,A.P., STENEVIK,E.K., SKOGEN,M., TITOV,O.V., TJELMELAND,S., ZABAVNIKOV,V.B., ZIRYANOV,S.B., ZHUKOVA,N.G., ØIEN,N. & AANES,S. (2005) Joint PINRO/IMR report on the state of the Barents Sea ecosystem 2005/2006. IMR/PINRO Joint Report Series,No. 3/2006. ISSN 1502-8828. p.122

SUMIDA,P.Y.G., YOSHINAGA,M.Y., SAINT–PASTOUS MADUREIRA,L.A. & HOVLAND,M. (2004) Seabed pockmarks associated with deep–water corals off SE Brazilian continental slope, Santos basin. Marine Geology 207:159–167

SUNDBY,S. (1976) Oceanographic conditions in Malangene Fugløybankene Tromsøflaket. An overview. Fisken og Havet, B1:1-53

SÆTRE,H.J. (1972) Strømmålinger i Tromsøsundet og Sandnessundet, Februar 1972, Report, Norwegian Hydrodynamic Laboratory, p.1-20

TAVIANI,M., REMIA,A., CORSELLI,C., FREIWALD,A., MALINVERNO,E., MASTROTOTARO,F., SAVINI,A. & TURSI,A. (2005) First geo-marine survey of living cold-water *Lophelia* reefs in the Ionian Sea (Medterranean basin). Facies 50:409–417

THOMPSON,JJ. & BRIGHT,T. (1980) Effects of an offshore drilling fluid on selected corals. In: Series Research on Environmental Fate and Effects of Drilling Fluids and Cuttings, 2:1044-1078. Washington, DC

THORSNES,T. (2003) Coral reefs and marine geology. In Focus 2003 No3, NGU

THIEM,Ø., RAVAGNAN,E., FOSSÅ,J.H. & BERNTSEN (2006) Food supply mechanisms for cold-water corals along a continental shelf edge. Journal of Marine Systems 60:207–219

TOROK,S. (2006) Deep-sea corals provide key to climate change, Wealth from Oceans Flagship CSIRO Marine & Atmospheric Research. Available from < http://www.csiro.au/science/ps1cw.html> Last updated: 7 March 2006

TYLER-WALTERS,H. (2005) *Lophelia* reefs. Marine Life Information Network: Biology and Sensitivity Key Information Sub-programme [on-line]. Plymouth: Marine Biological Association of the United Kingdom. [cited 13/09/2007]. Available from< http://www.marlin.ac.uk> Last accessed: 15 November 2008

VIKEBØ,F.B. & ÅDLANDSVIK, B. (2005) Circulation and hydrography off northern Norway — a regional ocean model study. The impact of climate on early stages of Arcto-Norwegian cod – A model approach, PhD Manuscript University of Bergen, Paper I, p.15–49

VORREN,T.O., HALD,M., EDVARDSEN,M. & LIND-HANSEN,O.W. (1983) Glacigenic sediments and sedimentary environments on continental shelves: General principles with a case study from the Norwegian shelf. Glacial Deposits in North-West Europe. J. Ehlers. Rotterdam, A. A. Balkema: 61-73

VORREN,T.O. & KRISTOFFERSEN,Y. (1986) Late Quaternary Sediments and Stratigraphy on the Continental Shelf of Troms and West Finnmark, Northern Norway. Quaternary Research Boreas 15:51-59

VORREN,T.O., LEBESBYE,E., ANDREASSEN,K. & LARSEN,K.B. (1989). Glacigenic sediments on a passive continental margin as exemplified by the Barents Sea. Marine Geology 85:251-272

VORREN,T.O., LEBESBYE,E. & LARSEN,K.B. (1990) Geometry and genesis of the glacigenic sediments in the southern Barents Sea. *In*: DOWDESWELL, J.A. & SCOURSE, J. D. (eds) Glacimarine Environments: Processes and Sediments. Geological Society, London, Special Publications, 53:269–288

VORREN,T.O. & LABERG,J.S. (1997) "Trough mouth fans -- palaeoclimate and ice-sheet monitors" Quaternary Science Reviews 16(8): 865

WESSEL,P. & SMITH,W.H.F. (2008) The Generic Mapping Tools GMT Version 4.3.0. Technical Reference and Cookbook p.211

WHEELER,A.J., KOZACHENKO,M., BEYER,A., FOUBERT,A., HUVENNE,V.A.I., KLAGES,M., MASSON,D.G., OLU-LE ROY,K. & THIEDE,J. (2005) Sedimentary processes and carbonate mounds in the Belgica Mound province, Porcupine Seabight, NE Atlantic. In, Friewald, A. and Roberts, J.M. (eds.) Cold-water corals and ecosystems. Berlin, Germany, Springer, p.571-603

WHEELER,A.J., BEYER,A., FREIWALD,A.DE HAAS,H., HUVENNE,V.A.I, KOZACHENKO,M., ROY,O.L. & OPDERBECKE,K. (2007) Morphology and environment of cold-water coral carbonate mounds on the NW European margin Earth Science, Geol Rundsch 96:37–56

WILSON,J.B. (1979) 'Patch' development of the deep-water coral *Lophelia pertusa* (L.) on Rockall bank. Journal marine biology Ass. U.K.59:165–177

WWF-World Wide Fund For Nature (2003) The Barents Sea- A sea of opportiunities…and threats. Petroleum activities and fragile nature. A WWF-Norway report. Executive summary

WWF-World Wide Fund For Nature (2004) Cold-water corals fragile havens in the deep, Gland Switzerland

WWF-World Wide Fund For Nature (2007) Oil Spill Response Challenges in Arctic Waters, WWF International Arctic

Appendix

Statistics of pockmarks

STATISTICS OF POCKMARKS

Pockmark	x	y	Bottom	SS	Depth	D (W-E)	Slope (E-W)	Slope (W-E)	D (N-S)	Slope (S-N)	Slope (N-S)	Volume (m³)
1	487430.68	7803360.95	216,57	214,50	2,07	37,90	4,37	6,65	42,70	8,12	6,38	1327,90
2	487518.61	7803334.41	214,73	212,00	2,73	45,90	4,78	6,86	52,10	6,97	5,69	2589,47
3	487755.58	7803779.18	216,90	212,50	4,40	47,90	9,64	11,06	65,20	6,16	6,79	5472,78
4	488023.50	7804177.04	203,05	200,70	2,35	51,00	6,99	8,34	53,80	5,01	4,57	2553,77
5	488092.01	7804271.04	204,04	199,00	5,04	42,50	8,28	7,96	66,40	8,08	7,02	5685,46
6	486390.38	7804561.37	254,31	248,00	6,31	104,30	6,09	7,14	92,30	3,57	3,73	24126,86
7	486251.73	7804625.31	248,65	244,80	3,85	45,70	9,05	6,63	82,90	5,50	7,24	5791,46
8	486191.13	7804819.85	241,36	237,00	4,36	41,10	4,90	2,80	78,20	5,63	4,99	5578,84
9	486268.01	7804846.11	242,69	239,20	3,49	70,20	8,43	8,42	106,60	4,19	4,27	10338,52
10	486183.47	7804940.80	238,77	236,50	2,27	52,70	4,08	3,42	47,60	2,83	6,61	2255,42
11	486340.69	7804940.29	243,99	238,00	5,99	85,70	6,92	6,94	99,00	5,69	7,41	20187,47
12	486511.27	7804927.99	243,88	241,00	2,88	55,30	7,24	5,42	63,30	4,60	5,13	3994,74
13	486420.36	7805015.32	244,74	239,50	5,24	66,00	7,67	8,86	102,00	4,92	6,62	14009,67
14	486417.42	7805009.32	244,84	240,00	4,84	55,10	6,25	5,61	82,00	3,53	5,13	8697,61
15	486351.52	7805119.13	247,29	241,20	6,09	95,40	6,77	6,58	110,60	5,03	7,84	25500,49
16	486471.29	7805126.61	246,52	241,50	5,02	70,90	7,15	7,74	137,50	5,39	5,67	19397,42
17	486585.28	7805094.80	244,23	240,50	3,73	60,20	10,77	6,76	80,90	4,72	7,16	7202,81
18	486661.73	7805075.55	242,46	238,20	4,26	41,30	5,31	10,05	77,40	5,22	7,39	5419,67
19	486592.41	7805282.90	248,33	243,70	4,63	63,70	6,96	8,20	139,10	4,29	7,19	16257,11
20	486929.75	7805179.51	241,25	239,00	2,25	48,70	5,68	6,98	67,80	2,46	3,89	2940,53
21	486871.70	7805254.49	244,30	241,70	2,60	34,10	4,91	6,53	71,40	3,54	4,70	2509,73
22	486931.41	7805357.94	246,47	241,60	4,87	72,10	6,24	6,31	111,70	4,34	4,49	15553,08
23	486586.33	7805489.83	255,98	252,48	3,51	114,30	6,26	8,47	187,50	3,56	4,75	63541,19
24	487168.27	7805671.93	240,19	238,00	2,19	67,00	6,00	2,84	69,90	5,58	3,66	4056,82
25	487257.18	7805668.08	240,90	238,00	2,90	65,70	4,92	5,49	86,60	5,20	4,71	6530,30

Notation SS = surronding seafloor (m)
D (W-E) = diameter in W-E direction (m)
D (N-S) = diameter in N-S direction (m)